A role for DNA-PKcs in G_2 checkpoint response and DNA end resection after exposure to ionizing radiation

Inaugural-Dissertation

zur

Erlangung des Doktorgrades

Dr. *rer. nat.*

der Fakultät für Biologie

an der

Universität Duisburg-Essen

Standort Essen

vorgelegt von

Rositsa Kirilova Dueva

aus Petrich, Bulgarien

Dezember, 2015

Die der vorliegenden Arbeit zugrunde liegenden Experimente wurden am Institut für Medizinische Strahlenbiologie an der Universität Duisburg-Essen, Standort Essen, durchgeführt.

1. Gutachter: Prof. Dr. Georg Iliakis

2. Gutachter: Prof. Dr. Andrea Musacchio

Vorsitzender des Prüfungsausschusses: Prof. Dr. Ralf Küppers

Tag der mündlichen Prüfung: 15. März 2016

“Success in not final, failure is not fatal: it is the courage to continue that counts.”

Winston Churchill

TABLE OF CONTENTS

LIST OF COMMONLY USED ABBREVIATIONS

53BP1	p53 binding protein 1
ADP	Adenosine diphosphate
A-EJ	Alternative end joining
A-NHEJ	Alternative non-homologous end joining
AT	Ataxia telangiectasia
ATM	Ataxia telangiectasia mutated
ATP	Adenosine triphosphate
ATR	Ataxia telangiectasia and Rad3-related
ATRIP	ATR-interacting protein
BASC	BRCA1-associated genome surveillance complex
BLM	Bloom syndrome helicase
B-NHEJ	Backup non-homologous end joining
BRCA1	Breast cancer susceptibility protein 1
BRCA2	Breast cancer susceptibility protein 2
BSA	Bovine serum albumin
CAK	CDK-activating kinase
CHK1	Checkpoint kinase 1
CHK2	Checkpoint kinase 2
CHO	Chinese hamster ovary cells
CDC25	Cell division cycle 25 phosphatase
CDK	Cyclin-dependent kinase
ClB1+	Cyclin B1 positive cell
c-NHEJ	Classical non-homologous end joining
CPT	Camptothecin
CSR	Class switch recombination

CtIP	CtBP-interacting protein
DAPI	4’,6-diamidino-2-phenylindole
DDR	DNA damage response
DMEM	Dulbecco’s Modified Eagle Medium
DMSO	Dimethylsulfoxid
DNA	Deoxyribonucleic acid
DNA2	DNA replication helicase/nuclease 2
DNA-PK	DNA-dependent protein kinase
DNA-PKcs	DNA-dependent protein kinase catalytic subunit
DSB	Double strand break
dsDNA	Double-stranded DNA
dsRNA	Double-stranded RNA
EDTA	Ethylenediaminetetraacetic acid
et al.	*et alii* (‘and others’)
EXO1	Exonuclease 1
FACS	Fluorescence-activated cell sorting
FBS	Fetal bovine serum
γH2AX	phosphorylated histone variant H2AX at Ser139
GFP	Green fluorescent protein
Gy	Gray (J/kg), unit of ionizing radiation dose
H3pS10	Histone H3 phosphorylated at Ser10
HEPES	4-(2-hydroxyethyl)-1-piperazineethanesulfonic acid
HR	Homologous recombination
HRR	Homologous recombination repair
HSP90	Heat shock protein 90
hTERT	Human telomerase reverse transcriptase

i.e.	*id est* (‘it is’)
IF	Immunofluorescence
IgA/E/G/M	Immunoglobulin A/E/G/M
IR	Ionizing radiation
IRIF	Ionizing radiation-induced foci
KAP-1	KRAB-associated protein 1
KARP-1	KU80 Autoantigen Related Protein-1
kDa	Kilodalton
LSCM	Laser scanning confocal microscopy
LET	Linear energy transfer
MDC1	Mediator of DNA damage checkpoint protein 1
MEM	Minimum Essential Medium
MI	Mitotic index
MRN	MRE11-RAD50-NBS1 complex
mRNA	Messenger RNA
mTOR	Mammalian target of rapamycin
NBS1	Nijmegen breakage syndrome 1 protein
NEAA	Non-essential amino acids
NEK1	Never-in-mitosis A related protein kinase 1
NHEJ	Non-homologous end joining
nt	Nucleotide
p53	Tumor protein 53
PAGE	Polyacrylamide gel electrophoresis
PARP1	Poly [ADP-ribose] polymerase 1
PAXX	Paralog of XRCC4 and XLF
PBG	Phosphate-buffered gelatin

PBS	Phosphate-buffered saline
PBS-T	Phosphate-buffered saline containing Tween®-20
PCNA	Proliferating cell nuclear antigen
PFA	Paraformaldehyde
PI	Propidium iodide
PIKK	Phosphatidylinositol-3 kinase-related kinase
PI3K	Phosphatidylinositol-3-kinase
PIN1	Peptidyl-prolyl *cis/trans* isomerase 1
RIPA buffer	Radioimmunoprecipitation assay buffer
PMT	Photomultiplier
PNK	Polynucleotide kinase
RAG1	Recombination activating gene 1
RAG2	Recombination activating gene 2
RAP80	Receptor-associated protein 80
RFC	Replication factor C
RGB	Resolving gel buffer
RIF1	Replication timing regulatory factor 1
RNA	Ribonucleic acid
RNAi	RNA interference
RNF8	Ring finger protein 8
RPA	Replication protein A
rpm	revolutions per minute
RT	Room temperature
SAC	Spindle assembly checkpoint
Ser	Serine
SCID	Severe combined immunodeficiency

SD	Standard deviation
SDS	Sodium dodecyl sulfate
SDS-PAGE	Sodium dodecyl sulfate polyacrylamide gel electrophoresis
SE	Standard error
Ser	Serine
SGB	Stacking gel buffer
siRNA	Small/short interfering RNA
SIRT6	Protein deacetylase Sirtuin-6
SMG1	Suppressor of morphogenesis in genitalia 1
ssDNA	Single-stranded DNA
S/T	Serine/Threonine
SQ/TQ	Serine or threonine followed by glutamine
TEMED	Tetramethylethylanediamine
Thr	Threonine
TOPBP1	DNA topoisomerase 2-binding protein 1
Tris	Tris(hydroxymethyl)aminomethane
TRRAP	Transformation/transcription domain-associated protein
Tyr	Tyrosine
V(D)J	Variable (diversity) joining
WB	Western blot
WB-TB	Western blot transfer buffer
WRN	Werner syndrome helicase
wt	wild type
XLF	XRCC4-like factor / Cernunnos
XRCC1/4	X-ray repair cross-complementing group 1/4

LIST OF FIGURES

LIST OF TABLES

ABSTRACT

DNA damage response (DDR) is a cellular network that comprises signaling from DNA lesions, including DNA double-strand breaks (DSBs), and their repair. ATM and ATR belong to the Phosphatidylinositol-3 kinase-related kinases (PIKK) family and are known as the master controllers of DDR signaling. It is generally accepted that ATM is activated by DSBs or chromatin modifications, while ATR operates in DNA replication and in response to DSBs becomes activated by single-stranded DNA regions at the DSB ends generated by DNA end resection. DNA-PK catalytic subunit (DNA-PKcs), a third member of the PIKK family, is an essential component of the classical non-homologous end joining (c-NHEJ) pathway of DSB repair. However, the catalytic function of DNA-PKcs in c-NHEJ has been extensively studied, while its role in DNA damage signaling still remains obscure.

In this thesis, we provide evidence of a contribution of DNA-PKcs in the checkpoint response as well, particularly in cells irradiated in S and G_2 phases of the cell cycle. The role of DNA-PKcs in this process appears to be specific as this effect is not observed with depletion of KU70/80, an essential factor for recruitment of DNA-PKcs at DSBs. Analysis of G_2 arrest and evaluation of the mitotic index using H3pS10 assay after exposure of cells to IR revealed that deficiency of DNA-PKcs or its chemical inactivation is linked with persistent G_2 checkpoint; in cells irradiated in S phase this hyper-activated checkpoint is entirely dependent on ATR, while in cells sustaining DNA damage in G_2 phase it relies on both ATM/ATR.

The requirement of ATR for the prolonged G_2 checkpoint in DNA-PKcs deficient background suggests extensive resection at DSB ends which could be visualized by immunostaining of RPA. Hence, the data demonstrate that DNA-PKcs may also contribute to DNA damage response via regulation of DNA end resection.

Evaluation of the effects of ATM and ATR kinases on the G_2 checkpoint and DNA end resection by using small molecule inhibitors point to a model where ATM, ATR and DNA-PKcs may work as a kinase module to effectively control the G_2 checkpoint and the process of resection after exposure to ionizing radiation.

1. INTRODUCTION

1.1. DNA damage induction by ionizing radiation

The genomes of eukaryotic cells are continuously threatened by natural background irradiation, such as cosmic rays and decay of radioactive isotopes in terrestrial environment. The use of diagnostic medical imaging, radiation therapy and nuclear accidents provide another source of artificial background irradiation.

Important feature of ionizing radiation (IR) is the localized release of large amounts of energy that is sufficient to eject orbital electrons from atoms and molecules, thereby ionizing them. The energy deposition per ionizing event is about 33 eV, which is enough to break a strong chemical bond (1). The direct action of IR refers to the absorption of energy directly by the target molecule and is characteristic for radiations with high linear energy transfer (LET) such as neutron or α-particles. In this thesis IR was generated artificially using X-rays. As a sparsely ionizing form of radiation (low LET), X-rays are predominantly causing cellular damage indirectly by interacting with other atoms or molecules in the cell, mainly water, as it represents 80% of cellular content. The resulted free radicals are very unstable, because they carry an unpaired orbital electron in their outer shell, and react quickly with the target molecules. The chemical changes from the breakage of bonds in the molecules lead to biological effects (1).

As a carrier of genetic information, nuclear DNA is the most critical target of IR where the formation of DNA double-strand breaks (DSBs) represents the most deleterious lesion with high probability to convert in heritable mutations or lethal events. Importantly, DSBs are also naturally occurring intermediates during programmed biological processes like V(D)J recombination and class switch recombination (CSR) that are required for the adaptive immune system (2). Recently, DSB formation as a physiological event has been reported to occur upon stimulation of neuronal activity (3).

In a healthy cell, the severe effect of IR-induced DSBs and their misrepair have to be avoided in order to preserve genomic stability and, in extreme cases, to suppress cancer development (4, 5). However, IR as a DNA damaging agent is frequently used in cancer therapy to induce mitotic and less frequently apoptotic cell death in

tumor cells (6). Since tumor cells are actively dividing and therefore probably more radiosensitive that resting cells (G_0), the cell cycle phase (described below) is of great importance for radiotherapy (7).

As shown in **Figure 1**, exposure of cells to IR results in many types of DSBs, whose presence in the cell has to be detected. Sensor proteins that can detect each type of DSB (if any) remain undefined.

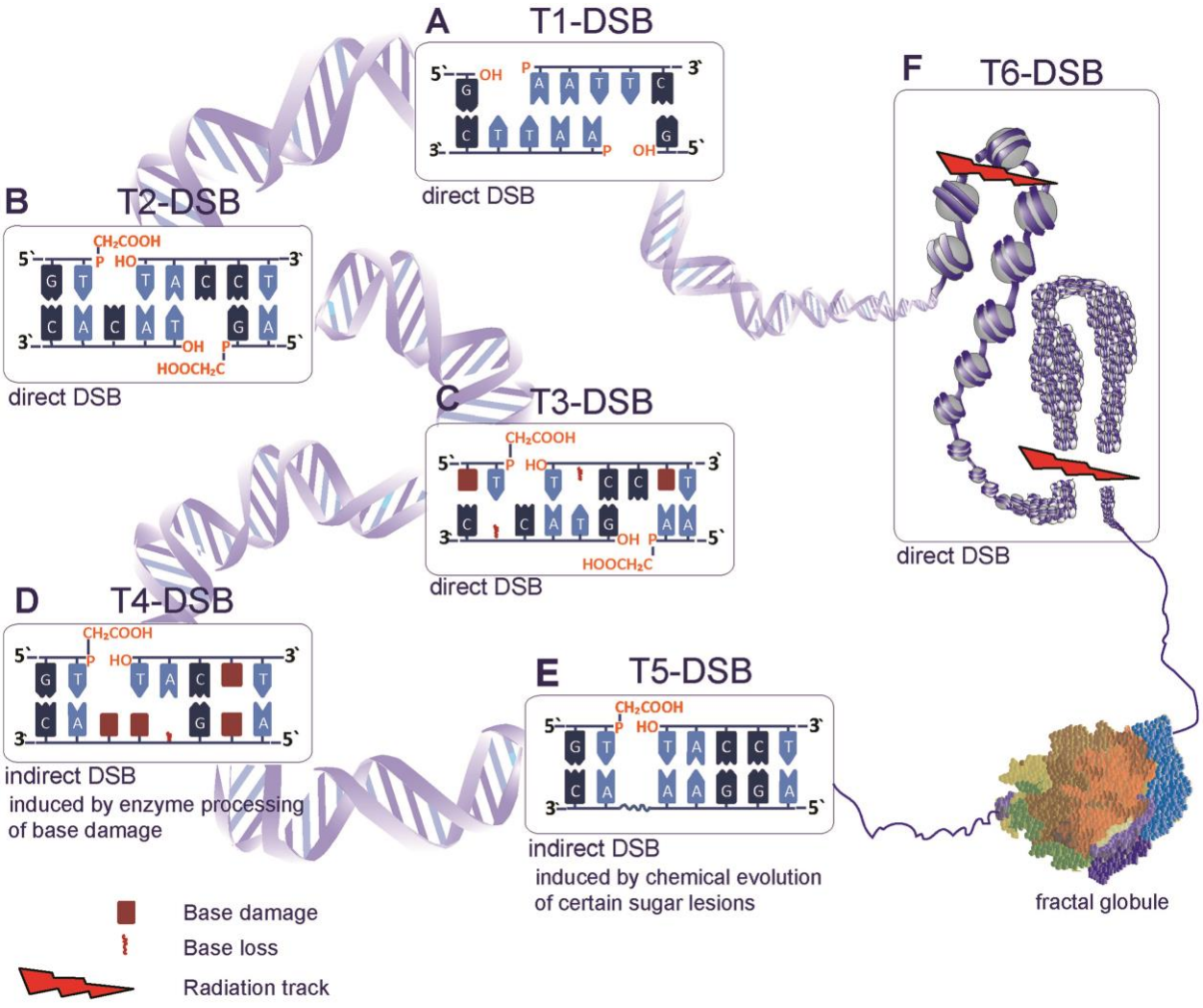

Figure 1: Different types of DSBs. (**A**) DSB with a 5'- phosphate and a 3'-OH group generated by restriction endonucleases, (**B**) IR-induced DSB with common 3'-phosphoglycolate and a 5'-OH at the ends, (**C**) Clustered lesions induced by clustered ionization events, where a DSB contains additional forms of DNA damage, (**D**) Indirect DSB converted from an initial single-stranded break (SSB) by enzymatic processing of opposing base damage, (**E**) Indirect DSB induced after temperature-sensitive chemical processing of sugar lesions opposite to a SSB, (**F**) Clustered DSBs that can affect chromatin stability by nucleosome loss or deletion of larger chromatin segments. *Figure obtained from Schipler and Iliakis, 2013 (8).*

Much is known about the sensor molecules that detect not the type of DSB but their conversion in common intermediates, for example, DNA discontinuity detected by KU70/80 and single-stranded DNA that becomes recognized by Replication Protein A (RPA). Such intermediates activate an intricate DNA repair machinery that is supported by signaling networks termed checkpoints. The checkpoint pathways interact with the cell-cycle control system by halting progression through G_1, S or G_2 phase, and thus provide time for faithful repair or prevent cell proliferation of potentially mutated cells.

1.2. Cell-cycle control system

Cell cycle progression requires high degree of synchronization among numerous enzymes to ensure faithful transfer of the genetic information over generations (9). The duplication of the genome requires correct order of events carried out by the cell-cycle control system. As a result, the initiation of each stage is dependent on the completion of the previous one (10). Before entering cell division, the cell requires metabolism and intake of nutrients, as well as duplication of its genome. This takes place in the interphase, which is the period between one M phase and the next (**Figure 2**). Cell division includes DNA replication occurring in S phase (S indicating *synthesis*), where each chromosome must be duplicated only once per cell cycle and with extreme precision to prevent development of heritable genetic aberrations in the daughter cell. Entry into mitosis is dependent on the completion of DNA replication (9).

The cell cycle contains two gap phases; the first gap (G_1) is before DNA replication and is the first phase within the interphase; it is known as growth phase, where the cell conducts all its metabolic activities and grows in size. The duration of G_1 phase varies among species and under unfavorable extracellular conditions like reduced growth factors signaling, cells usually enter the non-dividing G_0 state. Non-proliferating and differentiated cells remain in G_0 for long periods of time without resuming the cell cycle. Stem cells, in contrast, have the capacity to reenter the cell cycle and divide (9).

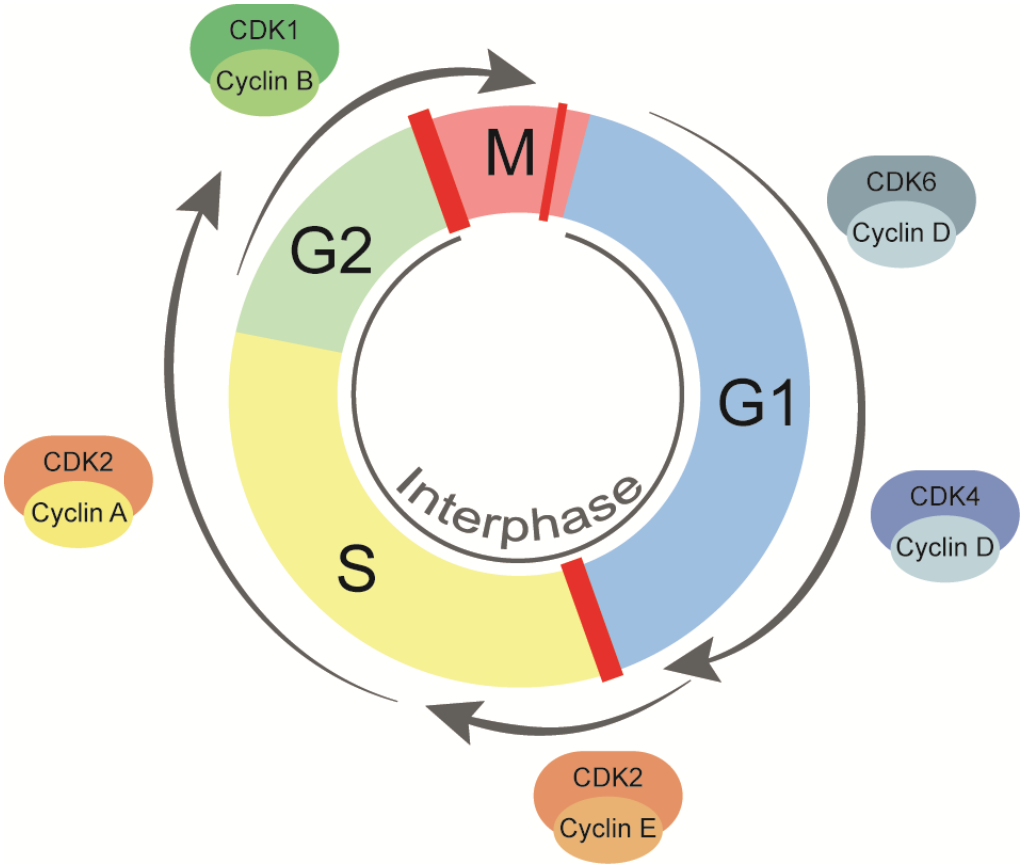

Figure 2: The cell-cycle control. Proper progression through the cell-cycle is ensured by three main checkpoints. Entry into S phase by overcoming the Restriction point (G_1/S checkpoint) is driven by G_1/S- and S-phase CDK-cyclin complexes. The different types of DNA replication checkpoint functioning throughout the S phase are not shown in the figure. Before onset of mitosis, which is triggered by M-phase CDK-cyclin complexes, cells undergo G_2/M checkpoint. In the end, the spindle checkpoint guarantees the precise separation of the duplicated chromosomes and therewith the metaphase-to-anaphase transition associated with destruction of cyclins (9). The arrows indicate the expression of the corresponding cyclins and activation of different CDK-cyclin complexes.

The second gap (G_2) occurs after DNA synthesis and is characterized by rapid cell growth and protein synthesis (11). The G_2 phase also provides additional time for the cell to correct replication errors during S phase. Hence, the major purpose of the gap phases in the cell cycle is to assist DNA replication and mitosis by monitoring whether the environmental conditions are suitable for entering the next phase. Some cells, particularly the early embryo of the frog *Xenopus laevis*, do not require gap phases in their cell cycle to prepare themselves for mitosis (9, 12).

In comparison to other cell cycle phases, the M phase is relatively short and is considered to be composed of nuclear division (mitosis), where the duplicated chromosomes are segregated and divided into daughter nuclei and cell division (cytokinesis) that allows distribution of cytoplasmic components into two individual daughter cells. In this way, each daughter cell obtains a complete and identical copy of the genome (9).

Key regulators of the cell-cycle control system are the **cyclin-dependent kinases (CDKs)**. CDKs are a family of enzymes that phosphorylate their protein substrates at serine/threonine residues. Cellular CDK levels remain constant but their activities oscillate as the cells progress through the cell cycle. CDKs are primarily regulated by different types of regulatory subunits called **cyclins**. This leads to formation of different CDK-cyclin complexes throughout the cell cycle (13, 14). Furthermore, CDKs can be activated by phosphorylation at a conserved threonine residue by CDK-activating kinase (CAK). In higher eukaryotes, the main candidate for CAK is the CDK7/Cyclin H/ménage-à-trois 1 (MAT1) complex (13, 15, 16). Inactivation of CDK-complexes involves ubiquitin-dependent proteolysis of cyclins, removing inhibitory phosphates from CDK active sites by CDC25 phosphatases or inhibitory tyrosine phosphorylation of CDK1 by Wee1 kinase. CDK-cyclin complexes can be also inactivated by inhibitory subunits like p21 and p27 (13, 17).

Proper progression through the cell cycle is governed by control mechanisms called **cell-cycle checkpoints** (10, 18). In G_1 checkpoint, when the conditions for cell proliferation are optimal, the S-phase CDK-cyclin complexes are activated, which then promote entry into S-phase by overcoming the restriction point. The second major checkpoint which allows entry into M phase is the G_2/M checkpoint, also known as DNA damage checkpoint. The G_2 checkpoint response prevents cells to enter mitosis with unfaithfully repaired DNA or incomplete DNA synthesis. The third major checkpoint is the spindle assembly checkpoint (SAC) in metaphase, which ensures proper mitosis and cytokinesis. Additionally, precise replication of the genome is ensured by different types of DNA replication checkpoint functioning throughout the S phase (19). In this thesis, the focus is placed on G_2 checkpoint regulation after DNA damage induction by ionizing radiation.

As sentinels for cell cycle progression, the cell cycle checkpoints regulate genome stability and their dysfunction may lead to cell death, increased susceptibility to DNA damaging agents and carcinogenesis (20).

1.3. Mammalian DNA damage checkpoint-control after exposure to IR

Cellular DNA damage induction by ionizing radiation activates essential checkpoint networks that halt progression through G_1 and G_2 phases of the cell cycle and slow down DNA synthesis. This favors restoration of DNA integrity by the repair mechanisms and thus protects against mutations, chromosomal aberrations and predisposition to cancer (21, 22).

DNA damage checkpoints are biochemical signaling pathways that sense various types of sequence alterations in the DNA. Checkpoint activation requires sensors of DNA damage, transducers and effectors (**Figure 3**). Transducer kinases amplify the damage signal from the sensor proteins by phosphorylating other kinases or downstream target proteins (effectors). At the effector level the DNA damage checkpoint connects with the cell-cycle control machinery (22).

The most well characterized DNA damage sensors are MRE11-RAD50-NBS1 (MRN) complex, KU70/80 heterodimer and poly(ADP-ribose)-Polymerase 1 (PARP1) (23). Candidates for such sensor molecules are also the PCNA-like proteins RAD1, RAD9 and HUS1, which were shown to form a DNA damage-responsive complex, and the RFC-like protein RAD17 (21, 24, 25). The breast cancer protein BRCA1 has also been linked to DNA damage sensing as a part of a large BRCA1-associated genome surveillance (BASC) complex together with ATM, MRN, Bloom's helicase (BLM) and mismatch proteins (MSH2/6 and MLH2) (26).

ATM and ATR serine/threonine kinases, both belonging to the phosphatidylinositol-3 kinase-related (PIKK) family, are the key signaling factors involved in DNA damage response (DDR) (27, 28). ATM and ATR share sequence similarities and many phosphorylation substrates. ATM gene product is mutated in patients suffering from Ataxia telangiectasia (AT), a rare autosomal recessive disease characterized by immune deficiency, neurodegeneration and cancer predisposition (29). Cells lacking ATM show a slow DNA synthesis and a defective DNA damage response (30).

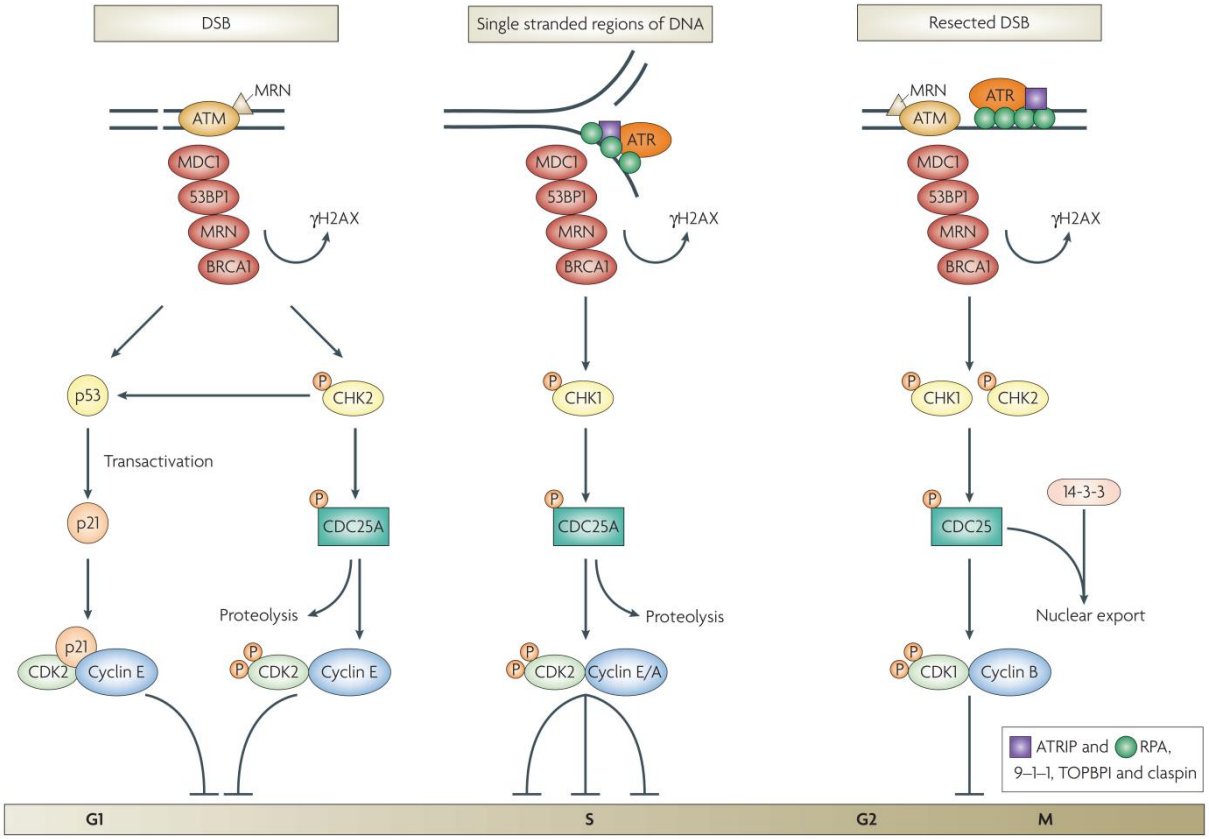

Figure 3: Mammalian DNA damage response pathways leading to cell cycle arrest. ATM and ATR kinases, both members of the PIKK family, are key components of the DNA damage signaling. In response to ionizing radiation ATM is activated by DSBs or changes in chromatin structure, while ATR responds to single-stranded DNA regions generated at DSB ends; therefore ATR is considered to have secondary function with reference to ATM in checkpoint development. Once activated, ATM and ATR phosphorylate many downstream targets that collectively promote cell-cycle arrest. See text for details. *Figure obrained from Löbrich and Jeggo, 2007 (31).*

ATR was shown to be essential for cell survival (32-34) and has been linked with Seckel syndrome which is associated with impaired DNA damage response and genomic instability (35, 36). The prevailing view is that in response to IR, ATM is recruited primarily by DSBs or changes in chromatin structure through MRN complex (37, 38) and is thought to have central role in activating DNA damage checkpoints leading to cell cycle arrest (39). In contrast, ATR is believed to function in perturbed DNA replication, and its activation by DSBs requires ATR-interacting protein (ATRIP), 9-1-1 complex (RAD9-HUS1-RAD1), TOPBP1, Claspin and the generation of ssDNA regions at DSB ends coated with RPA complexes, a process known as DNA end

resection (27, 40-44). Therefore, ATR is considered to have a secondary function with reference to ATM in checkpoint development and regulation (45, 46). Later on, the signal is amplified by mediator proteins like MDC1, 53BP1, MRN and BRCA1 and forwarded to the downstream effector kinases CHK1 and CHK2.

Two ATM-dependent G_1 checkpoints networks have been described. The fast response includes rapid phosphorylation of CHK2 by ATM leading to subsequent phosphorylation of CDC25A phosphatase, which in turn promotes proteolysis of CDC25A and therewith prevents activating dephosphorylation of CDK2 at Thr14 and Tyr15 (31). This fast branch of the G_1 arrest represents the DNA-damage sensing mechanism and may delay DNA synthesis. The second component of G_1/S checkpoint is slower since it utilizes transcriptional activation by the tumor suppressor p53 and protein synthesis of the CDK-inhibitor p21. Since p53 is involved in regulation of apoptosis and genomic integrity (47, 48), this aspect of the G_1/S checkpoint may be important for eliminating cells sustaining DNA-damage by apoptosis.

In S phase, collapsed or stalled replication forks activate ATR leading to phosphorylation of CHK1 and the subsequent degradation of CDC25A phosphatase. In this way the inhibitory phosphates masking the active site of CDK2 cannot be removed and inhibition of CDK2-Cyclin A/E complexes halts the entry into G_2 phase. This checkpoint response in S phase, also known as intra-S phase checkpoint, prevents firing of new replication origins and therewith slows down DNA replication.

DSBs in G_2 phase can directly activate ATM which leads to subsequent activation of CHK2. This in turn promotes phosphorylation of CDC25C at Ser216 to block its function. A parallel pathway in G_2 checkpoint is initiated by indirect activation of ATR via DSB end resection and subsequent phosphorylation of the checkpoint kinase CHK1. Phosphorylation of CDC25C phosphatase by CHK1 prevents removal of inhibitory phosphorylation of CDK1, which is essential for initiating mitosis (31, 49).

In addition, the DNA damage response involves regulation of CDK1-cyclinB complex activity by regulating the mRNA levels of cyclin B and its translocation from the cytoplasm during S and G_2 phases to the nucleus at the beginning of mitosis (50-52). Evidence also suggests the involvement of Never-in-mitosis A related protein

kinase 1 (NEK1) in checkpoint signaling, which was shown to function early in DNA damage checkpoint control independently of ATM and ATR signaling pathways (53, 54).

In summary, the widely held view is that the central players in DNA damage-induced checkpoints are ATM and ATR kinases, which initiate a phosphorylation signaling-cascade to transmit the damage signal. This results in inhibition of CDK-cyclin complexes and ensures cell cycle arrest. This delay in cell cycle progression does not only provide time for repair in the cell cycle phase where lesions are induced. Moreover, the DNA damage checkpoint ensures initial processing of the lesion and its safe transition into a cell cycle phase where repair can proceed optimally (22).

Therefore, the next section reviews DSB repair pathways and their dependence on cell cycle phase and checkpoint response.

1.4. Eukaryotic DSB repair pathways and their dependence on cell cycle phase and checkpoints

Two main repair pathways are capable of processing and rejoining DSBs and thus eliminating their adverse consequences – non-homologous end joining (NHEJ) and homologous recombination repair (HRR).

The classical or canonical NHEJ (c-NHEJ) is a fast process successfully eliminating DSBs within 10-30 minutes that simply rejoins DNA ends without necessarily restoring the original sequence around the break (**Figure 4**). Therefore, it is also considered as error-prone repair pathway. The essential feature of c-NHEJ is DNA-dependent protein kinase (DNA-PK) comprising KU70/80 heterodimer and an evolutionary new catalytic subunit DNA-PKcs (cs indicating *catalytic subunit*). Synapses of two DNA-PK complexes at the two broken ends provides a platform for repair by recruiting XRCC4/XLF/DNA ligase IV complex (55). Other factors that contribute to DSB end processing include, 53BP1, H2AX, Artemis, polynucleotide kinase (PNK), and DNA polymerases λ and μ (56). Nevertheless, evidence suggests that XRCC4 and XLF could act as a complex also in the early step of end joining and independently of Ligase IV where the filamentous structure of XRCC4-XLF may hold the DSB ends together (57-59). Recently, a paralog of XRCC4 and XLF, named

PAXX, was identified as a novel component of NHEJ machinery whose interaction with KU promotes end joining (60, 61).

C-NHEJ is not solely involved in repairing DSBs induced by IR; along with RAG-1 and RAG-2 (recombination-activating genes), the enzymes of NHEJ have been shown to be essential for V(D)J recombination, where DSBs are natural events. This process occurs in lymphocytes and involves the rearrangement of variable (V), diversity (D) and joining (J) segments on 'cut-and-paste' basis. This leads to a diverse repertoire of immunoglobulins and T-cell receptors (62). C-NHEJ is also required for class switch recombination (CSR) in B cells, a process that allows the change of antibody class from immunoglobulin M (IgM) to IgA/E/G (63).

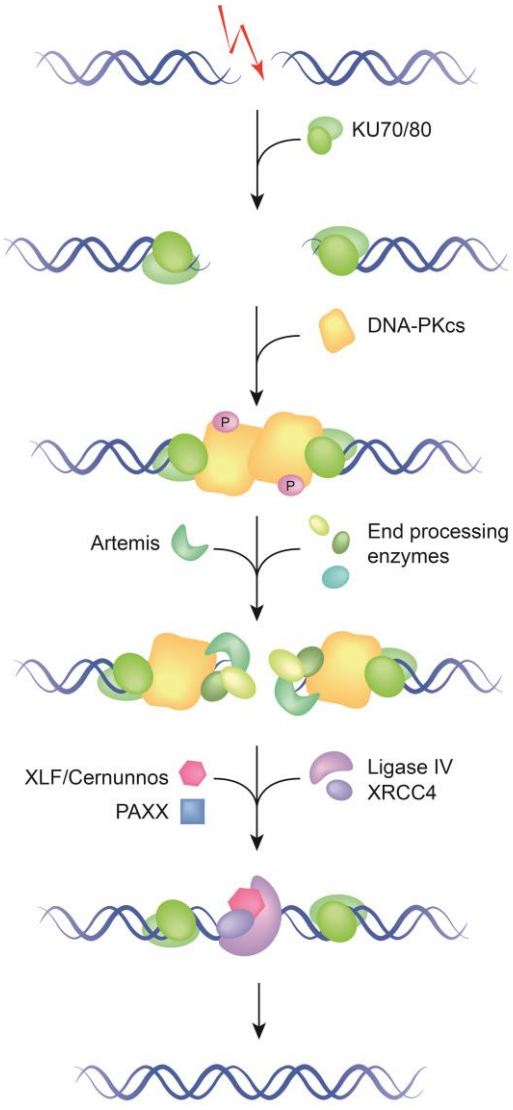

Figure 4: Schematic overview of classical non-homologous end joining (c-NHEJ). Crucial component of c-NHEJ is the enzymatically active DNA-PK complex, composed of a large catalytic subunit, termed DNA-PKcs, and DNA-binding factor KU70/KU80. As a heterodimer, KU70 and KU80 form a basket-shaped structure which enables the complex to slide along dsDNA with KU70 located proximal and KU80 distal to the end. The recruitment of DNA-PKcs guides KU70/80 to move inwards. After being processed, the ends are sealed by Ligase IV/XRCC4/XLF complex. The indicated phosphorylation events represent the post-translational modifications of DNA-PK complex, which result in dissociation of DNA-PKcs from the ends. Removal of KU70/80 is possibly due to ubiquitination (64). *Figure adapted from Dueva and Iliakis, 2013 (65).*

Although c-NHEJ is considered as error-prone repair pathway as it is associated with sequence alterations around the break, due to its high speed c-NHEJ is more efficient in suppressing translocations when compared to other alternative forms of end-joining operating with slower kinetics (described below) (65). Besides its high speed, Simsek and Jasin have further demonstrated that translocation formation is suppressed by the XRCC4/Ligase IV component of c-NHEJ (66). Therefore, c-NHEJ is considered a caretaker of genomic integrity and suppressor of tumor development (67, 68). C-NHEJ operates throughout the cell cycle and was shown to be independent of checkpoint response (69, 70).

In comparison to c-NHEJ, HRR is a slow process but accurate in restoring the original sequence in the vicinity of the break since it requires a homologous template or a sister chromatid (**Figure 5**). As a consequence, HRR is limited to S and G_2 phases of the cell cycle. Critical step in HRR is homology search and strand invasion in the donor DNA, which requires 3' single-stranded DNA (ssDNA) overhangs. The latter are produced by the combined action of DNA exonucleases and helicases which remove terminal nucleotides from the 5' ends, a process known as **DNA end resection** (71, 72). MRN complex promotes initial processing of broken DNA ends (73). Essential role for this short-range resection (50-100 nt) have CtBP-interacting protein (CtIP), and the tumor suppressor protein BRCA1 while the long-range resection (several thousand nt) is continued by Exonuclease 1 (EXO1), DNA2 helicase/nuclease and the Bloom helicase (BLM) (74-79). Hence, the MRN complex has two important roles in DDR – in checkpoint activation by recruiting ATM and in HRR initiation by promoting nucleolytic resection of DSB ends. The resulting long 3' ssDNA overhangs on both sides of the break are rapidly coated by RPA heterotrimer composed of RPA70, RPA32 and RPA14 subunits, where the binding size of one RPA molecule is ~30 nt (80, 81). Thereby, RPA stabilizes the ssDNA by preventing formation of secondary structures and protects it from nucleolytic cleavage. Notably, RPA-covered ssDNA serves as a platform for recruiting ATRIP and initiating ATR-CHK1 checkpoint signaling pathway and the 32-kDa subunit of RPA is a target of ATM, ATR and DNA-PKcs. In the following step, recombination mediators such as RAD52, RAD51 paralogs and the tumor suppressor BRCA2 assist

the displacement of RPA by RAD51 recombinase leading to the formation of RAD51-ssDNA nucleoprotein filament.

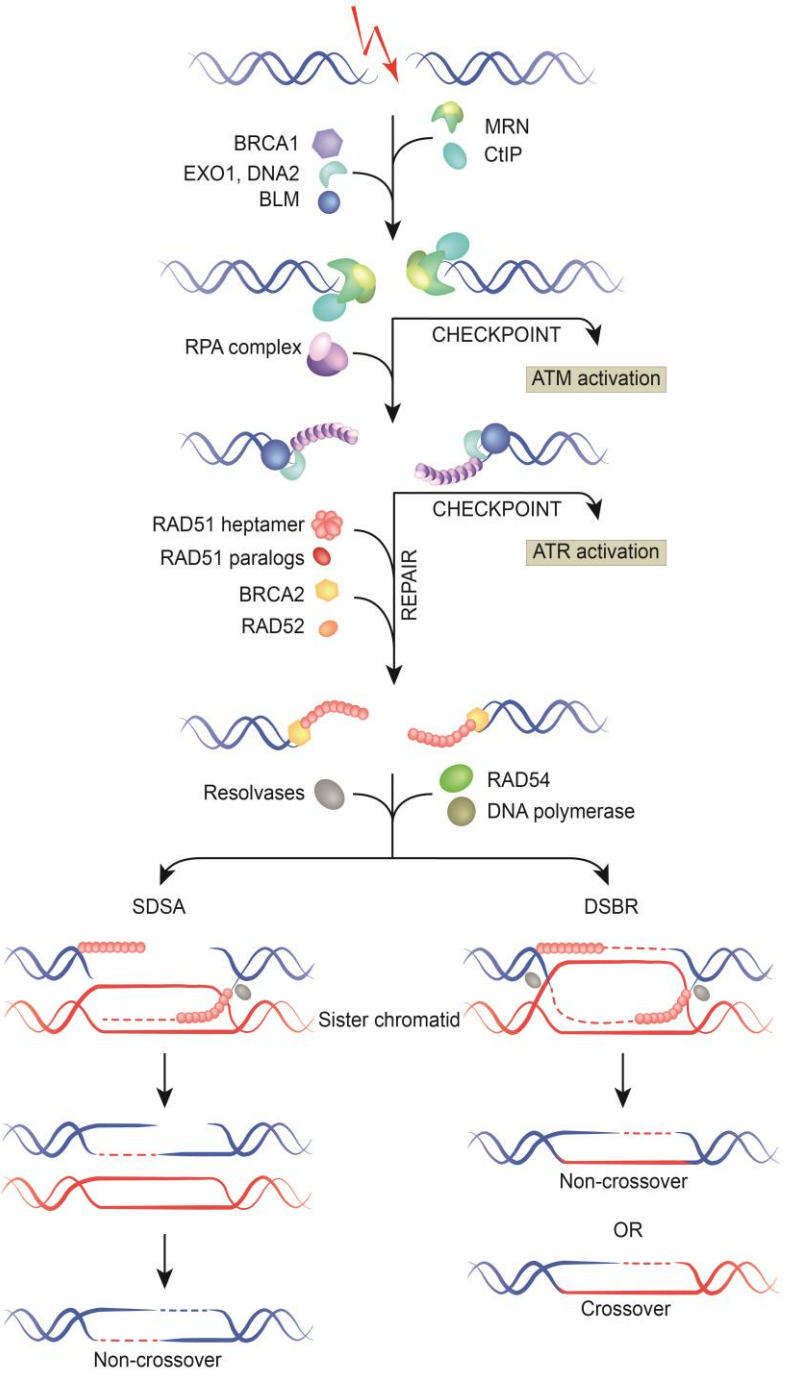

Figure 5: Schematic overview of homologous recombination repair (HRR). HRR relies on the formation of ssDNA-RPA intermediates generated by nucleolytic degradation of terminal nuleotides. Displacement of RPA by RAD51 recombinase ensures strand invasion with the template DNA sequence and homology search. Detailed description in text. *Figure adapted from Dueva and Iliakis, 2013 (65).*

The subsequent homology search and strand invasion into the template DNA sequence result in D-loop formation, where a polymerase starts synthesizing the complementary strand of ssDNA. The 3'-overhangs participate in the formation of Holliday junctions which in the last step of HRR become resolved resulting in restoration of the original sequence around the break with or without crossover (71).

In addition to these standard repair processes, mounting evidence supports the role of a third pathway in cells of higher eukaryotes considered to be an alternative form of end joining (a-EJ) that is independent of KU70/80 and DNA-PKcs (**Figure 6**) (82-85). It operates with slower repair kinetics than c-NHEJ and profits from microhomologies around the DNA ends, especially when the ends are processed by nucleases and end resection is initiated. This alternative form of end joining is considered as a backup non-homologous end joining (B-NHEJ) pathway, which becomes engaged at the DSB when either c-NHEJ or HRR fail to process the ends (65, 86). Throughout this thesis, the term a-EJ will be used to refer to this repair pathway.

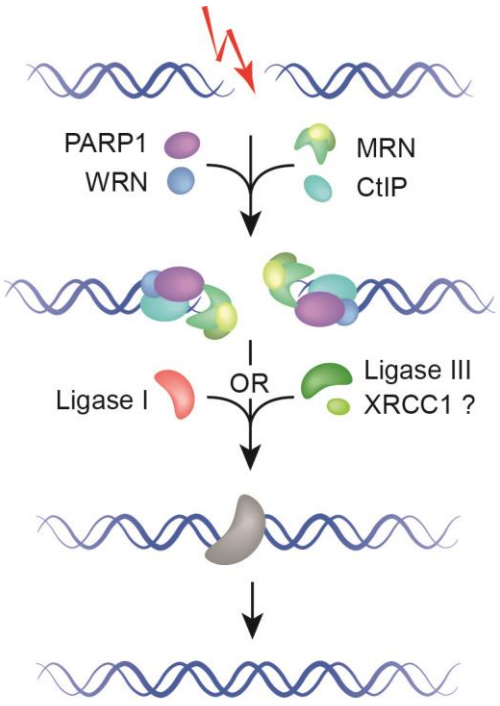

Figure 6: Alternative pathways of end joining (a-EJ) are considered highly inaccurate of restoring the original DNA sequence. See text for details. *Figure adapted from Dueva and Iliakis, 2013 (65).*

A-EJ has been characterized to be more error-prone than c-NHEJ with higher probability of deletions, sequence alterations around the break as well as with higher risk of translocation formation. Therefore, a-EJ is considered an ultimate source of genomic instability. Proteins implicated in a-EJ are Histone H1, PARP1, MRN, CtIP, as well as DNA ligase III or DNA ligase I that are involved in the rejoining step (87-90). A-EJ has been shown to operate in all cell cycle phases but is functionally enhanced in S and G_2 (91-93). Interestingly, data from our laboratory have shown that a-EJ is compromised in non-cycling (plateau phase) cells (94).

In conclusion, the error-prone NHEJ is predominantly used to preserve DNA integrity in higher eukaryotes throughout the cell cycle. In G_2 phase, however, HR additionally ensures DSBs repair in an error-free manner. The process of end resection is a crucial step during HR and once initiated, NHEJ factors cannot bind the ends and the DSB is committed to be repaired by HR. Therefore, the next chapter will focus on the factors coordinating initial processing of DNA ends.

1.5. Regulation of damage-induced DNA-end resection

Extensive processing of DNA ends by exonucleases leads to the formation of ssDNA-RPA intermediates that initiate ATR-dependent checkpoint signaling and engage homologous recombination to seal the break in S and G_2 phase. As the resected DNA ends could not be repaired by c-NHEJ and possibly the extended DNA end resection suppress a-EJ (95), it is intuitive to speculate that DNA end resection could be a critical step in repair pathway choice (96, 97). Moreover, the regulation of DNA end resection initiation is another important parameter of the repair pathway selection, which is controlled by a number of proteins (**Figure 7**) and requires extensive modifications of chromatin structure (98).

KU70/80 heterodimer, the DNA-binding component of DNA-PK complex, has extremely high affinity for dsDNA and is believed to be the first protein that binds directly the DSB ends. The subsequent recruitment of DNA-PKcs primes the DSB ends for direct ligation by classical NHEJ (85).

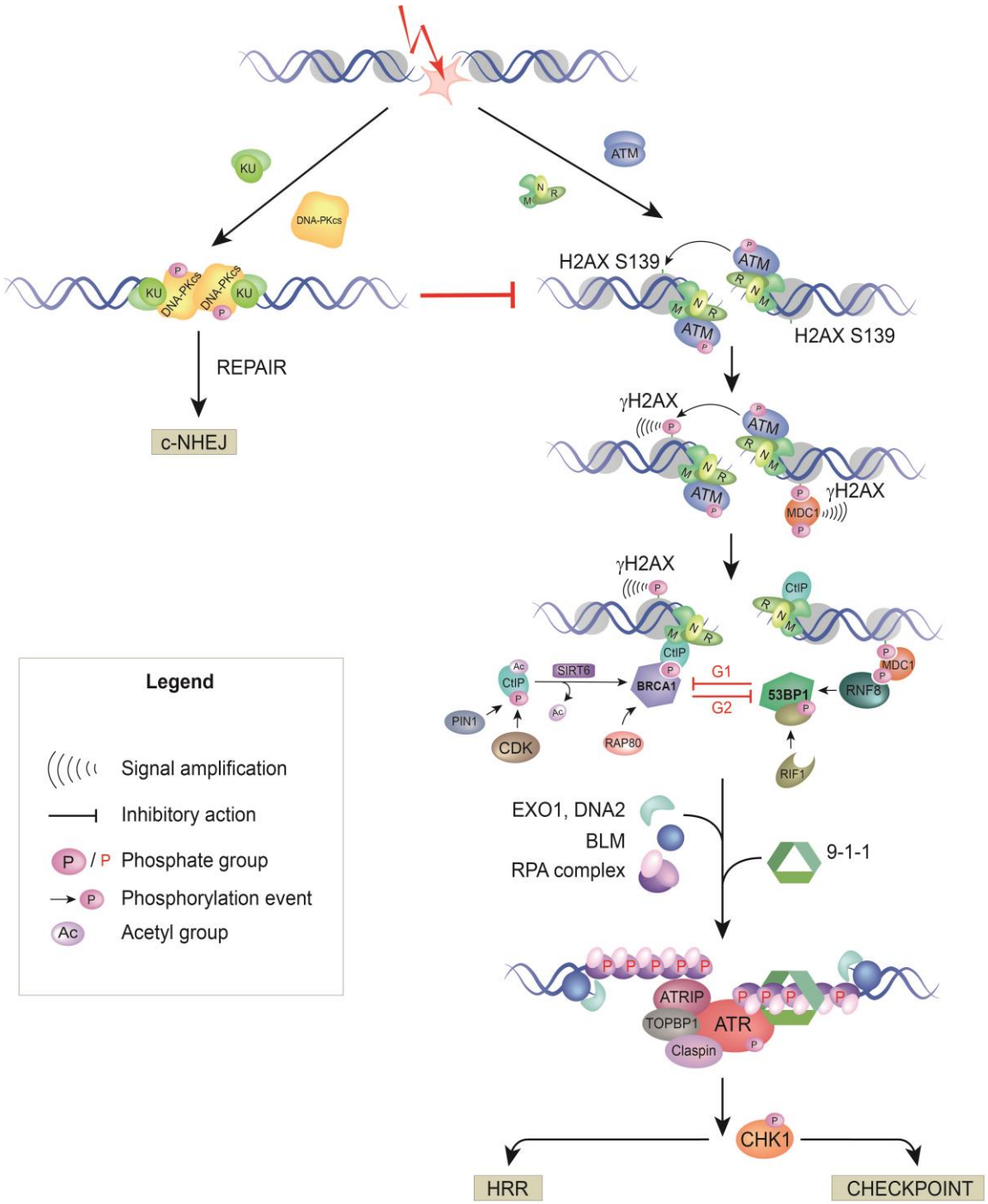

Figure 7: Regulation of DSB end resection and its impact on DNA damage response. Resection, the formation of ssDNA, at DNA ends occurs as an intermediate structure during DNA repair and replication. ATM stimulates the nucleolytic processing of DSBs, where MRN complex has a crucial function of recruiting and activating ATM. In response to DNA damage, histone variant H2AX becomes phosphorylated at Ser139 (termed γH2AX) by ATM. γH2AX, MDC1 and ATM form a positive feedback loop, where MDC1 binds γH2AX and further expands the DNA damage signals. 53BP1 has a protective role on DSB ends from resection and therefore promotes repair by c-NHEJ in G_1 phase. BRCA1 triggers HRR and suppresses 53BP1-dependent c-NHEJ in G_2 phase. The ssDNA regions, covered by RPA, serve as a substrate for checkpoint activation via ATR-Chk1 pathway. The hierarchical recruitment of resection factors is represented as precisely as possible. See text for details.

In comparison with KU70/80, MRN complex also has high affinity for DSB ends, and although KU70/80 seems to be the main opposing factor against mobilization of MRN to damaged chromatin (99), unpublished data from our laboratory suggest that KU and MRN possibly interact to fine-tune and control the fate of DSB.

In undamaged cells ATM exists as an inactive dimer which is rapidly activated upon DNA damage-induction by auto-phosphorylation at Ser1981. This modification induces dissociation of the inactive ATM dimer into active ATM monomers (100). MRN complex has an essential function in stimulation of ATM kinase activity by enhancing the stable binding between ATM and its substrates (101, 102). MRN consists of MRE11 (nuclease component), RAD50 (ATPase activity) and the Nijmegen breakage syndrome factor NBS1/Nibrin (Xrs2 in yeast). NBS1 has yet unknown enzymatic activity but is responsible for the nuclear localization of RAD50 and MRE11 (103). The retention of MRN to damaged chromatin is mediated through phospho-dependent interaction between NBS1 and Mediator of DNA damage checkpoint 1 (MDC1) (104).

In response to DNA damage, a phosphorylation of the histone variant H2AX at Serine 139 results in the formation of γH2AX, which has a significant role in the recruitment of DNA-damage-response proteins NBS1, 53BP1 and BRCA1 (105-107). Although *H2AX* gene is not essential for cell survival, H2AX deficiency is associated with increased radiosensitivity and pronounced repair defects (106). H2AX is primarily phosphorylated by ATM (108), where phosphorylated H2AX initiates recruitment of MDC1 and MRN complex to further amplify and propagate the DNA damage signal by recruitment of more ATM molecules, thus creating a positive feedback loop (107, 109-111). Phosphorylated MDC1 also promotes accumulation of the E3 ubiquitin ligase RNF8 to the DSB, which in turn ubiquitylates histone H2A and enables the recruitment of 53BP1 and BRCA1 (112).

RAD17 is a replication checkpoint clamp-loader that promotes ATR activation. Recently, Wang and colleagues have shown that RAD17 stimulates also ATM activation and DNA end resection by recruiting MRN complex to DSBs. RAD17 depletion is associated with impaired phosphorylation of ATM as well as of its substrates CHK2, NBS1, and γH2AX (25).

Sartori *et al.* first reported about the role of human CtIP in end resection, where it functionally interacts with MRN to promote HR (74). CtIP exhibits endonuclease activity with specificity for 5' flaps which is essential for cell survival in response to IR and topoisomerase poisons (113). Work by Sartori and colleagues demonstrated that the peptidyl-prolyl *cis/trans* isomerase 1 (PIN1) is involved in the regulation of DSB resection where PIN1 controls the stability of CtIP and its degradation (114). Recently, tetramerization of CtIP was shown to be required for proper DNA-end resection during homologous recombination (115). Another intriguing study by Jackson and colleagues provided evidence that the protein lysine deacetylase SIRT6 promotes end resection by deacetylation of CtIP. RNAi-mediated depletion of SIRT6 effectively reduces RPA foci number after camptothecin (CPT) treatment without affecting γH2AX foci formation (116).

CtIP was shown to associate with BRCA1 in late S and G_2 phases of the cell cycle, where CtIP-BRCA1 interaction depends on CDK-mediated phosphorylation of CtIP at Ser327 (79, 117). As an E3 ubiquitin ligase, BRCA1 also promotes ubiquitination of CtIP at multiple lysine residues without leading to its degradation, but by enhancing CtIP binding to chromatin after DNA damage-induction (118). A high-resolution assay to measure the extent of resection in eukaryotes, established by Huertas and colleagues, revealed that BRCA1 modulates the speed of CtIP-mediated resection, although the BRCA1-CtIP interaction is not essential for this process. Thus, under normal conditions BRCA1 increases the rate of end resection while abrogation of CtIP-BRCA1 interaction by CtIP-Ser327 mutation leads to shorter resected tracks (119).

MDC1 was identified to control the formation of damage-induced 53BP1, BRCA1 and NBS1 foci formation. 53BP1 and MDC1 are placed upstream of ATM, where both proteins activate ATM through independent pathways (120-122). A breakthrough study by Nussenzweig and colleagues demonstrated that 53BP1 inhibits resection in BRCA1-deficient cells. Thus, in S phase BRCA1 downregulates NHEJ and allows end resection by promoting removal of 53BP1. The authors proposed that 53BP1 and BRCA1 directly regulate repair pathway choice (123). In the same way, absence of 53BP1 is associated with ATM-dependent increase of end resection that favors the involvement of a-EJ pathways during class switch recombination (124). The

suppressive function of 53BP1 on end resection in G_1 is assisted by RIF1, where RIF1 recruitment relies on ATM-dependent 53BP1 phosphorylation (125-128). The ubiquitin-binding protein RAP80 was reported to recruit BRCA1 to DNA damage sites, implicating the involvement of ubiquitin-dependent signaling pathway in DDR (129-131). In a model proposed by Jeggo and colleagues, 53BP1, RAP80 and ubiquitin chains serve as a barrier for the process of resection and therefore promote NHEJ. However, in G_2 phase, BRCA1 is assisted by the de-ubiquitylating enzyme POH1 to fully remove 53BP1 from the break. The data suggest that BRCA1 alone is not sufficient for full clearance of 53BP1 (132). Once nucleolytic cleavage by MRN-CtIP-BRCA1 complex is initiated and RPA binds ssDNA, EXO1, DNA2 and the BLM helicase are recruited to facilitate extensive resection. Simultaneously, the 32-kDa subunit of RPA undergoes extensive phosphorylation by ATM, ATR and DNA-PK. RPA-ssDNA structures promote HRR and serve as a platform for ATR-mediated checkpoint signaling by recruiting the ATR activator ATRIP, the adapter proteins TOPBP1 and Claspin, and the checkpoint clamp 9-1-1 (133, 134). Therefore, ATR activation is considered to be mediated through ATM-dependent resection and contributes to checkpoint maintenance.

In summary, initiation of end resection is decisive for the repair pathway that will rejoin the DSB and influences the DNA damage response.

It appears that the catalytic subunit of DNA-PK does not fit into checkpoint control and regulation of DNA end resection owing to its key role in c-NHEJ. However, accumulating data generate evidence about a dual role of DNA-PKcs on c-NHEJ and HR (135-138) but the exact mechanism by which DNA-PKcs regulates HR is still unclear. Since this is not the only exception regarding non-canonical roles of DNA-PKcs, besides its necessity in c-NHEJ, the following section will review the role of this kinase in the DNA damage response and beyond.

1.6. The role of DNA-PK holoenzyme in DSB repair and beyond

1.6.1. The DNA-PK complex in DSB repair and its regulation

The first indication about a DNA-activated protein kinase in human cells was reported in 1985 by Anderson and colleagues, where they present evidence about dsDNA-dependent phosphorylation of multiple proteins in eukaryotic cells including the heat shock protein HSP90 (139). Now we know that DNA-dependent protein kinase (DNA-PK) is composed of a large catalytic subunit (DNA-PKcs, ~460 kDa, gene name *PRKDC*), and a dsDNA-binding component KU70/80 heterodimer (140). Originally, DNA-PKcs was termed *p350* (indicating a ~350 kDa ATP-binding polypeptide) (141). Due to its size, the crystal structure of DNA-PKcs at 6.6 Å resolution was resolved 25 years later, in 2010 (142). Despite the low resolution, the position of all known domains in a 3D model is now resolved (**Figure 8**). KU70/80 is a highly abundant protein complex initially identified as an autoimmune antigen. KU70/80 binds with high affinity dsDNA in a sequence independent manner and loads DNA-PKcs onto DNA (140, 143). The resulting association of KU70/80 with DNA-PKcs leads to the assembly of an enzymatically active complex with preference to phosphorylate SQ/TQ sequences (64, 143).

DNA-PKcs alone has a weak kinase activity in the presence of dsDNA, but the presence of KU70/80 increases its kinase activity 5-10 fold and also stabilizes the formation of the DNA-PKcs-KU-DNA complex (64). *In vitro* experiments with highly purified DNA-PKcs and KU70/80 revealed that under low salt conditions DNA-PKcs is able to bind dsDNA ends in the absence of KU70/80, while under higher salt conditions activation of DNA-PKcs is dependent on KU70/80 (144). Once activated, DNA-PK phosphorylates itself as well as other factors involved in NHEJ apparatus such as both KU subunits and XRCC4 (143).

DNA-PKcs belongs to the PIKK family together with ATM, ATR, mammalian target of rapamycin (mTOR), suppressor of morphogenesis in genitalia (SMG1) and transformation/transcription domain-associated protein (TRRAP) (145). Despite the sequence similarities to the PI3K family of kinases, PIKK family members are not lipid kinases and are referred as atypical protein kinases (146, 147).

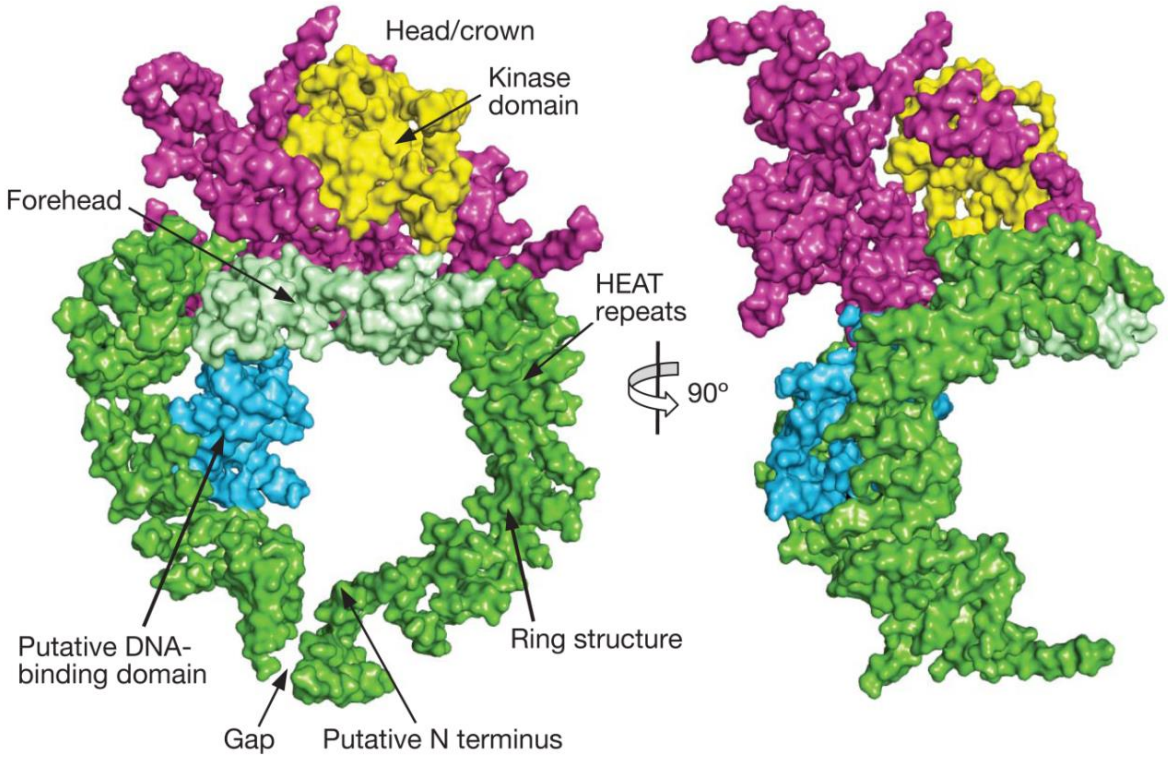

Figure 8: The structure of DNA-PK catalytic subunit: front (left) and side (right) view of the molecule. The many α-helical HEAT repeats (helix-turn-helix motifs), indicated with green, contribute to the formation of a ring structure. The head/crown region contains the C-terminal region that carries the FAT and FATC domains (magenta) and the kinase domain (yellow). Through the putative DNA-binding domain (cyan) DNA-PKcs may bind directly to DNA and become active independently of KU subunits. *Figure obtained from Sibanda et al. 2010, Nature (142).*

Unlike ATM and ATR, a clear DNA-PKcs homolog has not been identified in the genome of lower eukaryotes such as *Saccharomyces cerevisiae*. Interestingly, both KU70 and KU80 were shown to be present in distantly related organisms (from yeast to human) (148). However, rodents have much lower levels of both DNA-PKcs and KU than primate cells. The correlation between DNA-PK levels and species' life-span suggests that the evolutionary breakthrough of DNA-PKcs is a mechanism to enhance genomic stability (143).

Being involved in V(D)J recombination, loss of DNA-PKcs function leads to defective DSB repair and V(D)J recombination, and, thus, to hypersensitivity to IR and nonfunctional immune system. (149-153). This phenotype, defined as severe

combined immunodeficiency (SCID), has also been described in KU80-deficient mice (154, 155).

As already outlined above, free dsDNA ends and the DNA-binding factor KU70/80 represent the primary activators of DNA-PKcs. Another important mechanism of DNA-PK regulation is through posttranslational modifications. It has been reported that **extensive auto-phosphorylation of DNA-PKcs** results in inhibition of its kinase activity and release of DNA-PKcs from the breaks (156). Two major auto-phosphorylation site clusters, ABCDE and PQR, have been analyzed, while the phosphorylation sites L and M as well as N and JK clusters still remain undefined (**Figure 9**) (56, 138, 157). There are reports consistent with the model of activating DNA-PKcs by intra-molecular (*cis*) auto-phosphorylation, as well as in *trans* by the synapsed opposing complex (158-161). As a highly dynamic molecule, a conformational change at its N-terminus may also regulate its kinase activity independently of DNA or KU70/80 (162). Additionally, dissociation of DNA-PKcs from the complex with DNA is also stimulated through phosphorylation of DNA-PKcs by c-Abl tyrosine kinase. The binding of c-Abl to the KU association site at the carboxy-terminal domain of DNA-PKcs reveals antagonistic functions of KU and c-Abl toward DNA-PK activity (163, 164).

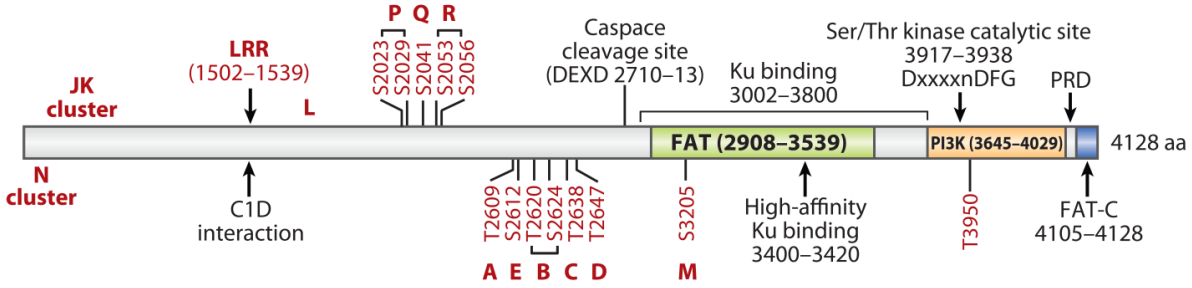

Figure 9: Domains within DNA-PK catalytic subunit. Auto-phosphorylation sites are shown in red. LRR indicates the leucin-rich region. FAT domain is called after the three kinases sharing the domain FRAP/mTOR, ATM and TRRAP. PI3K and PRD designate PI3 kinase domain and PI3K regulatory domain, respectively. FAT-C specifies the FAT domain at the extreme C-terminus. *Figure obtained from Lieber, 2010 (56).*

DNA-PKcs is also an *in vivo* substrate of other PIKK kinases like ATM and ATR as reported by several studies (135, 165, 166). Another post-translational event that

stimulates DNA-PKcs activity *in vitro* is the association of Poly-adenosine diphosphate (ADP)-ribose by PARP-1, which seems to be independent of KU70/80 (167).

In addition to the post-translational modifications, it has been reported that DNA-PK activity can also be regulated through protein-protein interactions. An example in this regard is the human KU80 Autoantigen Related Protein-1 (KARP-1) gene product, which is expressed from the KU80 locus through an upstream promoter and additional exons. This 9-kDa extended derivative of KU80 was reported to modulate DNA-PK activity (168, 169).

1.6.2. DNA-PKcs in the DNA damage checkpoint

DNA-PKcs is considered as a crucial component of c-NHEJ pathway, which is independent of checkpoint activation. Therefore, the role of DNA-PKcs in checkpoint signaling has been discounted. Nevertheless, DNA-PKcs has been shown to phosphorylate proteins involved in checkpoint signaling pathways.

A model was proposed, where DNA-PK together with ATM and ATR modulate p53 activity via phosphorylation of its N-terminus, which results in disruption of MDM2/p53 interaction and subsequent stabilization of p53 (143). This links DNA-PK to the regulation of G_1 checkpoint.

As briefly mentioned above, the 32-kDa subunit of the ssDNA-binding RPA is a target of ATM, ATR and DNA-PK, where Ser4 and Ser8 residues have been described to be DNA-PK-specific (170, 171). RPA-coated ssDNA intermediates during HRR activate ATR and therewith the G_2 checkpoint. In a proposed mechanism by Serrano *et al.* phosphorylation of RPA32 by DNA-PKcs and p53 by ATM and ATR leads to dissociation of p53-RPA complex and promotion of HR (172).

Since DNA-PKcs phosphorylates several substrates involved in checkpoint activation, an early study from 1997 proposed that the IR-induced cell cycle arrest in human cells lacking DNA-PK activity is abrogated. On the contrary, the DNA-PKcs-deficient cell line M059J not only did show proper G_2/M cell cycle arrest but also twenty-four hours after irradiation the fraction of G_2/M cells was significantly higher when compared to the DNA-PK-proficient cell line M059K (173). It has been

concluded that DNA-PKcs is not required for the activation of G_2 checkpoint and although DNA-PKcs phosphorylates DNA damage sensing molecules, other kinases may compensate for its absence (173).

Similar to G_2-checkpoint activation, our laboratory showed that DNA-PKcs is required for the recovery of IR-induced S-phase checkpoint as measured by total DNA synthesis. This effect seems to be DNA-PKcs specific and independent of c-NHEJ abrogation since other c-NHEJ components examined, Ligase IV, XRCC4 and KU80, failed to establish the phenotype observed in DNA-PKcs deficient cells (174). Similarly, Oakley and colleagues reported that DNA-PKcs defect is associated with impaired replication checkpoint and that DNA-PKcs contributes to CHK1 activation in response to hydroxyurea, CPT or etoposide treatment (175). The phosphorylation of RPA32 at Ser4/Ser8 by DNA-PKcs seems to be of great importance for the regulation of replication stress checkpoint activation (171).

Interestingly, a study by Tomimatsu *et al.* implicated DNA-PKcs in activating DNA damage response in ATM-deficient cells by phosphorylating DDR proteins involved in chromatin remodeling like KRAB-associated protein 1 (KAP-1) (176).

Hence, DNA-PK catalytic subunit appears to be important contributor to the recovery of IR-induced S- and G_2-checkpoints and its exact role in DNA damage signaling remains to be defined.

1.6.3. Other functions of DNA-PK in the cell

The kinase activity of DNA-PK has been extensively studied by virtue of its requirement for NHEJ and V(D)J recombination in mammalian cells (150, 177, 178). Nevertheless, accumulating data reveal damage-independent functions of DNA-PK, such as transcriptional modulation, viral infection, telomere protection and mitosis.

DNA-PKcs was originally found as a kinase that phosphorylates transcription factor Sp1 upon binding to GC-rich promoter sequences (179). Another study reported a regulatory role of DNA-PK on RNA polymerase II, which catalyzes DNA transcription (180). DNA-PKcs/KU70/KU80 complex, together with Topoisomerase IIβ, is also recruited to active transcription units (181). A more recent study implicates DNA-PKcs as a transcription modulator in prostate cancer progression (182). Other

data also implies a role for DNA-PKcs in mitosis which might be independently of KU and DNA damage (183-185).

DNA-PKcs was reported previously to suppress infection of cells with Herpes simplex virus by inhibiting viral replication (186, 187). Recently, DNA-PK activity has been implicated in HIV-1-induced CD4 lymphocyte death, which leads to immunodeficiency (188).

DNA-PKcs is also required for maintenance of the chromosome ends (telomeres) (189-191). If left unprotected, telomeres can be recognized as DSBs and their ‘repair’ may result in chromosome fusions that may lead to genomic instability.

All these findings define DNA-PKcs as a multifunctional kinase regulating many aspects of cellular physiology. This thesis focuses on the less-defined role of DNA-PKcs in DNA damage signaling, particularly G_2 checkpoint activation after ionizing radiation.

2. AIMS OF THE THESIS

DNA-PKcs is an evolutionally new DNA repair enzyme functioning as an alignment protein for broken DNA ends. DNA-PKcs is an abundant protein, as it represents up to 1% of total soluble protein from HeLa nuclei (192). The presence of DNA-PKcs in eukaryotic genomes shifts the predominant repair pathway for DSBs from HRR in yeast to NHEJ in primates, *i.e.* with increasing genome size genome integrity becomes more crucial than error-free repair. Since DNA-PKcs requires the KU70/80 heterodimer to be recruited to the break, one may ask why the cell has developed such a big protein (460 kDa) with auto-phosphorylation capacity, which is not capable to recognize a DNA break. The many phosphorylation sites of DNA-PKcs may lead to a series of conformational changes of the molecule and therewith to multiple functions in the cell beyond DSB repair.

As a central component of c-NHEJ, the contribution of DNA-PKcs to DNA double-strand repair is well characterized. DNA-PKcs' role in signaling and checkpoint response has been discounted and therefore requires in depth studies. Recent experiments from our laboratory provide evidence for a role of DNA-PKcs in checkpoint response, particularly for cells irradiated during S and G_2 phase of the cell cycle. The aim of this study is to contribute to this effort by investigating how DNA-PKcs contributes to checkpoint activation and development. Additionally, the role of the master signaling kinases ATM and ATR and a possible cross-talk between ATM/ATR and DNA-PKcs has been scrutinized.

To study the contribution of DNA-PKcs in checkpoint response the M059J cell line is commonly used, which fails to express the catalytic subunit of DNA-PK and is radiosensitive (193). Its paired and control counterpart cell line, which was isolated from the same tumor specimen, M059K, is relatively radioresistant, contains a functional catalytic subunit and expresses normal levels of DNA-PK activity (194).

Asynchronously growing cells exposed to IR activate DNA damage checkpoints, which result in cell cycle delay. The resulting abnormal cell cycle distribution is easily analyzed by measuring the DNA content of individual cells by fluorescence-activated cell sorting (FACS). Increase of the G_2 fraction of cells reflects activation of the G_2 checkpoint and cell cycle arrest in G_2 phase. The associated delayed mitosis can be

studied more precisely by the combined staining of DNA and mitotic marker proteins such as phosphorylated histone H3 at Ser10 that allows estimation of the mitotic index (MI). Furthermore, we sought to expand previously published G_2 arrest analyses (173) by using different doses of IR and multiple time-point intervals after irradiation.

In regard to the requirement of end resection for activating DNA damage checkpoint in G_2 phase, accumulation of RPA in the vicinity of the break was visualized as discrete foci by immunofluorescence (IF) and served as a marker for ongoing resection. With reference to G_2 checkpoint, the kinetics of RPA foci formation is studied in G_2 phase cells selected by appropriate staining. In an effort to unveil the contribution of each component of DNA-PK holoenzyme to the end resection process, we applied RNA interference (RNAi) to reduce the gene expression of KU70/80, combined with a specific inhibitor of DNA-PKcs.

The outcome of these experiments should clarify the role of DNA-PKcs on DNA damage response.

3. MATERIALS AND METHODS

3.1. Materials

3.1.1. Major laboratory apparatuses

Laboratory apparatus	Model	Provider
Cell and Particle Counter	Z2 Coulter Counter®	Beckman Coulter Inc., USA
Cell culture CO_2 incubators	MCO-18AC(UV)	Sanyo, Japan
Centrifuge	Multifuge™ 3S-R	Heraeus, Germany
Centrifuge (tabletop)	Biofuge Fresco™	Heraeus, Germany
Confocal laser scanning microscope	TCS SP5	Leica Microsystems, Germany
Electroporation device	Nucleofector™ I	Lonza Cologne GmbH, Germany
Flow cytometer	Gallios™	Beckman Coulter Inc., USA
Laminar flow cabinet	HERAsafe™	Heraeus, Germany
Imaging scanner	Typhoon 9400	GE Healthcare, USA
Infrared imaging system	Odyssey®	LI-COR Biosciences, Germany
Inverted phase contrast microscope	Motic AE31	Motic, China
NanoDrop™ spectrophotometer	ND-1000	Thermo Scientific, Germany
pH meter	InoLab®	WTW GmbH, Germany
SDS-PAGE equipment		Bio-Rad, USA
UV/VIS Spectrophotometer	UV-2401PC	Shimadzu, Japan
Wet transfer system		Bio-Rad, USA
X-ray machine, Isovolt 320 HS		General Electric, Pantak/Seifert

3.1.2. Cell lines

Name	Characteristics	Cell type	Growth media
Human cell lines			
82-6 hTERT	wt	fibroblast	MEM + 1% NEAA
M059K	repair-proficient	malignant glioblastoma	DMEM
M059J	DNA-PKcs deficient	malignant glioblastoma	DMEM
Mouse cell lines			
Exo1 wt	Exo1 proficient	mouse fibroblasts	DMEM
Exo1-/-	Exo1 knock-out	mouse fibroblasts	DMEM

3.1.3. Plasmids

Name	Characteristics	Provider
GFP expression vector	pEGFP-N1 vector	Clontech

3.1.4. Antibodies for immunofluorescence microscopy

Name	Specificity	Host / Type	Dilution	Provider
Primary antibodies				
Cyclin B1 (H433)	Human	Rabbit polyclonal	1/150	Santa Cruz
RPA70	Human, mouse	Mouse monoclonal	1/300	Kenny *et al.*, 1990 (195)
Secondary antibodies				
AlexaFluor®488	Mouse IgG	Goat polyclonal	1/400	Invitrogen
AlexaFluor®568	Rabbit IgG	Goat polyclonal	1/400	Invitrogen

3.1.5. Antibodies for western blot

Name	Specificity	Host / Type	Dilution	Provider
Primary antibodies				
KU70 (529)	Human	Mouse monoclonal	1/4.000	GeneTex
KU86 (H-300)	Human, mouse, rat	Rabbit polyclonal	1/5.000	Santa Cruz
CtIP (D76F7)	Human	Rabbit monoclonal	1/1.000	Cell Signaling
MRE11	Human, mouse, rat	Rabbit polyclonal	1/5.000	Novus Biologicals
NBS1	Human, mouse	Rabbit polyclonal	1/1.000	Novus Biologicals
GAPDH	Human, mouse, rat	Mouse monoclonal	1/10.000	Merck Millipore
α-Tubulin (AA13)	Human, mouse, rat	Mouse monoclonal	1/10.000	Sigma-Aldrich
Secondary antibodies				
IRDye® 680LT	Mouse IgG	Goat polyclonal	1/10.000	LI-COR Biosc.
IRDye® 680LT	Rabbit IgG	Goat polyclonal	1/10.000	LI-COR Biosc.
IRDye® 800CW	Mouse IgG	Goat polyclonal	1/10.000	LI-COR Biosc.
IRDye® 800CW	Rabbit IgG	Goat polyclonal	1/10.000	LI-COR Biosc.

3.1.6. Antibodies for flow cytometry

Name	Specificity	Host / Type	Dilution	Provider
Primary antibody				
Histone H3 (pS10)	Human, mouse	Rabbit polyclonal	1/5000	Abcam
Secondary antibody				
AlexaFluor®488	Rabbit IgG	Goat polyclonal	1/400	Invitrogen

3.1.7. Software

Software	Provider	Application
Adobe® Creative Suite® 6	Adobe Systems Inc., USA	Graphic design
EndNote® X7	Thomson Reuters, USA	Reference management
ImarisXT® 7.0	Bitplane Scientific Solutions, Switzerland	Immunofluorescence image analysis
Kaluza® 1.2 for Gallios	Beckman Coulter Inc., USA	Flow cytometry analysis
Leica Application Suite Advanced Fluorescence (LAS AF)	Leica Microsystems, Germany	Confocal microscopy image acquisition
Microsoft Office® 2010	Microsoft, USA	Word processing (Word), Data analysis and calculation (Excel)
WinCycle AV	Phoenix Flow Systems, USA	Cell cycle analysis
SigmaPlot® 11.0	Systat Software Inc., USA	Graphical presentation of data

3.1.8. Chemicals

Name	*Provider*
Aluminium sulfate, $Al_2(SO_4)_3$	Roth
Ammonium persulfate (APS)	Roth
Beta (β)-mercaptoethanol	Merck
Bromphenol blue	Sigma-Aldrich
Bovine serum albumin (BSA) fraction V	Roth
Calcium nitrate, $Ca(NO_3)_2$	Roth
CHK2i	Calbiochem
Coomassie brilliant blue G-250	Serva
4-(2-hydroxyethyl)-1-piperazineethanesulfonic acid (HEPES)	Roth
4’,6-diamidino-2-phenylindole (DAPI)	Serva
Dimethyl sulfoxide (DMSO)	Sigma-Aldrich
Disodium hydrogen phosphate, Na_2HPO_4	Roth
Ethanol absolute	Sigma-Aldrich
Ethylenediaminetetraacetic acid (EDTA)	Roth
Gelatin from cold water fish skin	Sigma-Aldrich
Glucose	Roth
Glycerol	Roth
Glycine	Roth
Hydrochloric acid, HCl	Roth
KU55933	Calbiochem
L-lactic acid	AppliChem
Magnesium chloride, $MgCl_2$	Sigma-Aldrich
Methanol absolute	Sigma-Aldrich
Mirin	Santa Cruz Biotechnology
Monosodium phosphate, NaH_2PO_4	Roth
Non-fat dry milk	Roth
NU7441	Tocris Bioscience
Paraformaldehyde (PFA)	Roth
Phosphoric acid, H_3PO_4	Roth
Potassium chloride, KCl	Roth

Potassium dihydrogen phosphate, KH_2PO_4	Roth
Potassium hydroxide, KOH	Roth
PromoFluor Antifade Reagent	PromoKine
Propidium iodide (PI)	Sigma-Aldrich
Protease inhibitor cocktail	Thermo Scientific
RIPA buffer	Thermo Scientific
RNasa A	Sigma-Aldrich
Rotiphorese® Gel 30 (37,5:1), 30% acrylamide/bis-acrylamide solution	Roth
Sodium chloride, NaCl	Roth
Sodium hydroxide, NaOH	Roth
Sodium dodecyl sulfate (SDS)	Roth
Sorbitol	Fluka
Tetramethylethylanediamine (TEMED)	Fluka
Tris(hydroxymethyl)aminomethane (Tris)	Roth
Triton X-100	Roth
Tween®-20 (polysorbate 20)	Roth
UCN01	Calbiochem
VE821	Haoyuan Chemexpress

3.1.9. Cell culture consumables

Name	*Provider*
Dulbecco's Modified Eagle Medium (DMEM)	Sigma-Aldrich
Fetal bovine serum (FBS)	Gibco Life Sciences
McCoy's 5A (Modified) Medium	Sigma-Aldrich
Minimum essential medium (MEM)	Sigma-Aldrich
Non-essential amino acids (NEAA)	Merck Millipore / Biochrom
Penicillin	Sigma-Aldrich
Phosphate-buffered saline (PBS)	Roth
Streptomycin	Sigma-Aldrich
Trypsin	Biochrom

3.2. Methods

3.2.1. Cell cultivation

Cell lines were maintained at 37 °C in a humidified incubator with 5 % CO_2. Cells were cultured as monolayers in 100 mm cell culture dishes with 15 ml of growth medium supplemented with 10 % fetal bovine serum (FBS), 100 µg/ml penicillin and 100 µg/ml streptomycin. The growth medium used for 82-6 hTERT was supplemented additionally with 1% non-essential amino acids (NEAA). Exponentially growing human cells were plated into 100 mm dishes at concentrations of 0.5-1.2x10^6 cells per dish and passaged every two days. Faster growing cells of other species were seeded in lower numbers.

For passaging or harvesting the cells, growth media was removed, the cell monolayer was washed once with 1x phosphate buffered saline (PBS) and subsequently with 2 ml of 0,05 % Trypsin-EDTA. To let the cells detach from the surface, the culture dishes were incubated for 3 min at 37°C. Trypsin was then inactivated by adding fresh growth media and cells were resuspended to avoid cell aggregation. For determination of the cell number an electronic particle counter (Beckman Coulter) was used.

Cells were discarded after approximately 30 passages to avoid genetic drift. After thawing frozen cells, the initial two passages were not used for experiments. All cells used in experiments were in the exponential phase of growth. Corresponding growth media and other supplements for cell culture are listed in **3.1.2**.

3.2.2. Cryopreservation of cells

For long-term storage, living cells were maintained at low temperatures using the protocol of *Borrelli et al. 1987* with dimethylsulfoxid (DMSO) as a cryoprotective agent (196). This freezing protocol ensures adequate recovery after thawing with no reduction in plating efficiency or delayed cell growth.

After trypsinization approximately 4x10^6 exponentially growing cells were centrifuged at 4°C and the pellet was gently resuspended in 250 µl of cold freezing solution A, containing 5 mM KH_2PO_4, 25 mM KOH, 30 mM NaCl, 0.5 mM $MgCl_2$, 20 mM L-lactic acid, 5 mM glucose, and 0.2 M sorbitol. Cells were further kept on ice. After addition

of 250 µl freezing solution B, which is identical to freezing solution A but supplemented with 20 % DMSO, cells were mixed thoroughly and immediately frozen at -150°C in cryovials.

The thawing procedure included rapid thawing of cells and their dilution in pre-warmed (37°C) growth medium at a density of ~2 x 10^6 cells per 100 mm cell culture dish. On the day after thawing the cells, the growth media was changed to remove DMSO.

3.2.3. X-ray irradiation

Irradiation of cells was carried out at room temperature (RT) using X-ray machine (GE Healthcare), operated at a maximum energy of 320 kV, 10 mA with 1.65 mm aluminium filter. To achieve an optimal dose rate, the distance between X-ray tube and irradiation table was adjusted according to the cell culture vessel. Thereby, 30-60 mm diameter cell-culture dishes and 25 cm^2 flasks were irradiated at a distance of 50 cm, while 100 mm diameter dishes and 75 cm^2 flasks were exposed to IR at 75 cm distance from the irradiation source. Additionally, rotation of the irradiation table during exposure reduced intensity fluctuations within the irradiation field. Different X-ray doses were applied to induce various numbers of DSBs. The dose rates at 50 cm and 75 cm distance were ~2.6 Gy/min and ~1.2 Gy/min, respectively. Controls were not exposed to irradiation. In order to avoid temperature fluctuations while performing H3pS10 assay, cells were irradiated on a thin-walled aluminium box filled with pre-warmed water.

3.2.4. Drug treatments

For treatments with kinase inhibitors, fresh and pre-warmed growth medium supplemented with each drug was added to the cells 1 hour before irradiation. Final concentrations of the drugs are listed below. Control cells were treated with the corresponding concentrations of DMSO. For the H3pS10 assay specifically, the growth media was not exchanged; rather the kinase inhibitors were dissolved in a small volume of media and distributed to each cell culture flask to reach the desired final concentration. After irradiation, as well as treatment with kinase inhibitors, the cells were returned in the incubator or in the warm-room for the specified time intervals.

All experiments for determination of mitotic index were performed in a warm-room located close to the irradiation source and specifically designed for highly sensitive assays susceptible to temperature fluctuations.

Table 1: Used drugs

Drug	Drug description	Designation	Working concentration
CHK2i	Specific inhibitor of CHK2		400 nM
KU55933	Specific inhibitor of ATM	ATMi	10 µM
Mirin	Inhibits MRE11 nuclease activity		75 µM
NU7441	Specific inhibitor of DNA-PKcs	DNA-PKi	5 µM
UCN01	Specific inhibitor of CHK1	CHK1i	100 nM
VE821	Specific inhibitor of ATR	ATRi	5 µM

3.2.5. Transfection of cells with siRNA

RNA interference (RNAi) is a conserved adaptive response where RNA molecules suppress post-translational gene expression by degradation of the target mRNA (197). As a research tool, RNAi via transfection is used to introduce double-stranded short interfering RNA (siRNA) molecules into cells in order to prevent gene expression.

Transfection is a non-viral method that enables the introduction of any naked nucleic acid molecules into cultured cells. In this thesis, transfection of siRNA duplexes into cultured eukaryotic cells was performed using Nucleofector® Technology (Lonza). This electroporation-based method developed by Amaxa® applies short electric pulses to temporarily destabilize the cell membrane and thus make it permeable. In this way, siRNA oligonucleotides in the surrounding media move into the cytoplasm.

Two days before transfection cells were seeded on 100 mm dishes. To avoid cell mortality and resistance to uptake macromolecules after transfection, cells were maintained in the log phase of growth. Cell density (confluency) at the time of nucleofection® was between 40-70% depending on the cell line.

siRNA duplexes were purchased from Eurogentec (if not stated otherwise). The constructs consisted of ~19 base pairs with 2-base deoxynucleotide overhangs (**Table 3**). Cells were harvested by trypsinization and centrifuged at 1200 rpm for 3 min. Up to 4 x 10^6 cells were resuspended in 100 µl of custom transfection buffer (80 mM NaCl, 5 mM KCl, 12 mM glucose, 25 mM HEPES, 40 mM

Na_2HPO_4/NaH_2PO_4, 20 mM $MgCl_2$, 0.4 mM $Ca(NO_3)_2$) and 200 pmol siRNA was added. Cells were then quickly transferred into an Ingenio® cuvette and subjected to nucleofection® with the corresponding program (**Table 2**). The sample was immediately removed from the cuvette and transferred into freshly prepared pre-warmed (37 °C) growth medium. The untreated control sample (mock-transfection) was comprised of cells that were not treated with siRNA but subjected to nucleofection® procedure. For immunofluorescence experiments, cells were directly plated in 30 mm dishes with glass coverslips and directly returned to the incubator. The transfected cells were used for experiments 48 hours after transfection. For western blot analysis cells were plated in 100 mm dishes and protein detection was performed 24 to 72 hours post transfection. Delivery efficiency of siRNA was confirmed using Green Fluorescent Protein (GFP) expression vector, where green fluorescence was measured by flow cytometry 24 hours after transfection. Thereby, the transfection efficiency is defined as the percentage of cells in the population expressing GFP protein.

Table 2: Nucleofector® programs

Cell line	Program
82-6 hTERT	X-23
M059K	X-01
M059J	X-01

Table 3: siRNA sequences

Target mRNA	siRNA sequence (5'→3')	Provider/Reference
CtIP	GCUAAAACAGGAACGAAUCdTdT	Yu and Chen, 2004 (117) Sartori *et al.*, 2007 (74)
DNA2	#9: AGACAAGGUUCCAGCGCCAdTdT	Peng *et al.*, 2012 (198)
DNA2	#11: AAGCACAGGUGUACCGAAAdTdT	
EXO1	CAAGCCUAUUCUCGUAUUUdTdT	Gravel *et al.* 2008, (199)
EXO1	#1	FlexiTube GeneSolution siRNA (Product no. 1027416), Qiagen
EXO1	#2	
EXO1	#7	
EXO1	#8	
KU70	GAGUGAAGAUGAGUUGACAdTdT	Britton *et al.*, 2013 (200)
MRE11	GGAGGUACGUCGUUUCAGAdTdT	Yuan and Chen, 2010 (201)
NBS1	#1:UAACCUUGUUGGCCUGAAGUAGAUG	Shiotani *et al.*, 2013 (202)
NBS1	#2: CCAACUAAAUUGCCAAGUAUU	

3.2.6. Flow cytometry analyses

3.2.6.1. Cell cycle analysis by flow cytometry

Flow cytometry analysis of cell suspensions stained with fluorescent dyes that bind to DNA enables the measurement of DNA content of individual cells. Propidium iodide (PI) has a red fluorescence and can be excited with an Argon laser (488 nm). PI stains all double-stranded nucleic acids; therefore the PI solution contains RNAase which clears away all dsRNA so that the bound PI reflects only the amount of DNA.

Prior to cell cycle analysis, cells were harvested, fixed in pre-chilled 70 % ethanol and stored at least over night at 4°C. Cells were then spun down, ethanol was aspirated and the cell pellet was resuspended in PI staining solution. After 15 min-incubation at 37°C in a water bath, cells were subjected for measurement of the DNA content on a Beckman Coulter Gallios® flow cytometer with a 620 nm bandpass filter. PI solution was not removed during measurement, where 10.000-20.000 events per condition were analyzed. Proper gating based on forward and side scattering was ensured to detect the cells of interest. Cell cycle analysis was performed using WinCycle™ software.

3.2.6.2. Bivariate flow cytometry

The histogram obtained with PI staining does not show the cells in mitosis (M), which have the same DNA content as cells in G_2 phase. Therefore, two-parameter (bivariate) flow cytometry was used for simultaneous analysis of DNA content and phospho-histone H3 (Ser10) staining as a marker of mitotic cells (203). In order to avoid temperature fluctuations, the cell harvesting procedure was performed with pre-warmed solutions in a warm-room with constant temperature of 37°C. On the day before the experiment, the caps of the cell culture flasks were closed to ensure steady state CO_2 atmosphere and the flasks were relocated from the incubator to the warm-room.

Cells were first washed briefly with PBS. Since mitotic cells are rounded up and can be easily detached mechanically from the surface, aspiration was avoided and the PBS solution was transferred to the 15 ml-Falcon® tube. Cells were then harvested by trypsinization and centrifuged for 5 min at 1200 rpm at 4°C. After fixation in pre-

chilled 70 % ethanol, cells were stored over night at -20°C. For immunofluorescent staining, cells were incubated for 5 min on ice with 500 µl of cold PBS containing 0.25 % Triton X-100 and centrifuged for 5 min at 4°C. After one-hour incubation at RT in 1 ml blocking buffer (PBG), the cells were stained with 100 µl of primary antibody (see **3.1.6**) diluted in blocking buffer on a shaker for 1 h at RT. Subsequently, the cells were spun down for 3 min at 1200 rpm and the supernatant with unbound antibody was aspirated. The cell pellet was washed once with 1 ml PBS and stained with secondary antibody as outlined above, but in the dark for 1 h. Finally, the cells were washed once with PBS, stained with propidium iodide and subjected to analysis. Totally 20.000 cells per condition were analyzed. Further acquisition of H3pS10-AlexaFluor® 488 signal was achieved by gating the fraction of diploid cells based on DNA-PI. Compensation was not applied for this kind of measurement. Data analysis was performed using Kaluza 1.2 software. The mitotic index was determined as the fraction of cells in mitosis.

Importantly, not more than 1 x 10^6 cells per sample were used for staining and minimum volume of PBS was used for washing, where ~50 µl of supernatant was left during aspiration in order to avoid losing cells after each centrifugation step.

Table 4: Solutions for flow cytometry

Name	Compounds
PBG	0.2 % gelatin 0.5 % BSA (fraction V) 1x PBS pH 7,4
Permeabilization solution	0.25 % Triton X-100 PBS pH 7,4
Propidium iodide (PI) staining	40 µg/ml propidium iodide 62 µg/ml RNaseA *Buffer for RNaseA, pH 7.6* 10 mM Tris 100 mM EDTA 50 mM NaCl *Buffer for PI staining* 0.1 M Tris 0.1 M NaCl 5 mM $MgCl_2$ 0.05 % Triton X-100

3.2.7. Immunofluorescent staining

For immunofluorescent detection of IR-induced foci (IRIF), cell were plated on 20 mm glass coverslips in 30 mm cell culture dishes and grown for two days. 82-6 hTERT cells were plated in a concentration of 80 000 cells per dish, while M059K and M059J cells were seeded in a concentration of 100 000 and 200 000 cells/dish, respectively. Prior to antibody staining, cells were transferred in fixative solution (PFA, 2% paraformaldehyde) for 15 min, washed once with PBS and then permeabilized with P-solution (100 mM Tris pH 7.4, 50 mM EDTA pH 8.0, 0.5 % Triton X-100) for 5 min at RT. Subsequently, cells were washed with PBS and blocked with phosphate-buffered gelatin (PBG: 0.2 % gelatin, 0.5 % bovine serum albumin, PBS) overnight at 4°C or at least 1 h at RT. For cell cycle analysis, the remaining cells were collected and fixed with pre-chilled 70 % ethanol.

All antibodies used for immunofluorescent staining were diluted in PBG (see **3.1.4**). For every coverslip 80-100 µl of antibody solution was added on a parafilm sheet. Coverslips were gently inverted with the cells facing down onto the drop of antibody solution. After incubating with primary antibodies 1.5 h at RT, cells were washed three times with PBS for 5 min and incubated with AlexaFluor®-conjugated secondary antibodies in dark for 1 h. To visualize nuclei, the cells were counterstained with 25 ng/ml 4',6-diamidino-2-phenylindole (DAPI) dissolved in PBS for 15-20 min at RT. Finally, cells were washed with PBS (3 times for 5 min) and mounted on microscopic slides using PromoFluor Antifade Reagent (PromoKine) diluted 1:1 with distilled water. After solidification of the mounting media in dark at RT, 3D-images were captured using confocal microscope (Leica Microsystems).

Table 5: Solutions for immunofluorescence

Name	Abbreviation	Compounds
4',6-diamidino-2-phenylindole	DAPI	25 ng/ml DAPI 1x PBS pH 7,4
Phosphate buffered gelatin (Blocking buffer)	PBG	0.2 % gelatin 0.5 % BSA (fraction V) 1x PBS pH 7,4
2% paraformaldehyde	PFA	2 % PFA in Milli-Q H_2O
Permeabilization solution	P-Solution	100 mM Tris pH 7,4 50 mM EDTA 0.5 % Triton X-100

3.2.8. Laser Scanning Confocal Microscopy

One of the most important advantages of laser scanning confocal microscopy (LSCM) toward conventional wide-field fluorescence microscopy is optical sectioning – the ability to obtain high-resolution pseudo 3D-images of a thin specimen at multiple depths. This eliminates the need for a microtome sectioning, which is usually used for epifluorescence microscopy.

The term 'confocal' refers to the focus of the final image which corresponds to the point of focus in the specimen. The elimination of out-of-focus information is obtained by a pinhole aperture situated in a conjugate plane in front of the detector (a photomultiplier, PMT) (**Figure 10**).

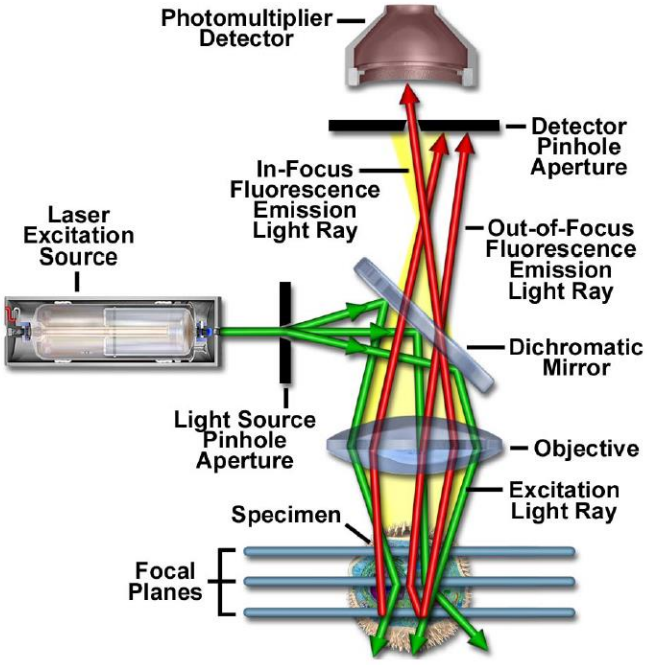

Figure 10: Schematic overview of confocal microscopy. Figure obtained from '*Laser Scanning Confocal Microscopy' from Claxton, Fellers and Davidson*

The pinhole regulates the diameter of the light beam and thus filters the unfocused background signal for the final image. Hence, the detector can detect only light that has passed through the pinhole (in-focus portion of light). Since the pinhole greatly reduces the amount of light in the final image, increase of signal intensity is achieved by a laser as an excitation source and a highly-sensitive PMT for better detection of the emission light. In contrast to the traditional mercury arc lamp, the laser generates

strong monochromatic light with a specific wavelength which can excite more fluorophores per fraction of time.

The laser beam in a LSCM system passing through a light source aperture is reflected by a dichroic mirror, recollected by an objective lens and directed to a fluorescently labeled specimen in a defined focal plane. The fluorescent emission from the specimen in the same focal plane passes back through the dichroic mirror and is transmitted to the PMT. Detection with PMT allows signal acquisition of one pixel per time. Therefore, the LSCM is equipped with motorized scanning mirrors (galvanometric scanner) which scan the horizontal laser beam across the specimen in a consecutive manner; one of the scanning mirrors moves the beam along the *x*-axis and the other in *y* direction. As a result, an optical section from the sample is generated that represents the image obtained from a single focal plane (*z*-section). Movement of the sample in the *z*-axis by a piezoelectric stage allows to collect series of multiple *z*-optical sections (*z*-stack) which then serve for digital reconstruction of the 3D structure by the provided software. This final image of the specimen contains only the in-focus information. Additionally, the use of multiple fluorescent dyes and lasers with different spectral characteristics (*i.e.* emission and excitation wavelengths) enables simultaneous detection of more than one target molecules within the same biological material.

3.2.9. Image acquisition and foci analysis

For IRIF analysis, immunofluorescently-stained cells were visualized with LAS AF software provided with the LCSM system (Leica).

In all experiments, a scanning step of 0.5 µm along the *z*-axis through the whole nuclei was set to obtain a *z*-stack (~10 µm). For each sample 5 to 10 fields were scanned to obtain an average of 30 G_2 phase cells per sample. The settings for each parameter are listed below. Parameters like laser intensity, PMT gain and offset varied between individual experiments but were kept constant within a single experiment. To avoid ‘spillover’ between different channels during simultaneous detection of multiple fluorescent dyes, each channel was scanned sequentially.

Foci analysis was performed by Imaris® software (Bitplane). Fluorescent spots with a diameter above 0.5 µm within each nucleus were determined as foci. Threshold

values of the pattern recognition parameters were kept constant during the whole analysis process. For data presentation were used 2D projections of the 3D renderings of all image stacks.

Table 6: Settings for image acquisition of Leica TCS-SP5

Parameter	Settings / Value
Objective	HCX PL APO lambda blue; 63.0x1.4 OIL UV
Pinhole	95.55 µm
Pixel size	200 nm
Resolution	1024 x 1024
Scan direction	bidirectional
Sequential scan	between stacks
Speed	400 Hz
Zoom factor	1.2
z-step size	0.5 µm

Table 7: Parameters for detection of fluorescent dyes by LSCM

Dyes	Excitation	Filter range
DAPI	405 nm	410-550 nm
AlexaFluor® 488	488 nm	495-550 nm
AlexaFluor® 568	594 nm	575-650 nm

3.2.10. Bradford protein assay

Bradford assay is a quick and sensitive colorimetric assay for quantitative analysis of total protein in solution in the range of 1 – 1500 mg/ml. The assay, first described by Marion Bradford in 1976 (204), is based on absorbance shift of the dye Coomassie Brilliant Blue G-250 when bound to proteins.

The unbound form of Coomassie (cationic) is reddish/brown and has a maximum absorption at 470 nm. Under acidic conditions, the dye binds to proteins, preferentially to basic amino acid residues (arginine, lysine and histidine), and the protein-bound dye becomes anionic and blue. The protein-dye complex results in a shift in the absorption spectrum from 470 to 595 nm, where the increase of absorption is proportional to the amount of bound dye, *i.e.* concentration of protein in the sample. Standard protein (BSA) in a linear concentration range from 0.1 to 2.0 mg/ml was used for calibration. Protein concentration was determined with UV-Vis spectrophotometer.

Table 8: Bradford reagent

Components	5x concentrate
Coomassie Brilliant Blue G-250	0.05 % (w/v)
Methanol / Ethanol	25 % (v/v)
Phosphoric acid (H_3PO_4)	45 % (v/v)

3.2.11. SDS-PAGE and immunoblotting

Conventional immunoblotting was applied to detect proteins of interest by separating them according to their molecular weight. Proteins from whole cell lysates were prepared with radioimmunoprecipitation assay (RIPA) buffer supplied with protease inhibitor cocktail according to manufacturer's instructions (Themo Scientific). Thereby, $1x10^6$ trypsinized human cells were lysed with 50-100 µl of RIPA buffer. 10-50 µg of the protein extracts were mixed 1:1 with 2x Laemmli sample buffer (LSB). Before loading on gels, the samples were denatured for 5 min at 96°C and spun down for 30 sec at 13.000 rpm. Protein extracts were resolved on 10 % sodium dodecyl sulfate (SDS) polyacrylamide gel with a constant voltage of 8,3 V/cm, a procedure termed SDS-polyacrylamide gel electrophoresis (SDS-PAGE).

For western blotting, the separated proteins from the SDS-polyacrylamide gel were transferred onto an Odyssey® 0.22 µm nitrocellulose membrane (LI-COR Biosciences) for 1h at 100 V by using wet transfer apparatus. Temperature of 4°C was kept constant during the entire transfer procedure. The membrane was blocked with 5 % non-fat dry milk in TBS-T (0.05 % Tween®-20 in 1x PBS) for 2 hours at RT and thereafter incubated with primary antibodies over night at 4°C. Primary antibodies were diluted in 2,5 % non-fat dry milk in PBS-T (1:1 dilution of WB blocking buffer with PBS-T) as listed in **3.1.5**. After washing 3 times (10 min each) with PBS-T, the membrane was incubated for 1 h at RT with secondary antibodies diluted in PBS-T. Prior to detection, the membrane was washed again as described above and let dry. For detecting the proteins of interest Odyssey® Infrared Imaging System (LI-COR Biosciences) was used.

Table 9: Solutions for SDS-PAGE and western blot wet transfer

Name	Abbreviation	Compounds
Solutions for SDS-PAGE		
Rotiphorese® Gel 30 (37,5:1)		
4x Stacking Gel buffer pH 6.8	SGB	0.5 M Tris-HCl 0.4 % SDS
4x Resolving Gel buffer, pH 8.8	RGB	1.5 M Tris-HCl 0.4 % SDS
1x Running buffer		0.025 M Tris-HCl 0.192 M glycine 0.1 % SDS
2x Laemmli sample loading buffer pH 6.8	LSB	0.065 M Tris-HCl 0.01 M EDTA 20 % glycerol 3 % SDS 0.02 % bromophenol blue 5 % β-mercaptoethanol
5 % Stacking gel		5 % Rotiphorese® Gel 30 0.125 M 4x SGB 0.1 % SDS 0.1 % APS 0.2 % TEMED
10 % Resolving gel		10 % Rotiphorese® Gel 30 0.37 M 4x RGB 0.1 % SDS 0.1 % APS 0.1% TEMED
Sensitive Coomassie solution for staining of SDS-PAGE gels		5 % aluminium sulfate 0.02% Coomassie Brilliant Blue G250 2 % (w/v) phosphoric acid 10 % ethanol
Solutions for western blot wet transfer		
4x Electrode buffer, pH 8.3		0.1 M Tris-HCl 0.7 M glycine
Western blot transfer buffer	WB-TB	25% 4x Electrode buffer 20 % methanol
Phosphate-buffered saline- Tween®-20 pH 7.6	PBS-T	1x PBS 0.05 % Tween®-20
Blocking buffer		5 % non-fat dry milk PBS-T

4. RESULTS

Part 1: How does DNA-PKcs contribute to G_2 checkpoint response?

4.1. Persistent G_2 checkpoint associated with DNA-PKcs deficiency is ATR-dependent

First reports discounted the involvement of DNA-PKcs in G_2 phase checkpoint and therefore did not consider it as a DSB signaling molecule (173). Rather, DNA-PKcs is thought to be exclusively implicated in DSB repair by c-NHEJ, where together with KU70/80 heterodimer comprise the DNA-PK holoenzyme. However, previous experiments from our laboratory indicate a possible role for DNA-PKcs in checkpoint regulation in cells irradiated in S and G_2 phase of the cell cycle (205). The contribution of DNA-PKcs to the G_2 checkpoint was investigated by utilizing two isogenic glioblastoma cell lines M059K and M059J isolated from the same tumor specimen (194). M059K cell line expresses normal level of DNA-PKcs activity, while M059J cells lack p350, the catalytic component of DNA-PK because of a frameshift mutation in *PRKDC* (*DNA-PKcs* gene) (193, 206, 207).

G_2 arrest after ionizing radiation can be investigated by one-parameter flow cytometry analysis using propidium iodide (PI) staining. PI is a fluorescent dye that binds to dsDNA and thus enables the measurement of DNA content (**Figure 11 A)**. Another approach to study specifically cells sustaining damage in G_2 phase is the two-parameter flow cytometry, combining PI and phospho-histone H3 (H3pS10) staining (**Figure 11 B**). Histone H3 is phosphorylated at Serine 10 during mitosis and staining with antibody against phospho-histone H3 ensures discrimination between G_2 and mitotic cells, where the reduction of the mitotic index is a direct indicator of the G_2 checkpoint response (203). A corresponding confocal image of Histone H3pS10 stained cells is shown on **Figure 12**.

Exposure of actively proliferating cells to IR leads to accumulation of cells at the G_2/M border, which resembles the increased G_2 fraction on the cell cycle histogram 6 hours after irradiation with 2Gy (**Figure 11 A**).

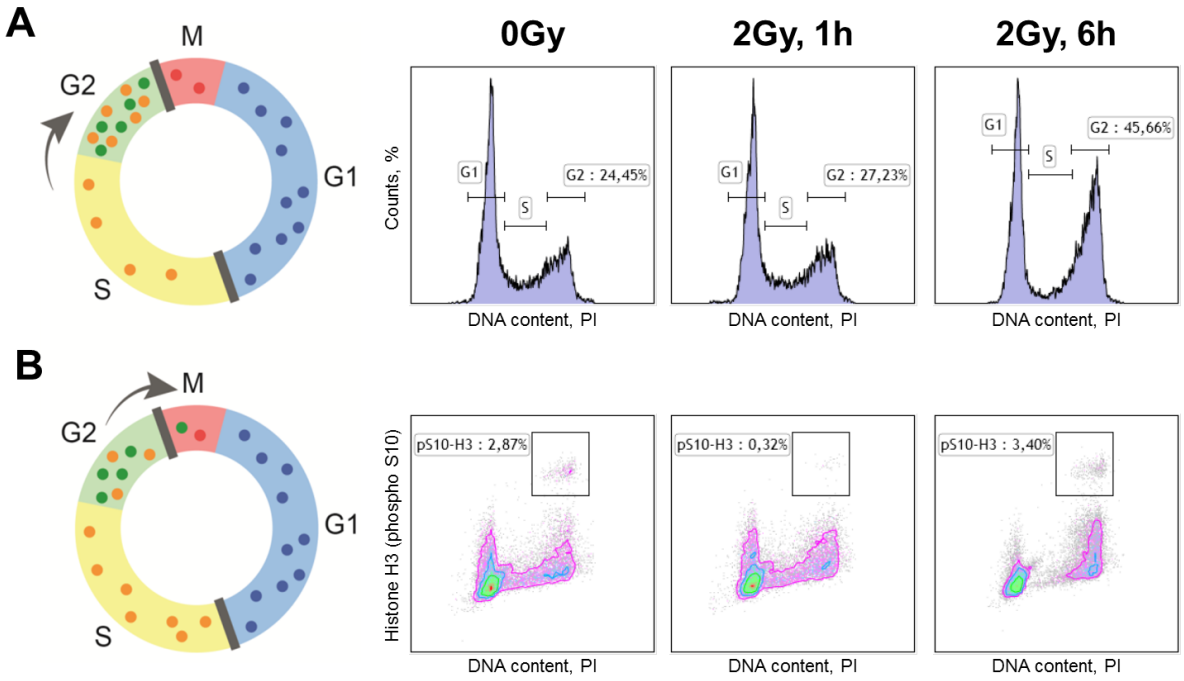

Figure 11: G_2 checkpoint assays. G_2 checkpoint can be studied by (**A**) staining the DNA with propidium iodide (PI) and measuring the percentage of cells in G_2 phase of the cell cycle. For a precise analysis of cell cycle distribution was used Multicycle AV™ software. Time frame of experiment is 0h to 24h post IR treatment. G_2 checkpoint activated specifically in cells irradiated in G_2 phase (**B**) can be studied by combined DNA (*x* axis) and phosphorylated Histone H3 at Ser10 (*y* axis) staining that allows discrimination between G_2 and mitotic cells and thus determination of the mitotic index (MI; percentage of cells in mitosis against total number of cells). Time frame of H3pS10 assay is 0-8 h post IR. The cells used as an example are actively growing 82-6 normal human fibroblasts immortalized with hTERT.

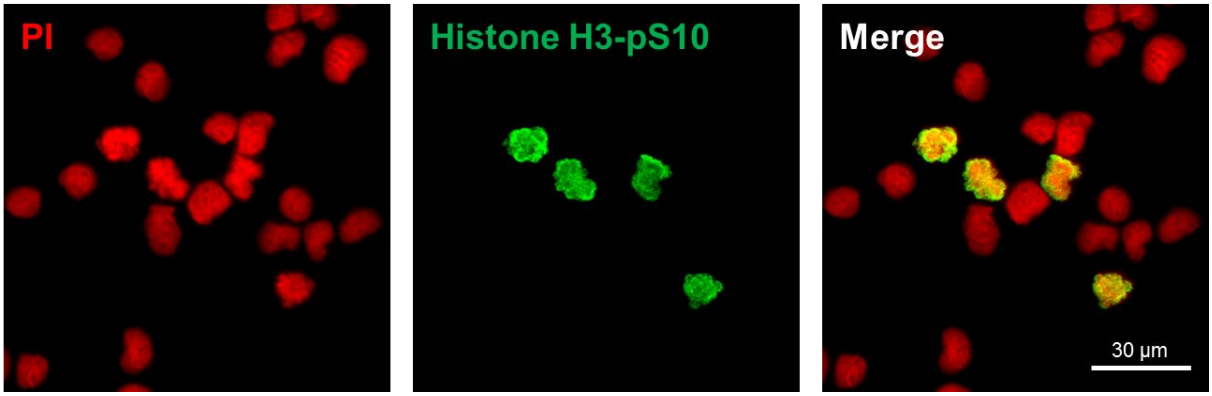

Figure 12: Confocal image of mitotic cells using Histone H3 (phospho S10) staining in ethanol-fixed M059J cells. Secondary antibody was conjugated to Alexa Fluor® 488. Nuclei were counterstained with propidium iodide (PI).

Since the accumulation of cells in G_2 phase arises through progression of cells from S phase, the increase of the G_2 fraction above the levels of unirradiated cells represents primarily the cells irradiated in S phase. Irradiation of asynchronous cell culture also results in delayed mitosis. As shown on **Figure 11 B**, the percentage of mitotic cells (represented in the gates) is decreased 2 hours after irradiation with 1Gy and reaches normal levels at the 6-hour time point.

As shown on **Figure 13**, exposure of cells to ionizing radiation causes a time-dependent increase in the fraction of G_2 cells. The G_2 arrest is also dose-dependent, as the fraction of G_2 cells rises with increasing doses of IR. Repair-proficient M059K cells irradiated with 1Gy show a slight increase of the G_2 fraction at the 3-hour time point, while the higher fraction of G_2 cells induced with 2Gy persists until 12 hours post IR. In both cases, the G_2 fraction of cells exposed to IR reaches the level of non-irradiated cells at 15 h. Notably, DNA-PKcs deficient cells show a more pronounced G_2 arrest after irradiation with the same doses when compared to the cell line with competent DNA-PKcs. Thereby, the increase in G_2 fraction and the maximum of G_2 percentage appears at later times. Slower recovery is observed at lower doses (0,5Gy and 1Gy IR), while with increasing the dose the cells fail to recover from the checkpoint-mediated arrest until 30 hours later. As outlined above, this response reflects activation of the G_2 checkpoint response predominantly in cells sustaining damage in S phase of the cell cycle.

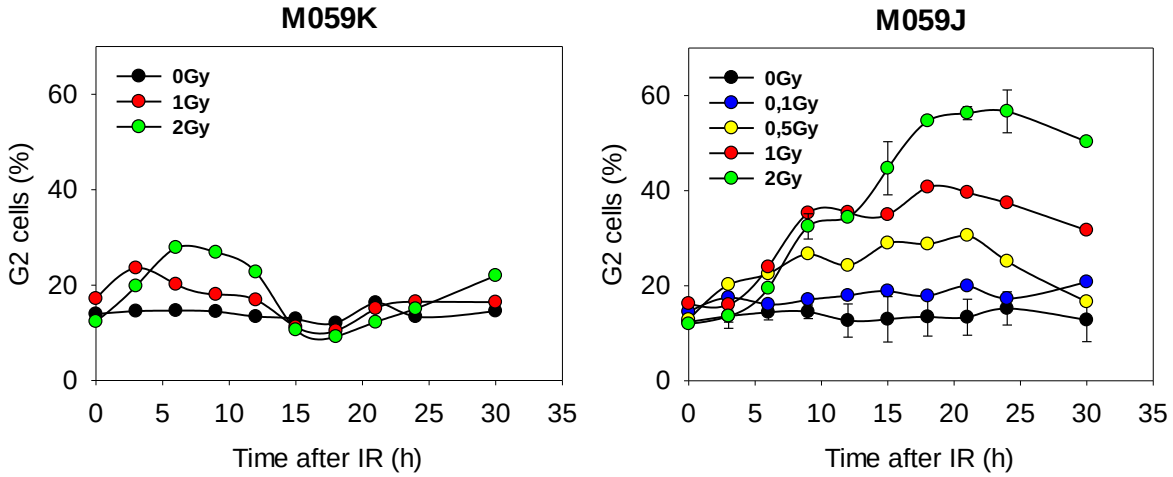

Figure 13: DNA-PKcs deficiency is associated with pronounced G_2 arrest. Exponentially growing M059K and M059J cells were exposed to different doses of IR and harvested every 3 hours. Cell cycle distribution was analyzed by single-parameter flow cytometry. The percentage of cells in G_2 is represented as a function of time. Data are compiled from two independent experiments (± SD).

This observation is also confirmed with the phospho-histone H3 assay (**Figure 14**). M059K cells show a rapid decrease in the normalized mitotic index almost to zero at 1h after IR, which reflects a stop in cell progression from G_2 into M phase. Progression to mitosis continues after the 2-hour time point and reaches control levels at 4 hours. This response represents induction of the G_2 checkpoint specifically in cells irradiated in G_2 phase, as predominantly G_2 cells reach M-phase within the timeframe of the experiment. In marked contrast to repair-proficient cells, the recovery from the G_2 checkpoint in DNA-PKcs deficient cells remains incomplete at the same times after irradiation suggesting DNA-PKcs dependence for the checkpoint response activation. This data are in agreement with another study, where the lack of DNA-PKcs is associated with persistent S phase checkpoint (174). Interestingly, the deficiency of several other components of classical NHEJ (Ligase IV, XRCC4 and KU80) fail to reproduce the phenotype of DNA-PKcs deficient cells (174). Since all of these mutants have a strong DNA repair defect, the lack of recovery in DNA-PKcs deficient cells cannot be explained exclusively by the repair deficiency.

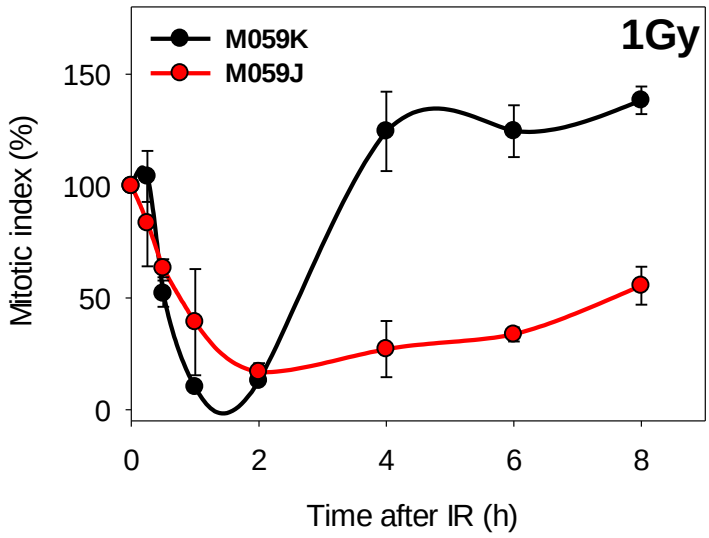

Figure 14: DNA-PKcs is required for recovery from G_2/M checkpoint after IR. The percentage of mitotic cells positive for H3pS10 normalized to the non-irradiated control is represented as a function of time after exposure to IR. Data from two independent experiments are presented (± SD).

The nature of DNA-PKcs activation and its role at DSB ends to orchestrate DNA repair raises a question whether chemical inhibition of DNA-PKcs kinase activity in M059K cells would have the same response as DNA-PKcs deficiency in M059J cells.

DNA-PKcs inactivation on cellular level is achieved by using specific small molecule inhibitors. Early generation of classical non-specific PI3K inhibitors involves Wortmannin, which is a non-competitive inhibitor that binds covalently to the kinase active site and was widely used in prior publications (208). Novel ATP-competitive inhibitors like NU7026 and NU7441 were found to be highly specific for DNA-PKcs (209-211).

For the experiments in this thesis, NU7441, a selective inhibitor of DNA-PKcs (to be referred as DNA-PKi), was used. The results shown on **Figure 15 A** clearly demonstrate that chemical inactivation of DNA-PKcs also results in persistent G_2 checkpoint indicating the essential function of DNA-PKcs kinase activity in the recovery from IR-induced cell cycle arrest (**Figure 15 A**, left panel). The off-target effect of DNA-PKi was ruled out by the experiment with M059J cells where NU7441 is ineffective (**Figure 15 A**, right panel).

The activation of the damage induced G_2 checkpoint is associated with the activity of ATM or ATR protein kinases. To elucidate which one of the remaining PIKK kinases is involved in the hyper-activated G_2 checkpoint in DNA-PKcs deficient cells, specific ATM (KU55933) and ATR (VE821) small molecule inhibitors were used (to be referred as ATMi and ATRi, respectively). Although ATMi prolongs the checkpoint in DNA-PKcs proficient M059K cells irradiated in S-phase, it shows no effect in M059J cells (**Figure 15 B**). The results with this inhibitor indicate that ATM is not involved in the maintenance of the prolonged checkpoint in DNA-PKcs deficient cells and implies the contribution of ATR. As expected, ATRi completely abrogated the G_2 checkpoint in M059J cells, as well as in DNA-PKcs proficient M059K cells irradiated in S-phase (**Figure 15 C**).

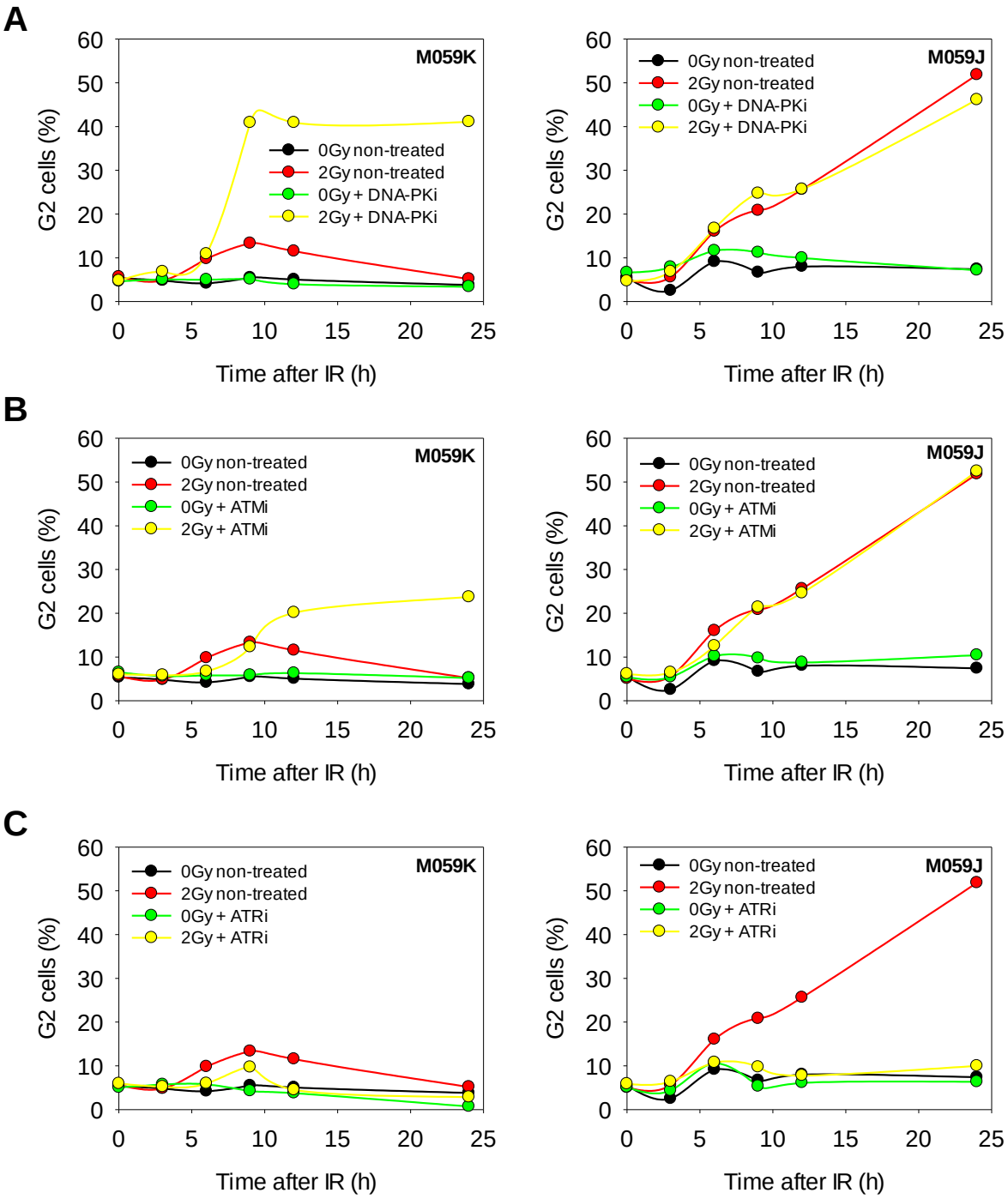

Figure 15: Effect of PIKK inhibitors on the G_2 arrest in M059K and M059J cells after exposure to IR. Actively growing M059K and M059J cells were pre-treated with different PIKK inhibitors 1 h prior to IR and maintained in the medium for the duration of the experiment (24 hours). Cells were harvested every 3 hours until 12 h following IR treatment and subjected to cell cycle analysis by flow cytometry. (**A**) 5 µM DNA-PKcs inhibitor NU7441, (**B**) 10 µM ATM inhibitor KU55933, (**C**) 5 µM ATR inhibitor VE821. Data presented from one experiment.

These observations reveal a possible cross-talk between DNA-PKcs and ATR in checkpoint signaling. Furthermore, the effect of DNA-PKcs deficiency, as well as DNA-PKcs inhibition seems to be stronger than that of ATM, which is thought to be a master conductor of the G_2 checkpoint response after induction of DNA damage by IR exposure. Interestingly, loss of ATR activity triggers normal progression of the cells through the cell cycle after IR. These results suggest that DNA-PKcs augments recovery from checkpoint arrest after exposure to IR and thus implicates DNA-PKcs in the regulation of checkpoint signaling together with ATM and ATR.

4.2. ATR regulates the G_2 checkpoint by integrating inputs from ATM and DNA-PKcs

Since M059K and M059J are both malignant glioma-derived cell lines, the effects of PIKK inhibitors on G_2/M checkpoint were next studied in the normal human fibroblast cell line 82-6 immortalized with hTERT (human telomerase reverse transcriptase) expression vector. This experiment was designed not only to answer the question whether these effects are cell type-specific, but also to verify the unexpected role of ATR on IR-induced checkpoint response in non-cancer cells. Another parameter included in this experimental setup was the applied dose (DSB-load), where cells were exposed to low (*i.e.* 2Gy) and high doses (*i.e.* 10Gy) of IR.

The results reveal that incubation of normal cells with DNA-PKi delays the recovery from the G_2 checkpoint after IR, while ATM inhibition leads to abrogation of the G_2 arrest at early time points post irradiation and moderate but persistent reduction of the mitotic index at later times. At 1 to 2h after IR, ATRi has similar effect to ATMi, but in contrast to ATMi, at later times ATRi results in control levels of mitotic cells, suggesting complete abrogation of the checkpoint response (**Figure 16 A**). These results are in line with the effects observed in M059K cells (**Figure 15**). Combinations of the PIKK inhibitors show that the DNA-PKi effect is abrogated either by ATMi or by ATRi indicating that the hyper-activated checkpoint due to the DNA-PKcs deficiency is abolished when ATM and/or ATR are inactive (**Figure 16 B**). Furthermore, combined treatment with ATRi and ATMi reveals that DNA-PKcs alone is not able to sustain IR-induced checkpoint. Interestingly, the ATM inhibitor shows a dose-dependent effect on checkpoint activation, as the higher dose of 10Gy further influences the outcome observed after irradiation with 2Gy (**Figure 16 A, C**). The

same response is observed with the combined treatment of DNA-PKi and ATMi (**Figure 16 B, D**). After 10Gy of irradiation, ATR inhibition results in a small initial drop followed by rapid increase in the mitotic index above normal levels, which may be explained by accumulation of cells at the G_2/M border due to the higher dose and their subsequent progression as an ensemble into mitosis. At a higher dose, either ATM or ATR alone are capable of activating moderately the G_2 checkpoint response (**Figure 16 D**, green and red lines respectively). The data suggest that the other remaining kinases ATM and DNA-PKcs cannot contribute to checkpoint development without ATR since they both remain active when ATRi is applied.

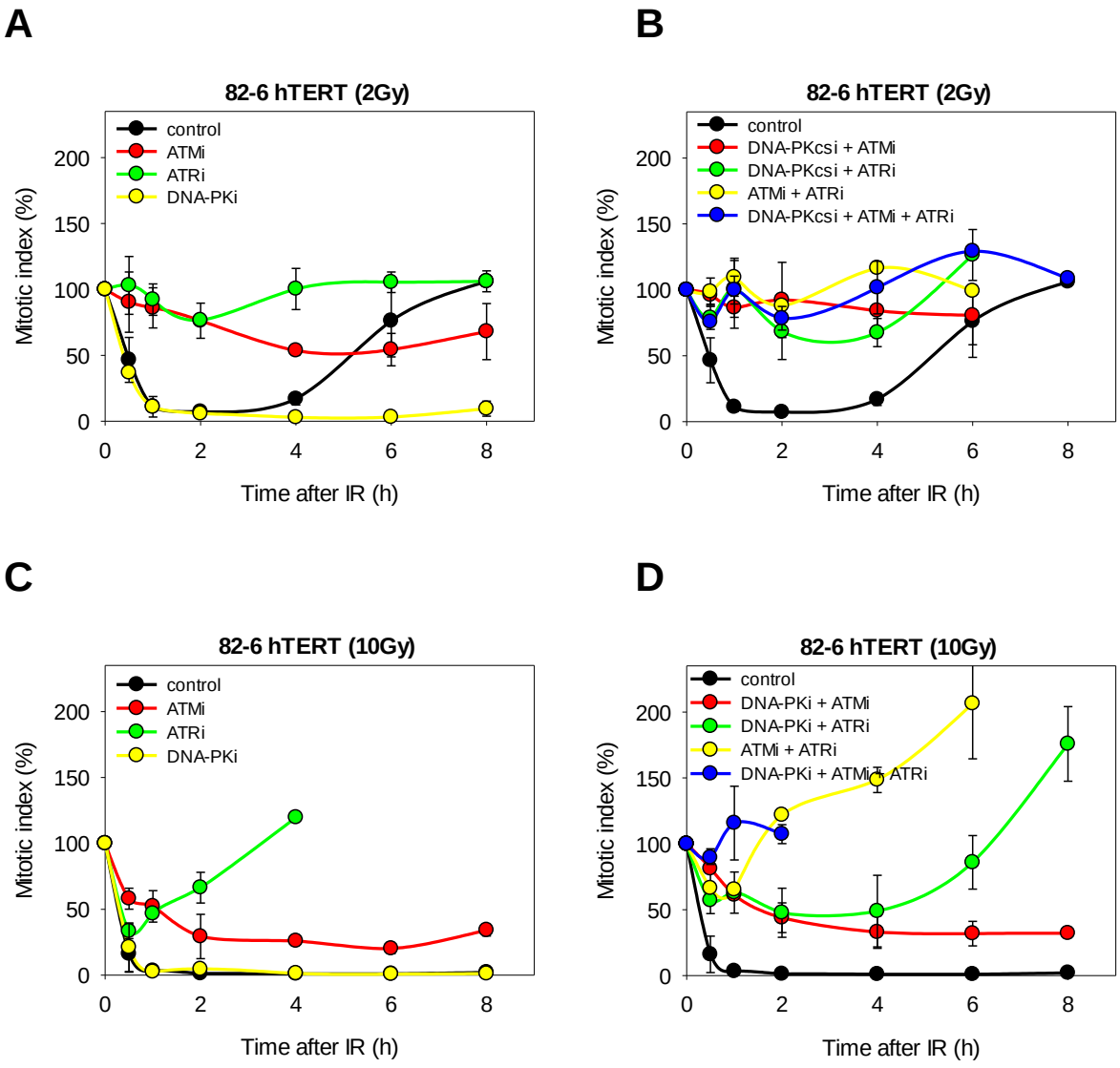

Figure 16: Multiple drugs effects on G_2/M progression of normal human fibroblasts after IR. Cells were treated with 5 µM NU7441 (DNA-PKcsi), 10 µM KU55933 (ATMi) and 5 µM VE821 (ATRi) 1 hour prior to IR. Cells were harvested at different time intervals after exposure to IR. Data obtained from two independent experiments (± SD).

All these results also suggest that ATR is not a minor contributor to G_2 checkpoint development and implicate the essential role of ATR for the manifestation of the G_2 checkpoint in cells sustaining damage in G_2 phase. Furthermore, the data imply that all three PIKK kinases may work as a module to regulate the DNA damage signaling and checkpoint response following exposure of cells to IR. In line with the above postulate, chemical inactivation of the kinase activity of the entire module leads to completely abrogated G_2 checkpoint independent of the radiation dose (**Figure 16 B, D**).

Further confirmation of the importance of the ATR arm of the G_2 checkpoint activation came from the results with inhibitor of the ATR-downstream kinase CHK1, UCN-01 (referred as CHK1i). As shown on **Figure 17**, inhibition of CHK1 results in a remarkable, although no complete, reduction of G_2 checkpoint, which suggests a cross-talk between ATR and CHK2. On the other hand, CDC25 may also become phosphorylated since the ATM-CHK2 arm is still active. However, this residual checkpoint could not be completely abrogated by inhibiting CHK2, although it was entirely reversed by ATM inhibition at a low dose (**Figure 17**, left panel). The same response was observed in M059J cell line (**Figure 18**).

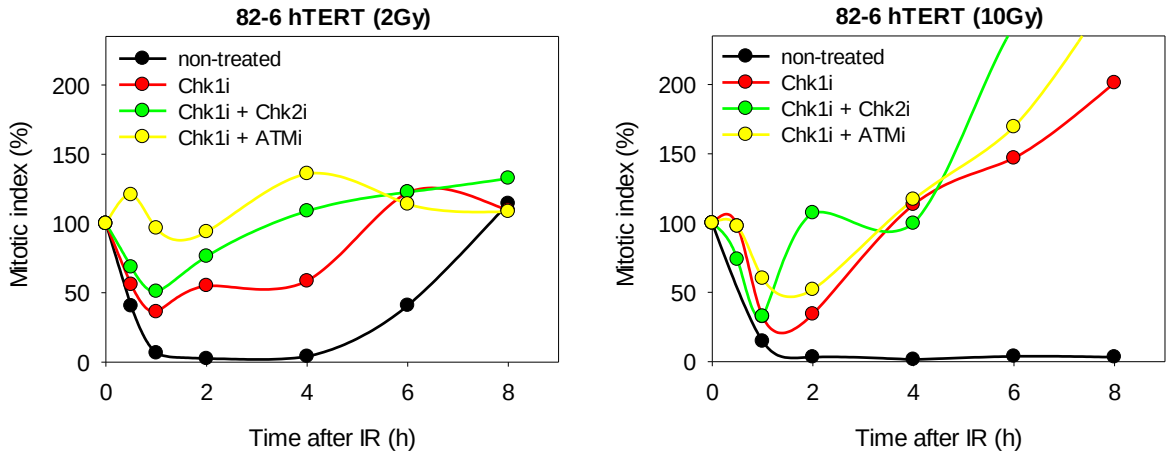

Figure 17: Multiple drugs effects on G_2/M progression of normal human fibroblasts after IR. Cells were pre-treated with 100nM Chk1i (UCN-01), 400nM Chk2i and 10 μM ATMi (KU55933). Data presented from one experiment.

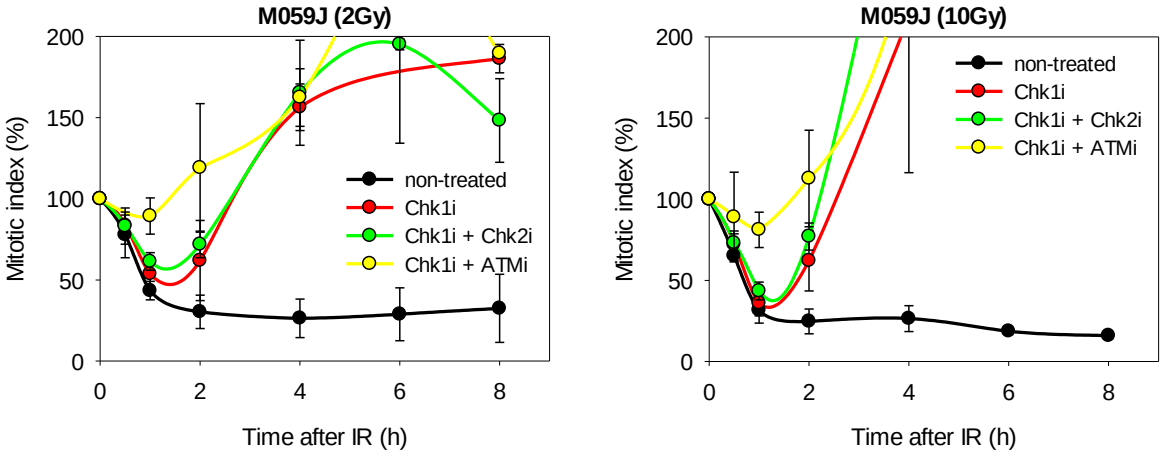

Figure 18: Multiple drugs effects on G_2/M progression of M059J cells after IR. Cells were treated with 100nM Chk1i (UCN-01), 400nM Chk2i and 10 µM ATMi (KU55933) 1 hour prior to irradiation. Data obtained from two independent experiments (± SD).

Since the hyper-activated G_2 checkpoint in DNA-PKcs-deficient cells is dependent on ATR activity and ATR requires DNA end resection at IR-generated DSBs, the hypothesis arose that under basal conditions resection is downregulated by DNA-PKcs. This implies that absence of DNA-PKcs leads to hyper-resection, which provokes ATR hyper-activation. Therefore, the next part of the thesis focuses on the role of DNA-PKcs in the process of DNA-end resection.

Part 2: Contribution of DNA-PK to the regulation of DNA-end resection

4.3. DNA-PKcs deficiency is associated with enhanced DNA end resection in G_2 phase

Next, to test the above hypothesis, the rate of DNA-end resection was studied in DNA-PKcs deficient cell line M059J and its counterpart M059K. RPA accumulation at the ssDNA overhangs was used as a read-out for ongoing DNA end resection. RPA foci were visualized in a population of irradiated G_2 cells selectively discriminated by Cyclin B1 staining. It is well documented that the Cyclin B level oscillates throughout the cell cycle with a maximum in S/G_2 phase and during mitosis, where Cyclin B1 is localized at the microtubules (212). Analysis of DNA end resection by IF revealed that the RPA70 foci number in DNA-PKcs deficient cell line is greatly increased as compared to the repair proficient cells (**Figure 19**).

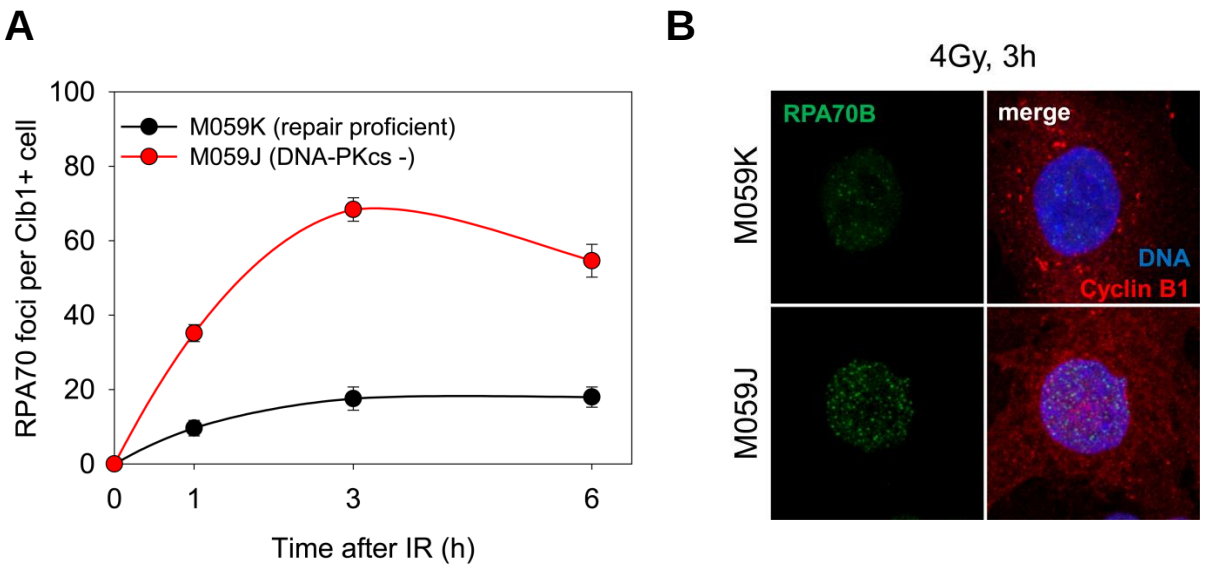

Figure 19: Immunofluorescence analysis of RPA70 foci number in M059K and M059J cells. (**A**) Kinetics of RPA70 foci formation in Cyclin B1 positive cells following exposure to 4Gy IR. Foci were scored in >30 nuclei per slide. (**B**) Representative immunofluorescence images of RPA70 foci (green) in Cyclin B1 positive cells (red). Nuclei were counter-stained with DAPI (blue). Representative data from one out of two independent experiments (± SE).

This observation indicates that under default conditions, DNA-PKcs may suppress DSB end resection in G_2 phase of the cell cycle. Therefore, in cells with DNA-PKcs deficient background the balance of DSB repair may be shifted toward HRR and a-EJ pathways that profit from resected DNA.

4.4. The role of KU heterodimer on end resection in M059K and M059J cells

KU70/80 binds directly DSB ends and serves as an anchor point for NHEJ proteins. Therefore, multiple previous studies assign functions to KU heterodimer, which include suppression of DNA end resection (213, 214). As KU70/80 is an integral part of the DNA-PK holoenzyme, we wished to investigate whether KU70/80 deficiency provokes similar responses as DNA-PKcs on DNA end resection. To investigate the role of KU heterodimer in the process of DNA end resection, we used siRNA-mediated depletion of KU70 in M059K and M059J cells.

As shown in **Figure 20 C**, the expression of KU70 can be reduced significantly by specific siRNA targeting KU70 mRNA. Both M059K and M059J cells transfected with siRNA against KU70 show reduced level of KU70 protein up to 48 hours after nucleofection® when compared to the control. However, the results from an immunofluorescent experiment with repair-proficient M059K cells do not show a significant increase of RPA foci number in KU70-depleted cells when compared with the mock-transfected control (**Figure 20 A**, left panel). This result does not resemble the effect of DNA-PKcs deficiency on RPA foci formation and argues against the negative role of KU70/80 on initiation of DNA end resection. Similarly, siRNA-mediated depletion of KU70 on top of DNA-PKcs deficiency (**Figure 20 A**, right panel) did not further increase RPA foci number at any of the time points following exposure to IR. In addition to RPA foci formation, the RPA foci intensity did not differ significantly between mock and siKU70-treatments in both cell lines, but the higher number of RPA foci in M059J cells is associated with a slightly increased foci intensity when compared to M059K cells (**Figure 20 B**).

In summary, these results show that KU70/80 alone is not sufficient to suppress the initiation of end resection under normal conditions and reinforce the notion that DNA-PKcs suppresses end resection independently of KU heterodimer.

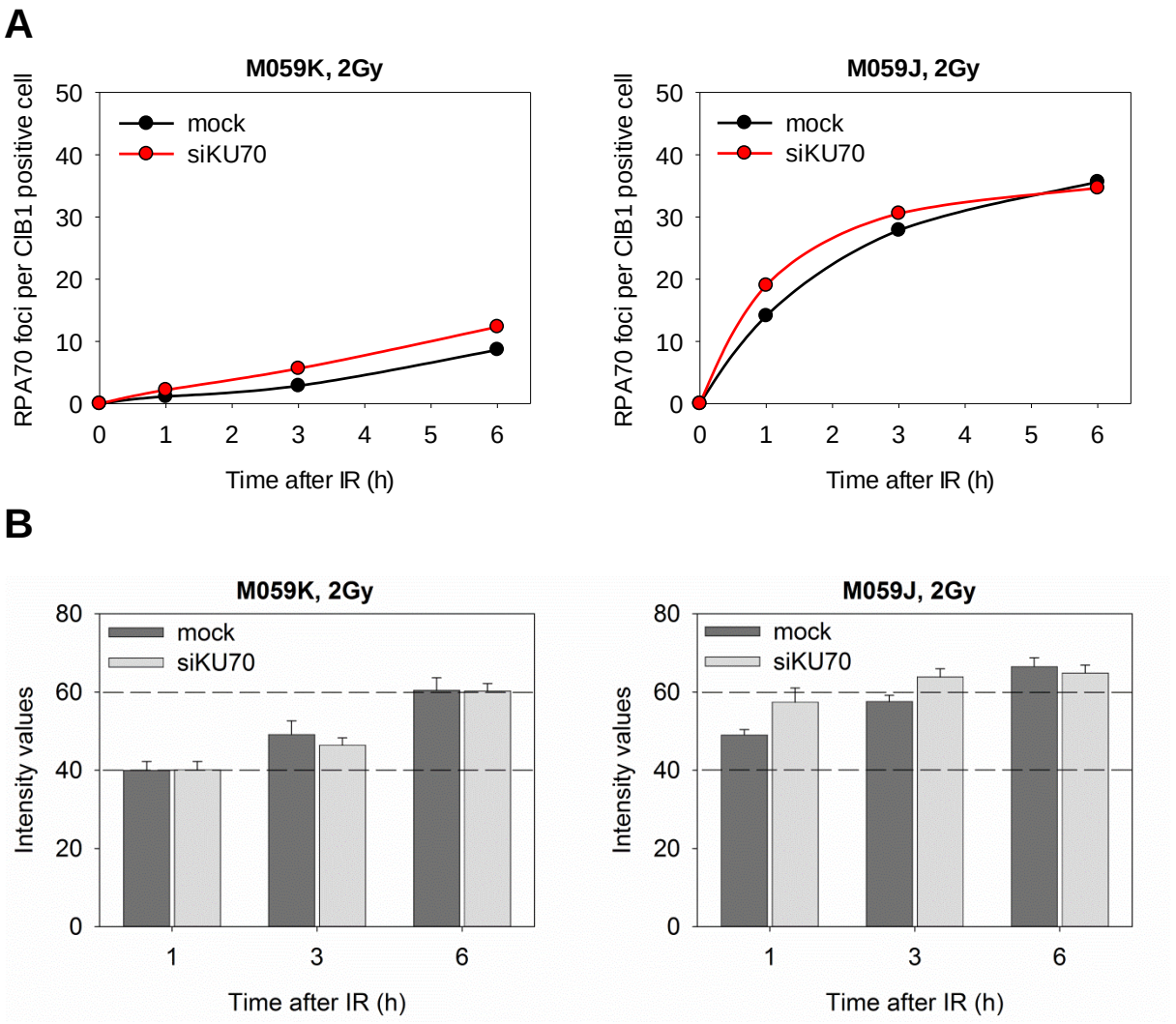

Figure 20: Effect of KU70 knock-down on DNA end resection. Analysis of RPA70 foci number (**A**) and intensity (**B**) in M059K and M059J cells. Foci number from the corresponding unirradiated controls at each time point was subtracted. In the mock-treated control cells were subjected to Nucleofection® in the absence of siRNA. The dashed lines serve to show the different levels of intensity values between the two cell lines. (**C**) Verification of KU70 knock-down by western blot 48 h after nucleofection®. 10 µg and 20 µg of total protein were loaded. Data obtained from one experiment (± SE).

4.5. DNA-PKcs actively regulates resection and G_2 checkpoint

To study the contribution of each component of the DNA-PK holoenzyme to the end resection process in more detail, an experiment in repair-proficient cell line M059K was designed applying RNA interference (RNAi) to reduce the gene expression of KU combined with a specific inhibitor of DNA-PKcs. This approach could answer the question whether the catalytic function of DNA-PKcs alone is necessary to suppress end resection. For a better comparison of the foci number in M059K cells, the dose of IR was increased from 2Gy in the previous experiment (**Figure 20**) to 4Gy. The remaining cells from each time point were analyzed by flow cytometry to monitor the G_2 arrest.

The results indicate that the level of KU70 stays relatively low even 72h after transfection with specific siRNA. Additionally, the knock-down of KU70 is associated with decreased expression of KU80 (**Figure 21 B**). The foci kinetics show a maximum RPA foci number at 6 hours after irradiation with 4Gy, and that the absence of KU70/80 does not significantly increase RPA foci number at later times post IR (**Figure 21 A**). This indicates that KU70/80 does not impair DNA end resection by blocking the DSB ends. Inactivation of DNA-PK catalytic subunit by NU7441 does not completely replicate the phenotype observed in M059J cell line in terms of RPA foci number. However, the DNA-PKcs inhibitor augments the RPA foci formation at later time points following exposure to radiation. Treatment with DNA-PKcs inhibitor on top of KU70/80 knock-down did not further alter RPA foci kinetics. Since in this experimental setup DNA-PKcs is present but catalytically inactive, these findings suggest that DNA-PKcs may actively regulate the end resection process through its catalytic function. This observation is confirmed by RPA foci kinetics in kinase-deficient CHO cells (unpublished data from our laboratory).

Once bound to the DSB ends, DNA-PKcs needs phosphorylation in order to detach from the break. Therefore, the delayed increase in RPA foci number in the presence of DNA-PKcs inhibitor implies that other kinases may contribute to the initial phosphorylation of DNA-PKcs. A possible candidate is ATM, which was shown to mediate DNA-PKcs phosphorylation at the Thr-2609 cluster (165).

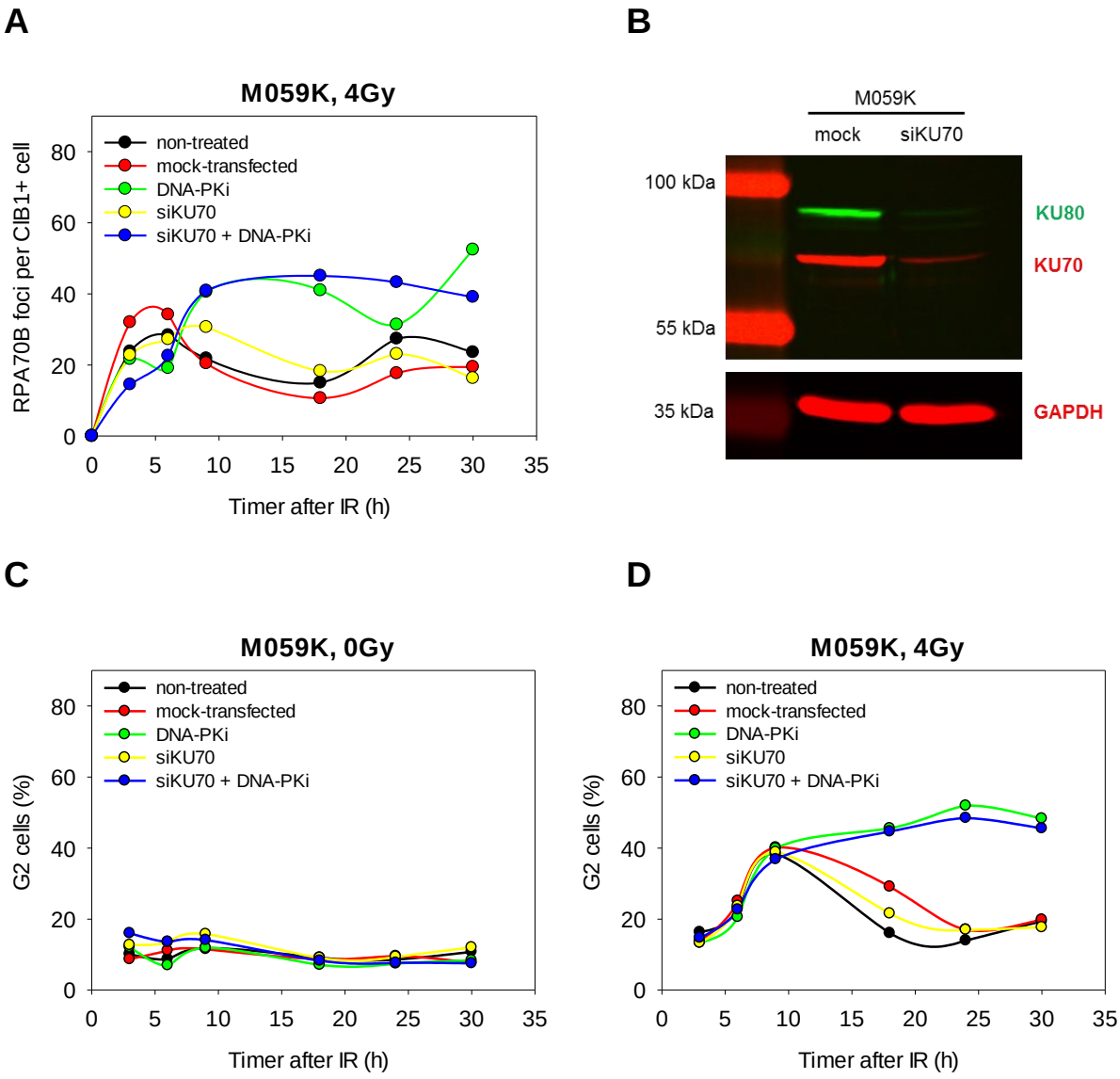

Figure 21: The role of DNA-PK holoenzyme on end resection in repair-proficient cells. (**A**) Kinetics of RPA70 foci formation in Cyclin B1 positive cells. Mock-transfected cells were subjected to nucleofection® program X-01 in the absence of siRNA and a fraction of these cells was treated with 5µM DNA-PKcs inhibitor NU7441. The foci number from the corresponding unirradiated controls at each time point was subtracted. (**B**) Western blot analysis of KU70 knock-down efficiency associated with decreased expression of KU80. Protein extracts were isolated on the day of experiment, 48h after nucleofection®. (**C, D**) G_2 arrest analysis by flow cytometry. Representative data from one out of two independent experiments.

Since KU70/80 appears to not regulate negatively resection under our experimental conditions, we speculated the effect of DNA-PKcs deficiency on G_2 checkpoint is DNA-PKcs-specific and not the result of c-NHEJ deficiency. Therefore, the remaining

cells from each sample were subjected to flow cytometry analysis to confirm that the G_2 checkpoint is not abrogated by KU70/80 depletion.

As shown on **Figure 21 C, D**, depletion of KU heterodimer does not affect the accumulation of cells in G_2 phase. In contrast, inhibition of DNA-PKcs results in prolonged G_2 arrest in non-depleted as well as in KU70/80-depleted cells.

In summary, the results in this section further support the notion that the catalytic subunit of DNA-PK may work independently of KU70/80 to regulate end resection and G_2 checkpoint development through its catalytic function.

4.6. Contribution of ATM and ATR to DSB end resection in the absence of DNA-PKcs

The unexpected role of ATR in G_2 checkpoint activation in response to ionizing radiation implies that ATR is dominantly involved in DNA damage recognition and checkpoint along with ATM and only not partially as frequently assumed. Another indication supporting this hypothesis comes from M059J cells, where the ATM level is reported to be post-transcriptionally reduced due to over-expression of miR-100 (microRNA 100) (215). Under these conditions, ATR may play a more prominent role in regulating resection. However, ATM signaling in M059J cells was shown to be intact (unpublished data from our laboratory).

To further study the sequence of PIKK kinase contribution to end resection, an experiment was designed, where M059J cells were treated with ATMi and ATRi 1 hour before or 30 minutes after IR and RPA foci formation was monitored up to 9 hours after damage induction. The results show that RPA foci reach their maximum 3-6 hours after irradiation (**Figure 22**). Pre-treatment with ATMi delays significantly RPA70 foci formation after IR indicating the essential function of ATM in the initiation of DNA-end resection (**Figure 22 A**, left panel). Although the level of ATM in DNA-PKcs deficient cells is low, ATM activity is evidently sufficient to trigger this process. This result also shows that ATR alone is not capable to initiate end resection at IR-induced DSBs in G_2 irradiated cells. Nevertheless, inactivation of ATR also reduces RPA70 foci number at the initial times after IR (1-3 hour window) implicating ATR also in initiation of the DNA-end resection. Chemical inhibition of

both ATM and ATR on top of DNA-PKcs deficiency provides the same response on RPA foci kinetics as ATMi alone.

Treatment with ATMi 30 min after exposure of cell to IR does not affect RPA foci number indicating that even after this short time after damage induction, the ATM-dependent contribution to signaling and resection regulation is completed. In contrast, inactivation of ATR 30 min post-IR diminishes significantly the number of RPA foci (**Figure 22 A,** right panel). These results show the key role of ATM for triggering the DNA damage signaling cascade and the response of ATR to ssDNA-RPA structures.

A

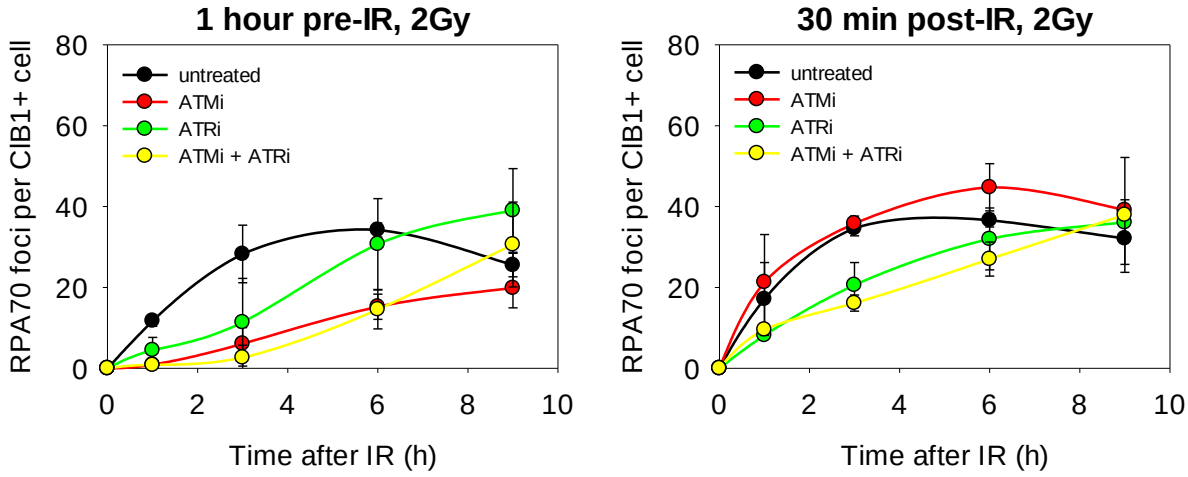

Figure 22: Effect of PIKK kinase inhibitors on RPA foci formation in M059J cells. Cells were treated with inhibitors 1 hour before (left panel) and 30 minutes after irradiation (right panel). ATM and ATR kinase activity was inhibited by 10µM KU55933 and 5µM VE821, respectively, and the inhibitors were left in the media for the duration of the experiment. (**A**) Kinetics of RPA70 foci formation in Cyclin B1 positive cells following exposure to 2Gy. Foci were scored in >30 nuclei per slide. (**B and C,** see below) Representative immunofluorescence images of RPA70 foci (green) in Cyclin B1 positive cells (red). Nuclei were counter-stained with DAPI (blue). Data obtained from two independent experiments (± SD).

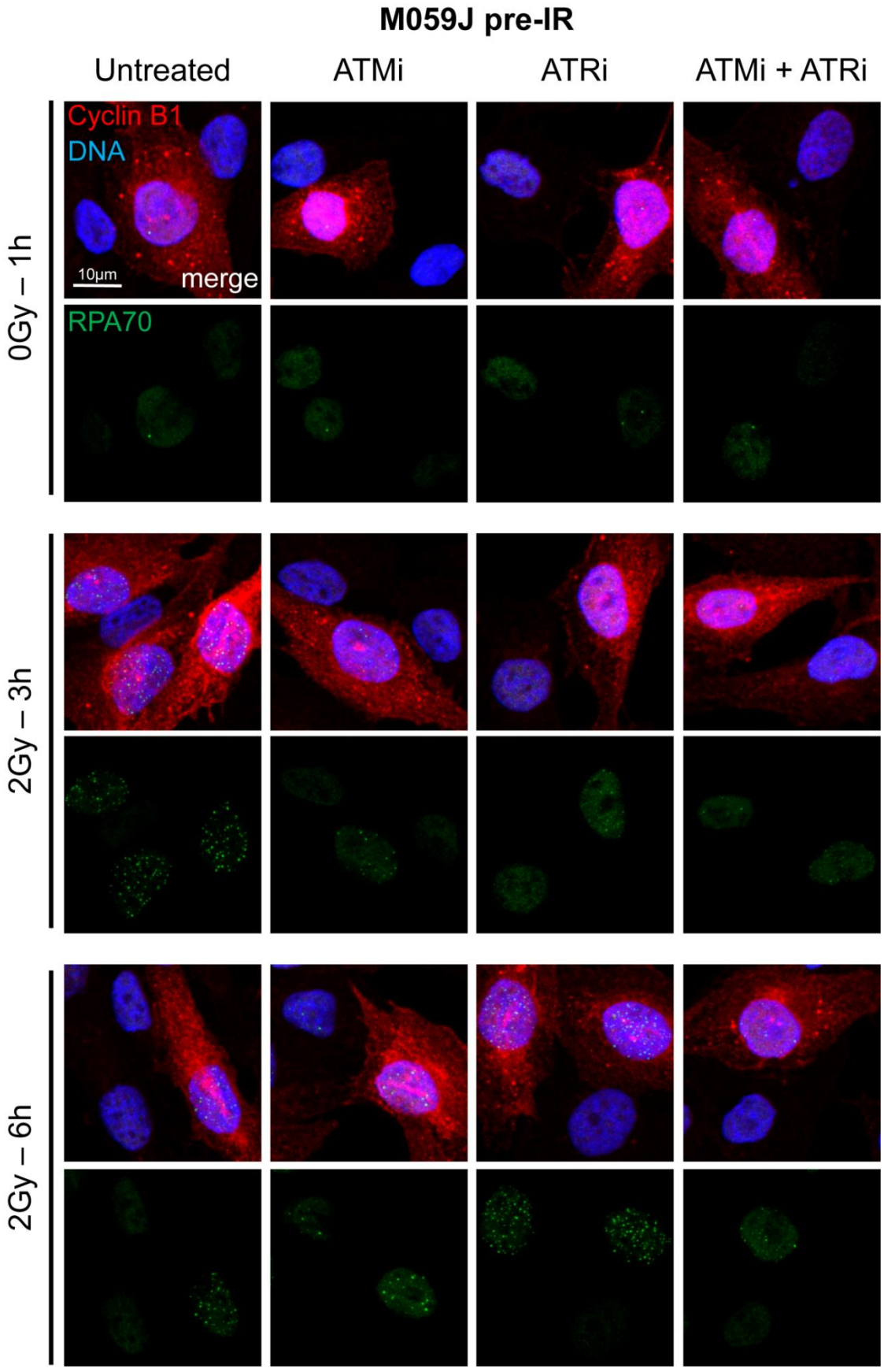

Figure 22B: Representative immunofluorescence images of RPA70 foci corresponding to Figure 22A, left panel

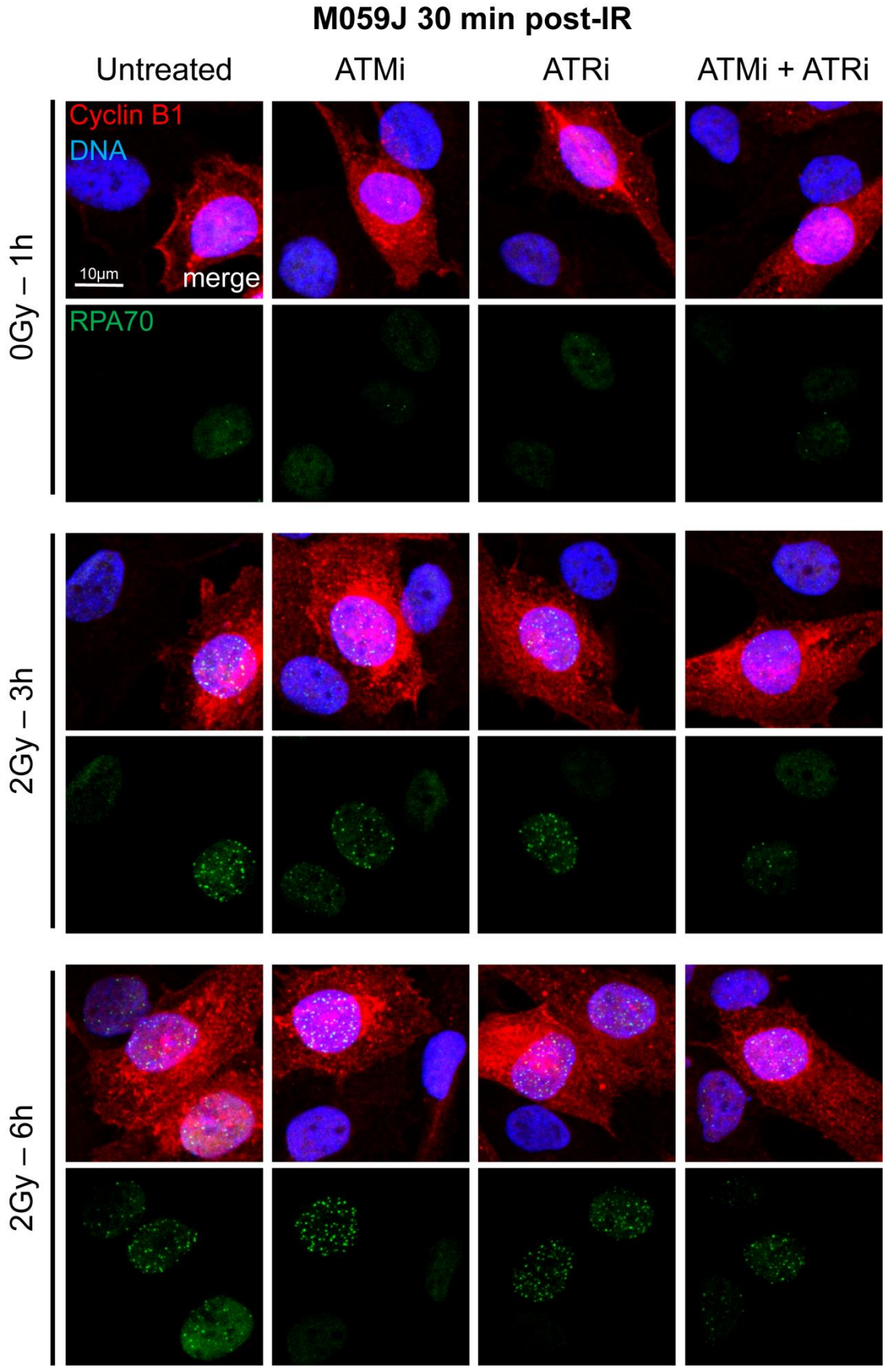

Figure 22C: Representative immunofluorescence images of RPA70 foci corresponding to Figure 22A, right panel

4.7. ATR is required for resection in G_2 phase in normal cells

Based on the observations that ATR may have a central role in G_2 checkpoint development under normal conditions, its activation by ssDNA-RPA structures must be essential.

To further explore the potential role of ATR in regulating the generation of ssDNA-RPA intermediates under normal conditions, similar experiments were performed with normal human fibroblast cell line 82-6 immortalized with hTERT using ATRi (**Figure 23**). Normal cells exposed to 4Gy of IR show similar response in terms of RPA foci kinetics as M059J cells exposed to 2Gy (**Figure 20**).

2.5μM ATRi does not affect RPA foci formation, whereas 5μM and 10μM of ATRi show similar response to that observed in M059J cells, with RPA foci numbers being reduced by a factor of 2. Pre-treatment with 20μM ATRi completely abolishes RPA foci formation. These results clearly show the attenuation of RPA foci formation with increasing concentrations of ATRi reflecting abrogated signaling at DSB ends in absence of ATR catalytic activity despite the presence of ATM activity. Data from our laboratory have shown that the number and intensity of phospho-ATM foci, as well as phosphorylation of CHK2 on Thr68, remain unaffected by ATRi or CHK1i. Seckel syndrome cells also exhibit intact ATM function (216).

A

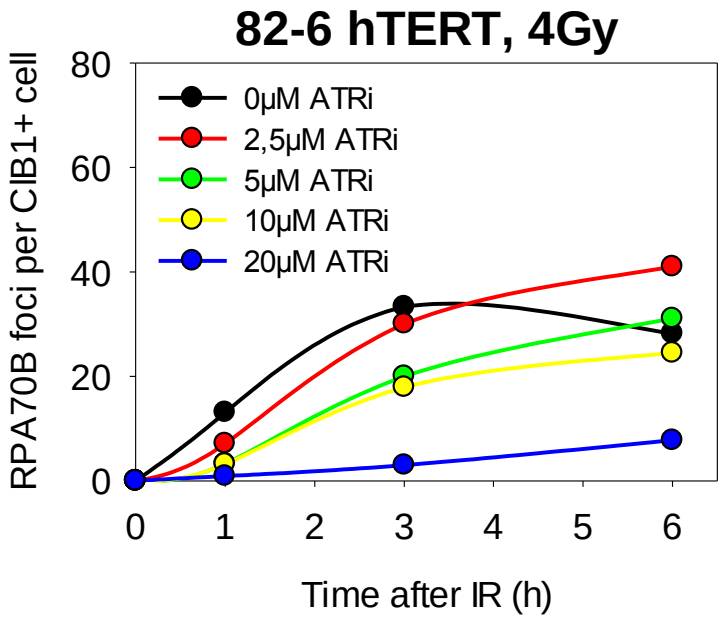

B

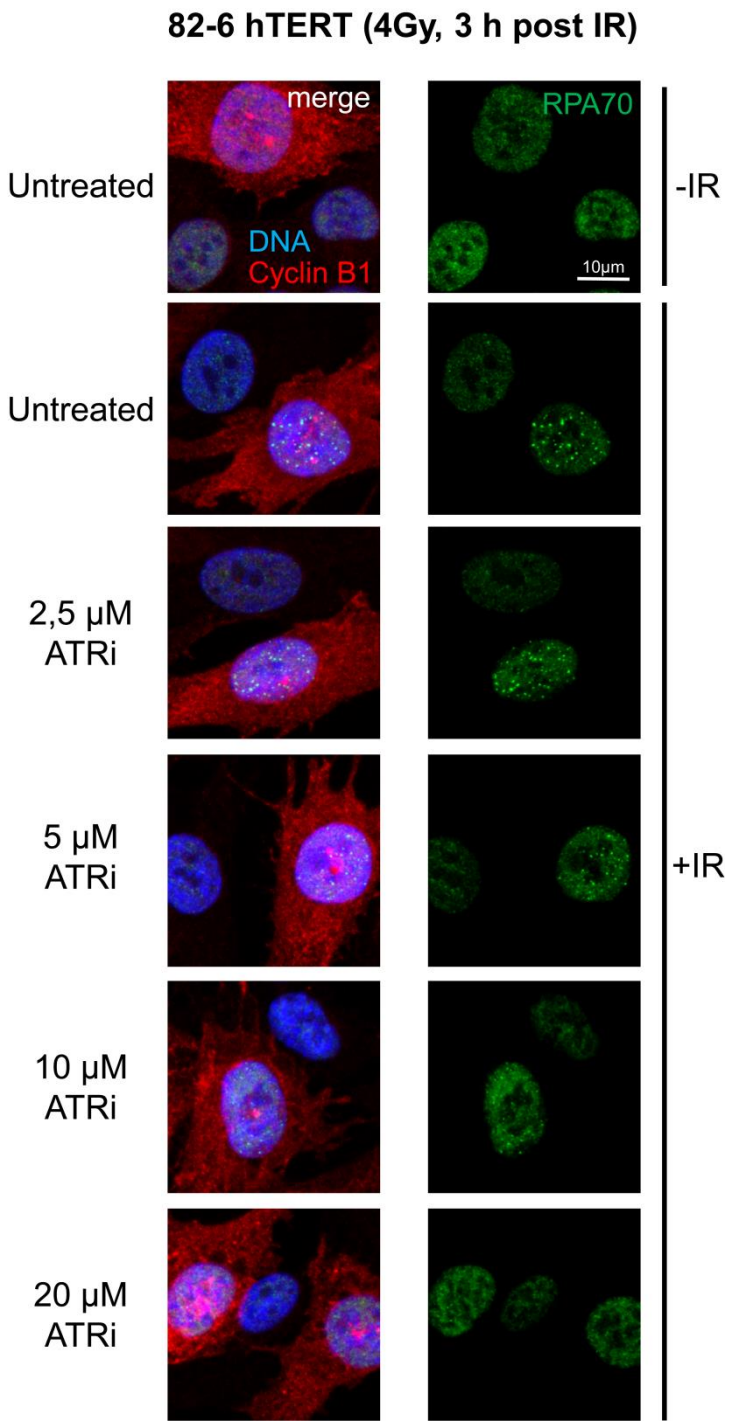

Figure 23: Effect of ATR inhibition on RPA foci formation in normal human fibroblasts. 82-6 cells were pre-treated with different concentrations of ATR inhibitor VE821 1h before exposure to IR and the inhibitor was left in the media for the duration of the experiment. Cells were collected at different time intervals after damage induction. The foci number from the corresponding unirradiated controls at each time point was subtracted. Data obtained from one experiment. (**A**) Kinetics of RPA70 foci formation in Cyclin B1 positive cells following exposure to 4Gy IR. (**B**) Representative immunofluorescence images of RPA70 foci (green) in Cyclin B1 positive cells (red). Nuclei were counter-stained with DAPI (blue).

4.8. Identifying factors involved in the elevated DSB end resection in DNA-PKcs deficient cells

To find out whether DNA-PKcs regulates the activity of enzymes responsible for DSB end resection, a screening of knockdowns of proteins involved in this process was performed – it comprised CtIP, MRN, EXO1 and DNA2. As repair-proficient cells in this experimental design we used normal human fibroblasts 82-6 hTERT.

CtIP has been implicated in initiating DSB end resection, homologous recombination and checkpoint signaling (74). The results show that depletion of CtIP (**Figure 24**) significantly reduces RPA70 foci formation in both cell lines (**Figure 25**).

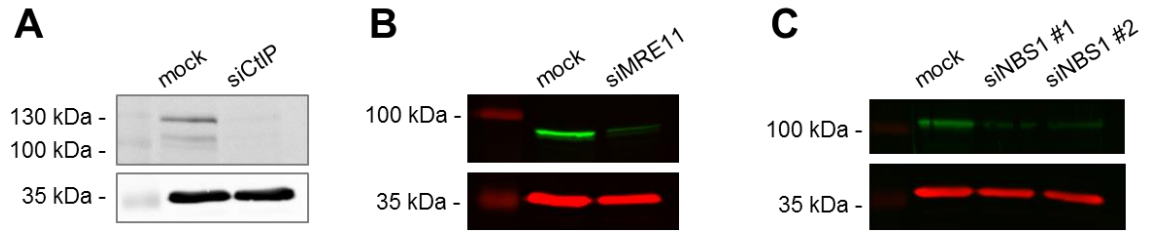

Figure 24: Western blot analysis of siRNA-treated M059J cells. Verification of CtIP (**A**), MRE11 (**B**) and NBS1 (**C**) knock-down efficiency 48 hours after transfection with siRNA. Equal amounts of total protein were loaded per lane (50µg for CtIP, 20µg for MRE11 and 30µg for NBS1 detection). Mock-transfected cells were subjected to nucleofection® program X-01 in the absence of siRNA. For siRNA-mediated depletion of NBS1 were tested two siRNA sequences. Samples were separated on 10% SDS polyacrylamide gel.

The MRN complex is engaged in sensing and signaling of DSBs and has been shown to operate in cooperation with CtIP (217). MRE11 has exo- and endonuclease activity. Therefore, we next sought to knock-down MRE11 and NBS1. The data show that although a sufficient level of knock-down of NBS1 was achieved (**Figure 24**) RPA70 foci formation was decreased in 82-6 hTERT, but not in M059J cells **Figure 26)**.

Similarly, the level of MRE11 depletion was efficient, but did not affect RPA70 foci number in any of the cell lines. However, indicative results were achieved when using the MRE11 inhibitor Mirin in combination with siMRE11, where pronounced effects on resection were recorded (**Figure 26 A, B**).

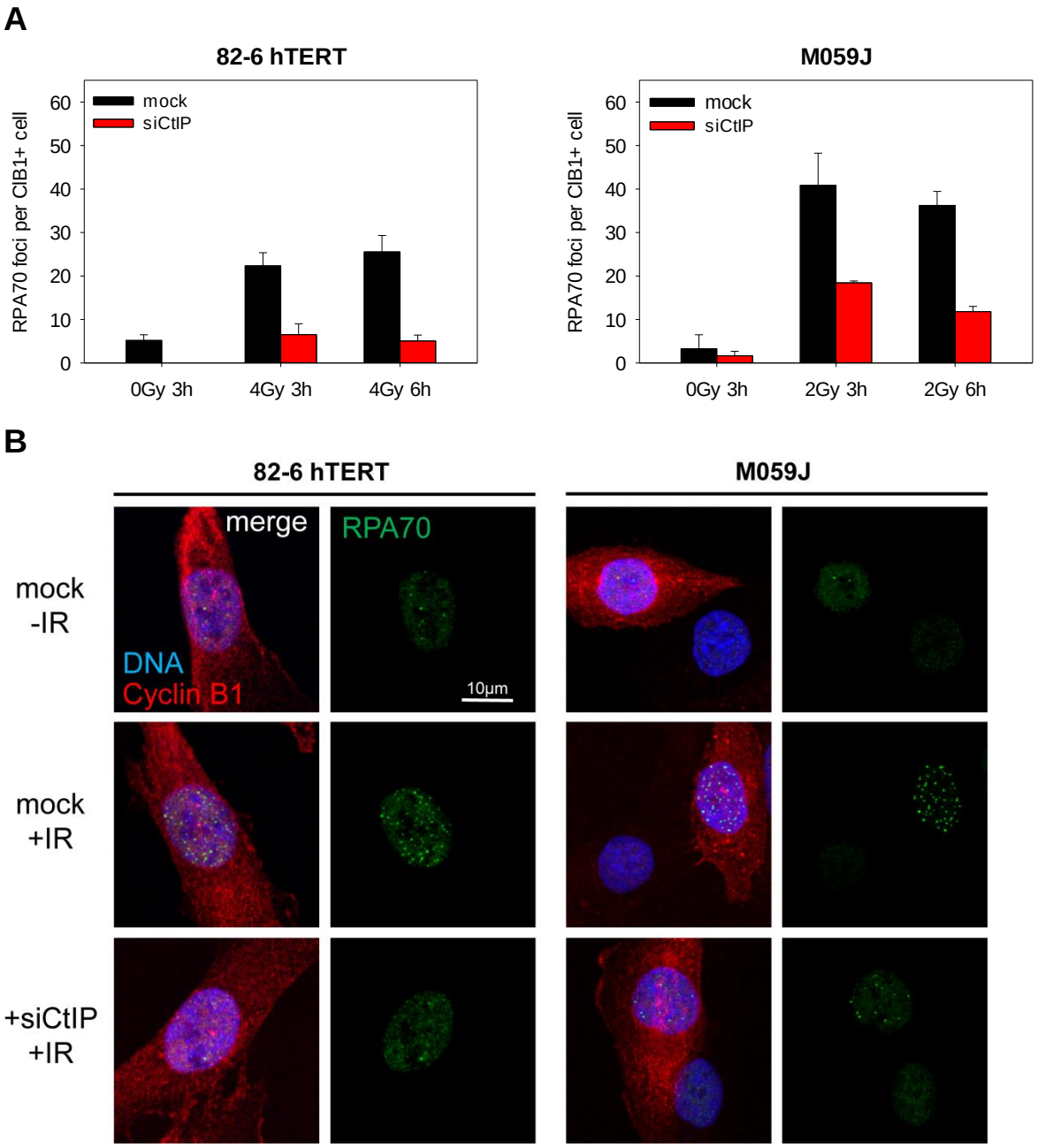

Figure 25: Effect of siRNA-mediated knock-down of CtIP on RPA foci formation. (**A**) RPA foci were scored in 82-6 hTERT and M059J cells positive for Cyclin B1 staining. Mock-nucleofection® was performed in the absence of siRNA. RPA foci formation was followed at 48 hours after transfection. Representative data from one experiment (82-6 hTERT) and one out of two (M059J) experiments (± SE). (**B**) Representative immunofluorescence images of RPA70 foci (green) in Cyclin B1 positive cells (red). Nuclei were counter-stained with DAPI (blue).

A possible explanation for MRE11 depletion alone results is that residual activity is sufficient for the observed effect. The double knock-down of MRE11 and NBS1 did not further affect RPA foci number (**Figure 26 B**, lower panel).

These observations identify MRN complex and CtIP as potential targets of DNA-PK catalytic subunit in the regulation of end resection under normal conditions. Next, we examined long-range resection mediated by EXO1 and DNA2.

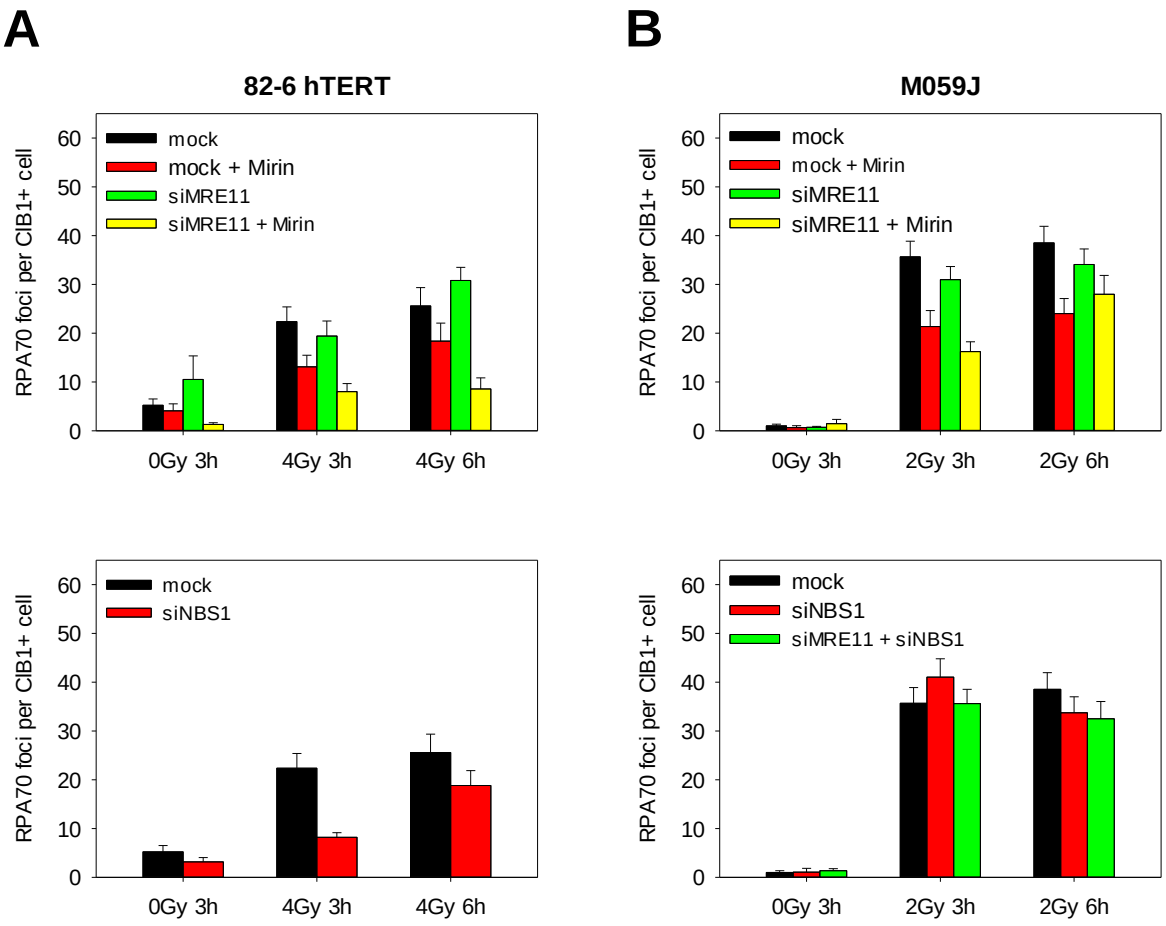

Figure 26: Contribution of MRN complex to DSB end resection. To evaluate the effect of MRN complex on RPA foci formation was applied mRNA interference targeting MRE11 and NBS1, as well as MRE11 inhibitor Mirin (75 mM). RPA foci were scored in 82-6 hTERT (**A**) and M059J (**B**) cells positive for Cyclin B1 staining. Mock-treated cells were exposed to nucleofection® in the absence of siRNA. Cells were irradiated 48 hours after transfection with siRNA. Data obtained from one experiment (± SE).

RPA70 foci formation was not attenuated in M059J cells transfected with different siRNA sequences against EXO1, rather RPA foci number becomes higher at the

6-hour time point after IR. Due to technical difficulties, EXO1 and DNA2 knockdowns could not be validated by western blotting. The effect of EXO1 depletion could be demonstrated in repair-proficient cells, where RPA foci were diminished (**Figure 27 A**).

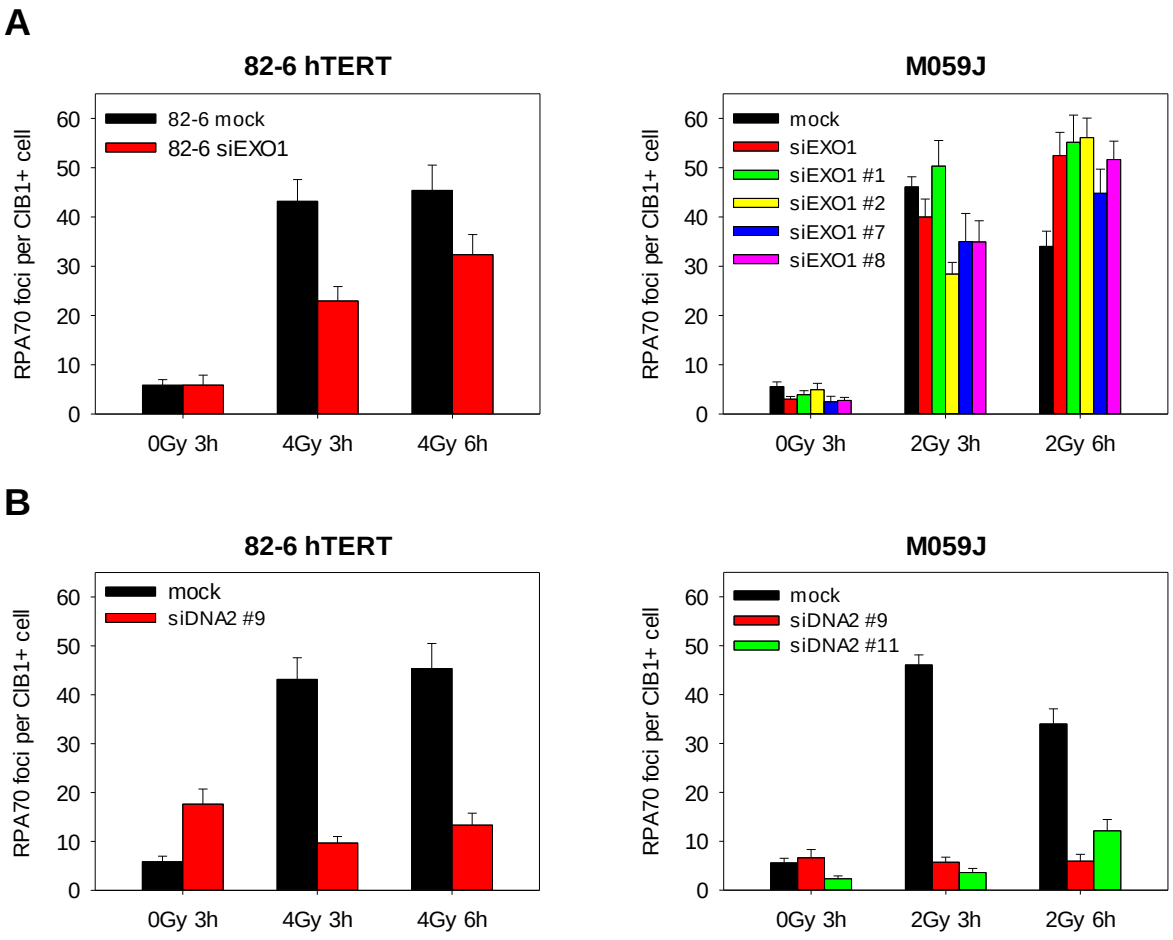

Figure 27: Effect of siRNA-mediated knock-down of EXO1 (A) and DNA2 (B) on RPA foci formation. RPA foci were scored in 82-6 hTERT and M059J cells positive for Cyclin B1 staining 48 hours after transfection with siRNA (± SD). Mock-nucleofection® was performed in the absence of siRNA. Data obtained from one experiment (± SE).

A similar effect is observed in Exo1-deficient cells (**Figure 28**), where RPA foci follow similar kinetics as observed in EXO1-depleted cells. In contrast, siRNA-mediated knockdown of DNA2 leads to very strong effect on RPA foci number in both 82-6 hTERT and M059J cells **Figure 27 B**.

In summary, CtIP, MRN complex and DNA2 stand out as strong candidates to be regulated/phosphorylated by DNA-PKcs.

In conclusion, our results provide evidence that DNA-PKcs regulates actively the G_2 checkpoint response and end resection, a function that does not require the KU70/80 DNA binding factor.

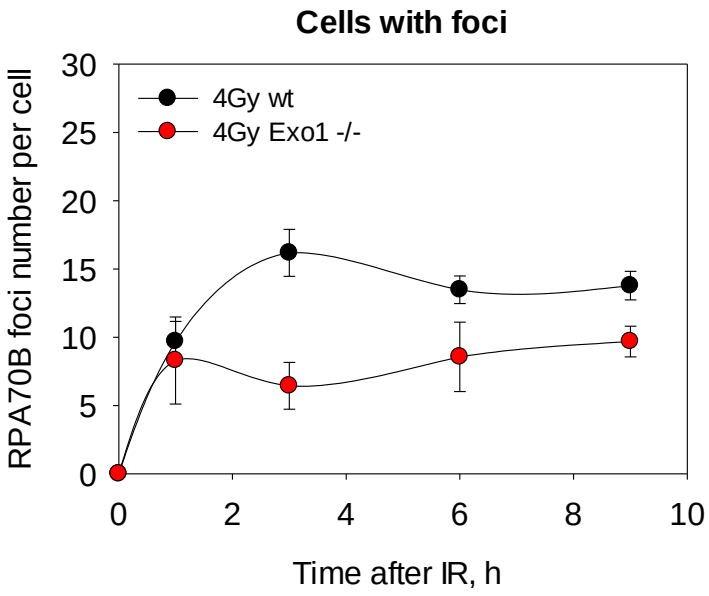

Figure 28: Effect of Exo1 deficiency on RPA foci kinetics. Insertion of Hygromycin cassette between exons 4 and 5 leads to disruption of *Exo1* gene locus in mouse embryonic fibroblasts (MEF) cells (218). Immunofluorescent Cyclin B1 staining in mouse cells was not successful, therefore the analysis of this this experiment were considered only cells with foci. Data obtained from one experiment (± SE).

In addition, our data suggest that in G_2 phase cells both ATM and ATR are required to sustain the checkpoint in response to DSBs since loss of either ATM or ATR causes its abrogation. At higher doses, this dependency is not present. Even more, ATR might not be a passive responder to ssDNA, rather ATR also regulates the end resection process.

Collectively, these data point to a kinase module consisting of ATM, ATR and DNA-PKcs, which regulates and fine-tunes the DNA damage response.

5. DISCUSSION

5.1. Contribution of DNA-PKcs to G_2 checkpoint response

DNA-PKcs is considered a key factor for c-NHEJ but not a component of checkpoint signaling. Our results, however, show that DNA-PKcs deficiency or chemical inactivation results in a hyper-activated checkpoint in cells sustaining damage in both S and G_2 phase of the cell cycle suggesting that DNA-PKcs plays an important role in checkpoint recovery. Inhibition of DNA-PKcs activity has even higher impact on G_2 arrest and decrease of the mitotic index than that of ATM inactivation in both S and G_2 phase cells. In DNA-PKcs deficient cells, the recovery from the checkpoint at 0.1Gy and 0.5Gy is possible although the checkpoint is dramatically prolonged. Interestingly, lack of recovery is observed with increasing radiation dose (*i.e.* at 1Gy and 2Gy). This means that at higher doses of IR the ATM/ATR component is over-activated, which is consistent with the observation that the hyper-activated G_2 checkpoint in DNA-PKcs deficient cells is ATR-dependent in S phase cells, and ATM/ATR dependent in G_2 phase irradiated cells.

Checkpoint activation in G_2 provides additional time for repair. In contrast to HRR, c-NHEJ is not considered to benefit from checkpoint signaling (69, 70). Our observations imply that DNA-PKcs does not control directly checkpoint activation through downstream kinases; rather under normal conditions DNA-PKcs forestalls the process of DNA end resection which triggers ATR and checkpoint activation. This is consistent with the major role of ATR in G_2 checkpoint response. DNA-PKcs deficiency, however, could prolong the time required for repair, as more breaks are resected and would require HR or a-EJ. This would be an indirect contribution of DNA-PKcs to G_2 checkpoint control.

Given the c-NHEJ deficiency of M059J cells, one may speculate that the enhanced G_2 checkpoint activation in these cells is not coupled with DNA-PKcs-deficiency itself; rather this mirrors the extended repair time required by HRR and a-EJ and the higher DSB load shunted in these repair pathways. However, reduced levels of KU70/80 in repair-proficient M059K cells did not affect checkpoint development. Iliakis and colleagues also have shown that the lack of recovery of IR-induced replication arrest,

representing the activation of the S-phase checkpoint, is DNA-PKcs-specific as it is not observed with other components of c-NHEJ (174).

Since DNA-PKcs deficiency is associated with reduced expression of ATM (219), it might be that the enhanced G_2 checkpoint on DNA-PKcs deficient background is due to the low level of ATM. Yet, the ATM level in M059J cells seems to be sufficient for signaling since DNA end resection is significantly abrogated by treatment with ATM inhibitor. In addition, combined treatment of 82-6 fibroblasts with DNA-PKcs and ATM inhibitors completely abrogated the persistent checkpoint induced by DNA-PKcs inhibitor alone, as measured by H3pS10 assay. Moreover, Tomimatsu *et al.* demonstrated the contribution of DNA-PKcs to the development of ATR-mediated checkpoint in ATM-deficient cells, where DNA-PKcs was shown to phosphorylate proteins involved in chromatin remodeling like KAP-1 (176).

Alternatively, DNA-PKcs may contribute actively to G_2 checkpoint regulation through direct interactions with ATM/ATR. Evidence suggests that in response to replication stress DNA-PKcs is required for optimal ATR-CHK1 signaling by regulating CHK1 protein expression and stability of CHK1-Claspin complex (220). *In vitro* studies by Vidal-Eychenie *et al.* also describe interactions between DNA-PKcs and ATR. In their proposed model KU mediates the recruitment of DNA-PKcs to the break, which in turn phosphorylates RPA and promotes ATR activation (221). Hence, abrogation of RPA phosphorylation sites by Alanine residues or treatment with DNA-PKcs inhibitor would affect ATR activation and therewith the checkpoint response, which is indeed not in line with all of our observations. This speculation needs to be carefully examined *in vivo*.

ATM was also shown to be required for the full phosphorylation-mediated activation of DNA-PKcs upon IR where ATM is critical for the phosphorylation of Thr-2609 cluster of DNA-PKcs (165). Whether abrogation of this phosphorylation event influences the G_2 checkpoint activation and maintenance by affecting DNA-PKcs activity deserves further investigation.

In summary, the prolonged checkpoint response observed under DNA-PKcs deficiency in cells sustaining damage in S phase is dependent on ATR. In contrast, this checkpoint activation in G_2 phase cells is abrogated by either ATM or ATR

inhibition, as well as by inactivation of the downstream kinases CHK1 and CHK2. These observations, combined with the data in the literature, suggest a functional crosstalk between DNA-PKcs and ATM/ATR in order to effectively control the G_2 checkpoint. The coordination within the module is abrogated by inhibition of any of these kinases, where only DNA-PKcs deficiency results in prominent G_2 checkpoint arrest - an effect that seems not to be coupled with c-NHEJ deficiency.

5.2. DNA-PKcs influences the G_2 checkpoint activation and maintenance through regulation of DNA end resection

Absence of DNA-PKcs in M059J cells shuttles the DSBs into HRR or a-EJ, which operate with slower kinetics that c-NHEJ. Therefore, the hyper-activated checkpoint response in absence of DNA-PKcs would be favorable for repair pathways that need time. RPA foci analysis by immunofluorescence is an established method for measuring the accumulation of RPA to ssDNA, which is used as a readout for DNA end resection during homologous recombination, and also activates the ATR/CHK1 signaling pathway. Interestingly, the increased resection in M059J system correlates with the enhanced G_2 checkpoint response.

The higher number of RPA foci in DNA-PKcs deficient cells suggests that under normal conditions DNA-PKcs suppresses end resection in G_2 phase and therewith homologous recombination. This agrees with a study by Nickoloff and colleagues, showing that DNA-PKcs suppresses HR as measured by HR substrates containing I-*Sce*I sites in DNA-PKcs defective Chinese hamster ovary (V3) cells and isogenic derivatives complemented with human DNA-PKcs cDNA. Complementation of DNA-PKcs resulted in lower levels of both DSB-induced and spontaneous HR frequencies (222). Moreover, DNA-PK's ability to suppress HR was shown to be dependent on its kinase activity, where its phosphorylation status is thought to help define the repair pathway choice. Thereby, phosphorylation of the ABCDE cluster seems to be of great importance for promoting HR, while phosphorylation of the PQR cluster would inhibit it (135, 138).

Moreover, unpublished data from our laboratory have shown that RAD51 foci in DNA-PKcs deficient M059J cell line also increase, when compared to repair-proficient M059K cells, and remain unresolved at later time points after IR, meaning

that HR in M059J cells could be aberrant. A study by Dip and Naegeli has shown that DNA-PKcs can recognize and associate with synthetic four-way Holliday junctions independently of KU70/80 and DNA ends (223). Given the higher residual number of RAD51 foci in M059J cells, this suggests that DNA-PKcs deficiency may be associated with abrogation of homologous recombination at the step of Holliday junction resolution. It is therefore plausible that DNA-PKcs may also regulate proteins involved in branch migration or Holliday junction resolution during homologous recombination. Hence, in cells with DNA-PKcs deficient background the persistent RPA foci may result from branch migration in the wrong direction.

Since HR requires extensive chromatin modifications, it is also possible that HR is abrogated in the absence of DNA-PKcs because more breaks are committed to be repaired by HR and chromatin opens up which may destabilize it. This assumption is supported by the higher residual number of γH2AX foci associated with DNA-PKcs deficiency (unpublished data from our laboratory).

The kinetics of RPA foci formation in repair-proficient M059K cells treated with the DNA-PKcs inhibitor does not completely resemble the phenotype observed in M059J cells where DNA-PKcs is absent. Increase of RPA foci number is observed at later times, which may be explained by NU7441 preventing DNA-PK's auto-phosphorylation and therewith its dissociation from the ends. Blocking the DNA ends in turn may hamper not only NHEJ but also HR by restricting the function of exonucleases. Nevertheless, the data from this experiment further imply that the catalytic activity of DNA-PKcs suppresses extensive resection of the DSB ends.

The experiments with siRNA-mediated KU70 knockdown in M059K cells provide evidence that DNA-PKcs may be activated in the absence of its regulatory subunit KU70/80, which is believed to recruit DNA-PKcs to DNA ends. Together, these results lead to a possible model shown on **Figure 29 (1)**, where under normal conditions DNA-PKcs downregulates resection independently of KU70/80. Nevertheless, it could be that despite the marked reduction of KU70/80 expression by approximately 90 %, very low level of KU70/80 is needed to secure recruitment of DNA-PKcs to DSBs. Indeed, this model is further supported by the evidence suggesting that under low salt conditions DNA-PKcs is capable of binding DNA ends

and becomes activated independently of KU70/80 (144). Meek *et al.* also reported a strong enzymatic activation of DNA-PKcs independently of DNA and KU70/80 through a conformational change of its N-terminus (162).

(2) The substantial increase of RPA foci in DNA-PKcs deficient cells leads to a second hypothesis suggesting that once KU70/80 is bound to DNA, the absence of DNA-PKcs may be favorable for the recruitment of other DNA repair factors. There is data suggesting that the KU-MRE11 interaction after IR is stronger under these conditions (224), although other studies show the opposing results (99). It is therefore conceivable that loss of DNA-PKcs may potentiate the interaction between KU and the MRN complex, which then can recruit ATM and CtIP to initiate resection. Whether this possible interaction of KU-MRN is sufficient for initiating resection in the absence of DNA-PKcs needs to be consolidated.

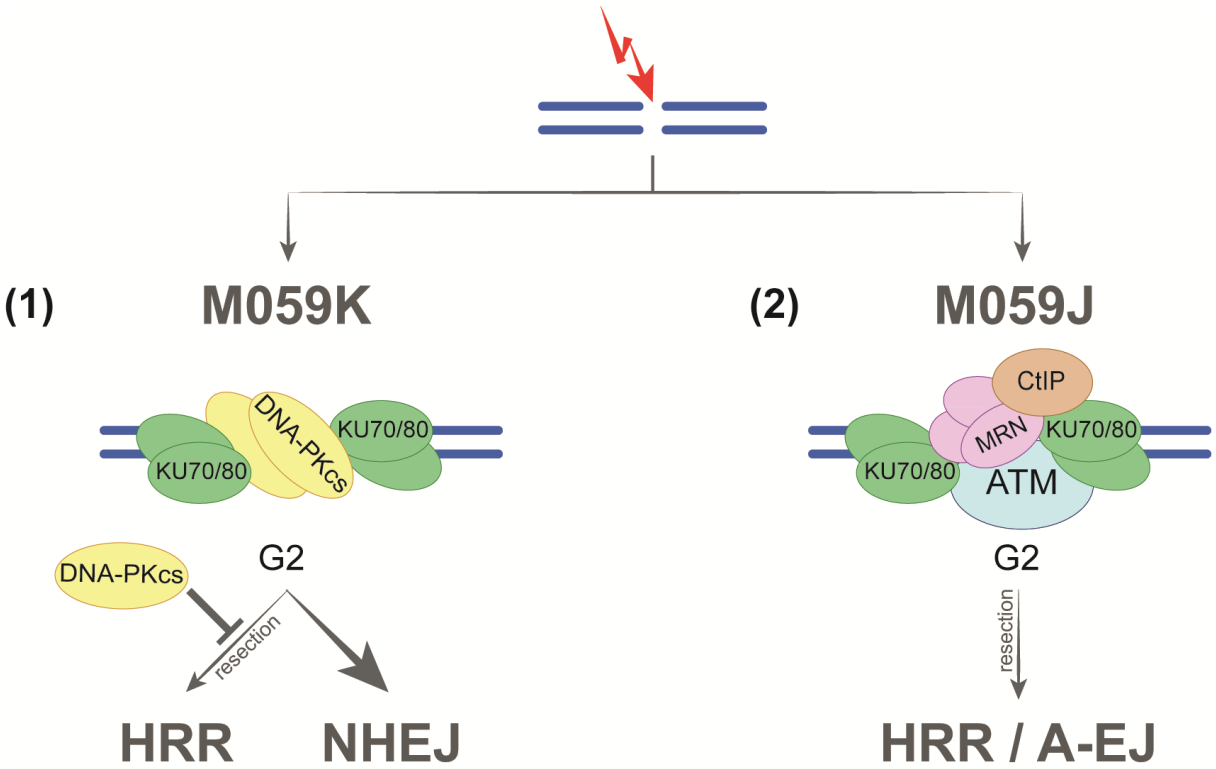

Figure 29: Two possible models for downregulation of DNA end resection by DNA-PK catalytic subunit. (**1**) Under basal conditions, DNA-PKcs may regulate end resection in G_2 phase independently of KU70/80. (**2**) Resection factors might gain profit from the absence of DNA-PKcs.

Nevertheless, the KU heterodimer was reported to negatively regulate HRR by blocking the ends for resection (214, 225). Moreover, KU deficiency was shown to be associated with remarkably increased DSB-induced HR when compared to cells lacking DNA-PKcs, as measured using the DR-GFP reporter (226). The data from our experiments do not support the role of KU-binding factor alone in suppressing initiation of resection and HR, not only under normal conditions but also in cells with deficient DNA-PKcs. However, this conclusion could not be reached with mouse cells depleted of KU70, where deficiency of KU70 results in marked increase of RPA and RAD51 foci number in comparison to the control (unpublished data from our laboratory).

While this work was in progress, an *in vitro* study by Zhou and Paull demonstrated that DNA-PKcs, together with MRN and ATM, regulates resection, where MRN can overcome the inhibitory activity of DNA-PKcs on EXO1 (227). Our data also link DNA-PKcs to MRN and CtIP in initiating resection since knockdown of either CtIP or abrogation of MRN activity in M059J cells reduces RPA foci number. However, the nuclease responsible for the long-range resection in M059J cells appears to be DNA2. Transfection of M059J cells with two different siRNA sequences against DNA2 resulted in a significant decrease of RPA foci number, while depletion of EXO1 showed a prominent effect on RPA foci number in 82-6 fibroblasts but not in M059J cells.

In conclusion, hyper-resection in DNA-PKcs deficient M059J cells shunts DSBs in G_2 phase toward HRR or a-EJ, which also explains the higher number of translocations in DNA-PKcs deficient cells (unpublished data from our laboratory). Our observations suggest that DNA-PKcs regulates the process of DNA resection, thus implicating its enzymatic activities in both c-NHEJ and HRR.

5.3. DNA-PKcs-deficiency does parallel its chemical inactivation

Our results clearly indicate that in case of G_2 checkpoint small molecule DNA-PKcs inhibitor has identical effect on G_2 arrest as the absence of DNA-PKcs protein. However, at the resection level, chemical inactivation of DNA-PKcs does not completely parallel the effect on RPA foci observed in DNA-PKcs deficient cells. The latter implies that enzymatically inactive DNA-PKcs associated with the break has an

inhibitory effect on HR by suppressing resection. This result is reminiscent of a study describing an 'interactive competition' between HR and NHEJ by using another specific DNA-PK inhibitor (136).

Consequently, DNA-PKcs may regulate checkpoint response independently of KU70/80. Thus, the hyper-activated checkpoint after treatment with the DNA-PKcs inhibitor, or DNA-PKcs deficiency, provides time for repair by HRR or a-EJ, but resection of DSB ends originally directed to c-NHEJ is limited since exonucleases have no access to the ends. This may explain why in the case of DNA-PKcs' chemical inhibition in M059K checkpoint activation does not correlate with the rate of resection as observed in M059J cells.

5.4. A model integrating ATR, ATM and DNA-PKcs to effectively control G_2 checkpoint and DNA end resection

ATM is thought to be central to DNA damage signaling (39). The sequential engagement of ATM and ATR in DNA damage response is well described in the literature where ATM is believed to be the primary kinase initiating end resection (228, 229). It is therefore not surprising that in normal cells deficiency of ATM leads to abrogated checkpoint in cells sustaining damage in G_2 phase. With increasing the DSB load, the role of ATM in sustaining the checkpoint becomes more prominent. ATM deficiency or inactivation of ATM activity by specific inhibitors is also associated with delayed formation of RPA foci.

DSB repair by HR requires resection of the ends, which then triggers ATR activation. Since in higher eukaryotes only ~10-20% of the DSBs are thought to be repaired by HR (230), the contribution of ATR in checkpoint development in response to DSBs is typically thought to be limited. Although ATR is assigned to DNA replication stress and requires ssDNA for activation in response to DSBs, our data provide compelling evidence that ATR is also essential for checkpoint activation and maintenance in response to IR. This observation places the role of ATR beyond the replication checkpoint control.

Moreover, the reduction of RPA foci number in the presence of ATR inhibitor in both 82-6 fibroblasts and M059J cells implies that ATR may not be a passive responder to

resection; rather ATR might actively regulate the initiation of end resection process. Kousholt *et al.* have shown that the rapid activation of ATR downstream target CHK1 precedes initiation of resection. In addition, CtIP-mediated end resection was shown to be required for the sustained checkpoint signaling but not for its initiation, which leads to the assumption that checkpoint activation is independent of end resection and points to the above indicated role of ATM (231).

Furthermore, CHK1 inhibition results in residual checkpoint activation at the early time points after IR. Despite this small initial drop of the mitotic index, ATR seems to be involved in G_2 checkpoint activation and maintenance predominantly through CHK1 (232).

Since both ATM and ATR promote end resection in G_2 phase and checkpoint response, inhibition of each of them results in abrogation of both G_2 checkpoint response and of end resection. Unlike ATM and ATR, DNA-PKcs deficiency results in enhanced G_2 checkpoint activation combined with excessive DSB end resection. This suggests that ATM/ATR and DNA-PKcs have opposing roles in the process of resection. Under normal conditions DNA-PKcs prevents ATR upregulation and over-resection that may be unfavorable for c-NHEJ. The upregulation of ATR activity in DNA-PKcs deficient background but also in ATM deficient cells (233) suggests that ATM and ATR cannot substitute DNA-PKcs for the recovery from the checkpoint.

Together, our data demonstrate the contribution of DNA-PKcs to G_2 checkpoint and end resection suggesting that DNA-PKcs is involved in a functional kinase module together with ATM/ATR in order to effectively control the DNA damage response and optimize end processing. Based on our observations, if the DNA-PKcs component of this module is missing, which is also associated with reduced ATM level, the cell tries to ‘compensate’ for its absence via up-regulation of ATR. In addition, under normal conditions DNA-PKcs may regulate homologous recombination through ATR. Although the view about ‘mechanistic/direct competition between NHEJ and HR’ in DSB repair is strengthened by many publications (135, 222, 226, 234, 235), we suggest that pathway choice is not only dictated by the cell cycle phase and chromatin status; rather it is a highly regulated process by all three PIKK kinases. In

this module ATR seems to have a complete control on G_2 checkpoint response and also to regulate resection. The exact mechanism remains to be elucidated.

6. SUMMARY

The data from our experiments revealed that DNA-PKcs deficiency is associated with persistent G_2 checkpoint that in cells sustaining damage in S phase of the cell cycle is dependent on ATR, while in cells irradiated in G_2 phase it strongly relies on both ATM/ATR. The hyper-activation of the G_2 checkpoint seems to be DNA-PKcs-specific as it is not observed after depletion of KU70/80, and is associated with enhanced resection at IR-generated DSBs as analyzed by RPA foci formation. However, chemical inactivation of DNA-PKcs does not completely replicate the increased level of RPA foci observed in DNA-PKcs deficient cells. Nevertheless, this result suggests that the DNA-PKcs' catalytic function may be essential in order to actively regulate the process of DNA end resection.

To identify potential targets of DNA-PKcs in DSB end resection, we applied RNAi screening and found that CtIP, MRN complex and DNA2 nuclease/helicase are good candidates to be regulated by DNA-PKcs kinase activity. Subsequent *in vitro*, as well as immunoprecipitation experiments are needed to confirm the interaction of DNA-PKcs with the proposed targets.

Administration of specific ATM and ATR kinase inhibitors as well as inhibitors of their downstream targets CHK1 and CHK2 revealed that ATM inactivation is associated with less enhanced G_2 checkpoint activation and significant decrease of DNA end resection following exposure to IR in comparison to elimination of DNA-PKcs activity. Interestingly, the data also point to contribution of ATR in the regulation of G_2 checkpoint and DNA end resection through CHK1 not only in DNA-PKcs deficient but also in normal cells, suggesting that ATR does not only passively respond to ssDNA but may actively regulate the initial steps of these processes.

Collectively, these results link DNA-PKcs to checkpoint response activation via regulation of DNA end resection and imply a cross-talk between the three PIKK kinases ATM, ATR and DNA-PKcs.

REFERENCES

1. Hall EJ, Giaccia AJ. Radiobiology for the Radiologist. Sixth Edition ed. Philadelphia, Baltimore, New York, London, Buenos Aires, Hong Kong, Sydney, Tokyo: Lippincott Williams & Wilkins; 2006.

2. Khanna KK, Jackson SP. DNA double-strand breaks: signaling, repair and the cancer connection. Nat Genet. 2001;27:247-54.

3. Madabhushi R, Gao F, Pfenning AR, Pan L, Yamakawa S, Seo J, et al. Activity-Induced DNA Breaks Govern the Expression of Neuronal Early-Response Genes. Cell. 2015;161(7):1592-605.

4. Friedberg EC, Walker GC, Siede W, Wood RD, Schultz RA, Ellenberger T. DNA Repair and Mutagenesis. Second Edition ed. Washington, D.C.: ASM Press; 2006.

5. Vamvakas S, Vock EH, Lutz KW. On the role of DNA double-strand breaks in toxicity and carcinogenesis. Critical Reviews in Toxicology. 1997;27:155-74.

6. Fuks Z, Weichselbaum RR. Radiation Therapy. In: Mendelsohn J, Howley PM, Israel MA, Liotta LA, editors. The Molecular Basis of Cancer. Philadelphia, London, Toronto, Montreal, Sydney, Tokyo: W.B. Saunders Company; 1995. p. 401-31.

7. Pawlik TM, Keyomarsi K. Role of cell cycle in mediating sensitivity to radiotherapy. International journal of radiation oncology, biology, physics. 2004;59(4):928-42.

8. Schipler A, Iliakis G. DNA double-strand-break complexity levels and their possible contributions to the probability for error-prone processing and repair pathway choice. Nucleic Acids Res. 2013;41(16):7589-605.

9. Morgan DO. The Cell Cycle - Principles of control. London: New Science Press Ltd; 2007. 297 p.

10. Hartwell LH, Weinert TA. Checkpoints: Controls that ensure the order of cell cycle events. Science. 1989;246:629-34.

11. Rao P, Johnson RT. Mammalian cell fusion: Studies on the regulation of DNA synthesis and mitosis. Nature. 1970;225:159-64.

12. Liskay RM. Absence of a measurable G2 phase in two Chinese hamster cell lines. Proceedings of the National Academy of Sciences of the United States of America. 1977;74(4):1622-5.

13. Morgan DO. Principles of CDK regulation. Nature. 1995;374:131-4.

14. Satyanarayana A, Kaldis P. Mammalian cell-cycle regulation: several Cdks, numerous cyclins and diverse compensatory mechanisms. Oncogene. 2009;28:2925-39.

15. Fisher RP, Morgan DO. A novel cyclin associates with MO15/CDK7 to form the CDK-activating kinase. Cell. 1994;78:713-24.

16. Nigg EA. Cyclin-dependent kinase 7: at the cross-roads of transcription, DNA repair and cell cycle control? Current opinion in cell biology. 1996;8(3):312-7.

17. Murray A. Cyclin Ubiquitination: The destructive end of mitosis. Cell. 1995;81:149-52.

18. Lukas J, Lukas C, Bartek J. Mammalian cell cycle checkpoints: signalling pathways and their organization in space and time. DNA Repair. 2004;3:997-1007.

19. Bartek J, Lukas C, Lukas J. Checking on DNA damage in S phase. Nature reviews Molecular cell biology. 2004;5(10):792-804.

20. Kastan MB, Bartek J. Cell-cycle checkpoints and cancer. Nature. 2004;432:316-23.

21. Zhou BB, Elledge SJ. The DNA damage response: putting checkpoints in perspective. Nature. 2000;408:433-9.

22. Iliakis G, Wang Y, Guan J, Wang H. DNA damage checkpoint control in cells exposed to ionizing radiation. Oncogene. 2003;22:5834-47.

23. Ciccia A, Elledge SJ. The DNA Damage Response: Making It Safe to Play with Knives. Mol Cell. 2010;40(2):179-204.

24. Volkmer E, Karnitz LM. Human Homologs of Schizosaccharomyces pombe Rad1, Hus1, and Rad9 Form a DNA Damage-responsive Protein Complex. J Biol Chem. 1999;274:567-70.

25. Wang Q, Goldstein M, Alexander P, Wakeman TP, Sun T, Feng J, et al. Rad17 recruits the MRE11-RAD50-NBS1 complex to regulate the cellular response to DNA double-strand breaks. EMBO J. 2014;33(8):862-77.

26. Wang Y, Cortez D, Yazdi P, Neff N, Elledge SJ, Qin J. BASC, a super complex of BRCA1-associated proteins involved in the recognition and repair of aberrant DNA structures. Genes Dev. 2000;14:927-39.

27. Cimprich KA, Cortez D. ATR: an essential regulator of genome integrity. Nat Rev Mol Cell Biol. 2008;9(8):616-27.

28. Maréchal A, Zou L. DNA Damage Sensing by the ATM and ATR Kinases. Cold Spring Harb Perspect Biol. 2013;5(9):a12716.

29. McKinnon PJ. ATM and ataxia telangiectasia. EMBO Rep. 2004;5:772-6.

30. Kastan MB, Lim DS. The many substrates and functions of ATM. Nature reviews Molecular cell biology. 2000;1(3):179-86.

31. Löbrich M, Jeggo PA. The impact of a negligent G2/M checkpoint on genomic instability and cancer induction. Nat Rev Cancer. 2007;7(11):861-9.

32. Cliby WA, Roberts CJ, Cimprich KA, Stringer CM, Lamb JR, Schreiber SL, et al. Overexpression of a kinase-inactive ATR protein causes sensitivity to DNA-damaging agents and defects in cell cycle checkpoints. EMBO J. 1998;17(1):159-69.

33. Brown EJ, Baltimore D. *ATR* disruption leads to chromosomal fragmentation and early embryonic lethality. Genes Dev. 2000;14(4):397-402.

34. de Klein A, Muijtjens M, van Os R, Verhoeven Y, Smit B, Carr AM, et al. Targeted disruption of the cell-cycle checkpoint gene ATR leads to early embryonic lethality in mice. Curr Biol. 2000;10(8):479-82.

35. O'Driscoll M, Ruiz-Perez VL, Woods CG, Jeggo PA, Goodship JA. A splicing mutation affecting expression of ataxia-telangiectasia and Rad3-related protein (ATR) results in Seckel syndrome. Nat Genet. 2003;33:497-501.

36. Alderton GK, Joenje H, Varon R, Borglum AD, Jeggo PA, O'Driscoll M. Seckel syndrome exhibits cellular features demonstrating defects in the ATR-signalling pathway. Hum Mol Genet. 2004;13(24):3127-38.

37. Lee JH, Paull TT. Activation and regulation of ATM kinase activity in response to DNA double-strand breaks. Oncogene. 2007;26(56):7741-8.

38. Bakkenist CJ, Kastan MB. Chromatin perturbations during the DNA damage response in higher eukaryotes. DNA Repair. 2015;in press.

39. Lavin MF. Ataxia-telangiectasia: from a rare disorder to a paradigm for cell signalling and cancer. Nat Rev Mol Cell Biol. 2008;9(10):759-69.

40. Cortez D, Guntuku S, Qin J, Elledge SJ. ATR and ATRIP: Partners in Checkpoint Signaling. Science. 2001;294:1713-6.

41. Zou L, Elledge SJ. Sensing DNA Damage Through ATRIP Recognition of RPA-ssDNA Complexes. Science. 2003;300:1542-8.

42. Kumagai A, Lee J, Yoo HY, Dunphy WG. TopBP1 Activates the ATR-ATRIP Complex. Cell. 2006;124(5):943-55.

43. Lee J, Kumagai A, Dunphy WG. The Rad9-Hus1-Rad1 checkpoint clamp regulates interaction of TopBP1 with ATR. J Biol Chem. 2007;282(38):28036-44.

44. Shiotani B, Zou L. ATR signaling at a glance. J Cell Sci. 2009;122:301-4.

45. Yoo HY, Kumagai A, Shevchenko A, Shevchenko A, Dunphy WG. Ataxia-telangiectasia Mutated (ATM)-dependent Activation of ATR Occurs through Phosphorylation of TopBP1 by ATM. J Biol Chem. 2007;282(24):17501-6.

46. Abraham RT. Cell cycle checkpoint signaling through the ATM and ATR kinases. Genes Dev. 2001;15:2177-96.

47. Hickman ES, Moroni MC, Helin K. The role fo p53 and pRB in apoptosis and cancer. Curr Opin Genet Dev. 2002;12:60-6.

48. Albrechtsen N, Dornreiter I, Grosse F, Kim E, Wiesmüller L, Deppert W. Maintenance of genomic integrity by p53: complementary roles for activated and non-activated p53. Oncogene. 1999;18:7706-17.

49. Bartek J, Lukas J. Chk1 and Chk2 kinases in checkpoint control and cancer. Cancer Cell. 2003;3(5):421-9.

50. Muschel RJ, Zhang HB, Iliakis G. Cyclin B expression in HeLa cells during the G2 block induced by ionizing radiation. Cancer Res. 1991;51:5113-7.

51. Muschel RJ, Zhang HB, Iliakis G, McKenna WG. Effects of ionizing radiation on cyclin expression in HeLa cells. Radiat Res. 1992;132:153-7.

52. Pines J, Hunter T. Human cyclins A and B1 are differentially located in the cell and undergo cell cycle-dependent nuclear transport. J Cell Biol. 1991;115:1-17.

53. Chen Y, Chen P-L, Chen C-F, Jiang X, Riley DJ. Never-in-mitosis related kinase 1 functions in DNA damage response and checkpoint control. Cell Cycle. 2008;7(20):3194-201.

54. Chen Y, Chen C-F, Riley DJ, Chen P-L. Nek1 kinase functions in DNA damage response and checkpoint control through a pathway independent of ATM and ATR. Cell Cycle. 2011;10(4):655-63.

55. Wang H, Zhao-Chong Z, Perrault AR, Cheng X, Qin W, Iliakis G. Genetic evidence for the involvement of DNA ligase IV in the DNA-PK-dependent pathway of non-homologous end joining in mammalian cells. Nucleic Acids Res. 2001;29:1653-60.

56. Lieber MR. The Mechanism of Double-Strand DNA Break Repair by the Nonhomologous DNA End-Joining Pathway. Annu Rev Biochem. 2010;79:1.-.31.

57. Andres SN, Vergnes A, Ristic D, Wyman C, Modesti M, Junop M. A human XRCC4–XLF complex bridges DNA. Nucleic Acids Res. 2012;40(4):1868-78.

58. Roy S, Andres SN, Vergnes A, Neal JA, Xu Y, Yu Y, et al. XRCC4's interaction with XLF is required for coding (but not signal) end joining. Nucleic Acids Res. 2012;40(4):1684-94.

59. Roy S, de Melo AJ, Xu Y, Tadi SK, Négrel A, Hendrickson E, et al. XRCC4/XLF Interaction Is Variably Required for DNA Repair and Is Not Required for Ligase IV Stimulation. Mol Cell Biol. 2015;35(17):3017-28.

60. Ochi T, Blackford AN, Coates J, Jhujh S, Mehmood S, Tamura N, et al. PAXX, a paralog of XRCC4 and XLF, interacts with Ku to promote DNA double-strand break repair. Science. 2015;347(6218):185-8.

61. Xing M, Yang M, Huo W, Feng F, Wei L, Jiang W, et al. Interactome analysis identifies a new paralogue of XRCC4 in non-homologous end joining DNA repair pathway. Nat Commun. 2015;6:6233.

62. Lieber MR, Ma Y, Pannicke U, Schwarz K. The mechanism of vertebrate nonhomologous DNA end joining and its role in V(D)J recombination. DNA Repair. 2004;3:817-26.

63. Lieber MR, Yu K, Raghavan SC. Roles of nonhomologous DNA end joining, V(D)J recombination, and class switch recombination in chromosomal translocations. DNA Repair. 2006;5(9-10):1234-45.

64. Jette N, Lees-Miller SP. The DNA-dependent protein kinase: A multifunctional protein kinase with roles in DNA double strand break repair and mitosis. Prog Biophys Mol Biol. 2015;117(2-3):194-205.

65. Dueva R, Iliakis G. Alternative pathways of non-homologous end joining (NHEJ) in genomic instability and cancer. Transl Cancer Res. 2013;2(3):163-77.

66. Simsek D, Jasin M. Alternative end-joining is suppressed by the canonical NHEJ component Xrcc4-ligase IV during chromosomal translocation formation. Nat Struct Mol Biol. 2010;17(4):410-6.

67. Burma S, Chen BPC, Chen DJ. Role of non-homologous end joining (NHEJ) in maintaining genomic integrity. DNA Repair. 2006;5(9-10):1042-8.

68. Ferguson DO, Sekiguchi JM, Chang S, Frank KM, Gao Y, DePinho RA, et al. The nonhomologous end-joining pathway of DNA repair is required for genomic stability and the suppression of translocations. Proc Natl Acad Sci USA. 2000;97(12):6630-3.

69. Wang X, Wang H, Iliakis G, Wang Y. Caffeine-induced radiosensitization is independent of non-homologous end joining of DNA double strand breaks. Radiat Res. 2003;159:426-32.

70. Wang H, Wang H, Powell SN, Iliakis G, Wang Y. ATR Affecting Cell Radiosensitivity Is Dependent on Homologous Recombination Repair but Independent of Nonhomologous End Joining. Cancer Res. 2004;64:7139-43.

71. San Filippo J, Sung P, Klein H. Mechanism of Eukaryotic Homologous Recombination. Annu Rev Biochem. 2008;77:229-57.

72. Mimitou EP, Symington LS. DNA end resection: Many nucleases make light work. DNA Repair. 2009;8(9):983-95.

73. D'Amours D, Jackson SP. The Mre11 Complex: At the Crossroads of DNA Repair and Checkpoint Signalling. Nature Reviews. 2002;3:317-27.

74. Sartori AA, Lukas C, Coates J, Mistrik M, Fu S, Bartek J, et al. Human CtIP promotes DNA end resection. Nature. 2007;450:509-14.

75. Nimonkar AV, Özsoy AZ, Genschel J, Modrich P, Kowalczykowski SC. Human exonuclease 1 and BLM helicase interact to resect DNA and initiate DNA repair. Proc Natl Acad Sci USA. 2008;105(44):16906-11.

76. Nimonkar AV, Genschel J, Kinoshita E, Polaczek P, Campbell JL, Wyman C, et al. BLM-DNA2-RPA-MRN and EXO1-BLM-RPA-MRN constitute two DNA end resection machineries for human DNA break repair. Genes Dev. 2011;25(4):350-62.

77. Karanja KK, Cox SW, Duxin JP, Stewart SA, Campbell JL. DNA2 and EXO1 in replication-coupled, homology-directed repair and in the interplay between HDR and the FA/BRCA network. Cell Cycle. 2012;11(21):3983-96.

78. Dolganov GM, Maser RS, Novikov A, Tosto L, Chong S, Bressan DA, et al. Human Rad50 Is Physically Associated with Human Mre11: Identification of a Conserved Multiprotein Complex Implicated in Recombinational DNA Repair. Mol Cell Biol. 1996;16:4832-41.

79. Chen L, Nievera CJ, Lee AY-L, Wu X. Cell Cycle-dependent Complex Formation of BRCA1{middle dot}CtIP{middle dot}MRN Is Important for DNA Double-strand Break Repair. J Biol Chem. 2008;283(12):7713-20.

80. Kim C, Snyder RO, Wold MS. Binding properties of replication protein A from human and yeast cells. Mol Cell Biol. 1992;12:3050-9.

81. Blackwell LJ, Borowiec JA. Human replication protein A binds single-stranded DNA in two distinct complexes. Molecular and cellular biology. 1994;14(6):3993-4001.

82. Wang H, Perrault AR, Takeda Y, Qin W, Wang H, Iliakis G. Biochemical evidence for Ku-independent backup pathways of NHEJ. Nucleic Acids Res. 2003;31:5377-88.

83. Terzoudi GI, Singh SK, Pantelias GE, Iliakis G. Premature chromosome condensation reveals DNA-PK independent pathways of chromosome break repair. Int J Oncol. 2008;31(1):145-52.

84. Cheong N, Perrault AR, Wang H, Wachsberger P, Mammen P, Jackson I, et al. DNA-PK-independent rejoining of DNA double-strand breaks in human cell extracts *in vitro*. Int J Radiat Biol. 1999;75:67-81.

85. Mladenov E, Iliakis G. Induction and Repair of DNA Double Strand Breaks: The Increasing Spectrum of Non-homologous End Joining Pathways. Mutat Res. 2011;711:61-72.

86. Perrault R, Wang H, Wang M, Rosidi B, Iliakis G. Backup Pathways of NHEJ Are Suppressed by DNA-PK. J Cell Biochem. 2004;92:781-94.

87. Rosidi B, Wang M, Wu W, Sharma A, Wang H, Iliakis G. Histone H1 functions as a stimulatory factor in backup pathways of NHEJ. Nucleic Acids Res. 2008;36(5):1610-23.

88. Wang M, Wu W, Wu W, Rosidi B, Zhang L, Wang H, et al. PARP-1 and Ku compete for repair of DNA double strand breaks by distinct NHEJ pathways. Nucleic Acids Res. 2006;34(21):6170-82.

89. Wang H, Rosidi B, Perrault R, Wang M, Zhang L, Windhofer F, et al. DNA Ligase III as a Candidate Component of Backup Pathways of Nonhomologous End Joining. Cancer Res. 2005;65(10):4020-30.

90. Soni A, Siemann M, Grabos M, Murmann T, Pantelias GE, Iliakis G. Requirement for Parp-1 and DNA ligases 1 or 3 but not of Xrcc1 in chromosomal translocation formation by backup end joining. Nucleic Acids Res. 2014;42(10):6380-92.

91. Wu W, Wang M, Mussfeldt T, Iliakis G. Enhanced Use of Backup Pathways of NHEJ in G_2 in Chinese Hamster Mutant Cells with Defects in the Classical Pathway of NHEJ. Radiat Res. 2008;170:512-20.

92. Iliakis G. Backup pathways of NHEJ in cells of higher eukaryotes: Cell cycle dependence. Radiother Oncol. 2009;92:310-5.

93. Wu W, Wang M, Wu W, Singh SK, Mussfeldt T, Iliakis G. Repair of radiation induced DNA double strand breaks by backup NHEJ is enhanced in G2. DNA Repair. 2008;7(2):329-38.

94. Singh SK, Wu W, Zhang L, Klammer H, Wang M, Iliakis G. Widespread Dependence of Backup NHEJ on Growth State: Ramifications for the Use of DNA-PK Inhibitors. Int J Radiat Oncol Biol Phys. 2011;79(2):540-8.

95. Deng SK, Gibb B, de Almeida MJ, Greene EC, Symington LS. RPA antagonizes microhomology-mediated repair of DNA double-strand breaks. Nat Struct Mol Biol. 2014;21(4):405-12.

96. Huertas P. DNA resection in eukaryotes: deciding how to fix the break. Nat Struct Mol Biol. 2010;17(1):11-6.

97. Symington LS, Gautier J. Double-Strand Break End Resection and Repair Pathway Choice. Annu Rev Genet. 2011;45:247-71.

98. Moore JD, Krebs JE. Histone modifications and DNA double-strand break repair. Biochem Cell Biol. 2004;82:446-52.

99. Cheng Q, Barboule N, Frit P, Gomez D, Bombarde O, Couderc B, et al. Ku counteracts mobilization of PARP1 and MRN in chromatin damaged with DNA double-strand breaks. Nucleic Acids Res. 2011;39(22):9605-19.

100. Bakkenist CJ, Kastan MB. DNA damage activates ATM through intermolecular autophosphorylation and dimer dissociation. Nature. 2003;421:499-506.

101. Lee J-H, Paull TT. Direct Activation of the ATM Protein Kinase by the Mre11/Rad50/Nbs1 Complex. Science. 2004;304:93-100.

102. Lee J-H, Paull TT. ATM Activation by DNA Double-Strand Breaks Through the Mre11-Rad50-Nbs1 Complex. Science. 2005;308(5721):551-4.

103. Zhang Y, Zhou J, Lim CUK. The role of NBS1 in DNA double strand break repair, telomere stability, and cell cycle checkpoint control. Cell Res. 2006;16:45-54.

104. Chapman JR, Jackson SP. Phospho-dependent interactions between NBS1 and MDC1 mediate chromatin retention of the MRN complex at sites of DNA damage. EMBO Rep. 2008;9(8):795-801.

105. Rogakou EP, Pilch DR, Orr AH, Ivanova VS, Bonner WM. DNA double-stranded breaks induce histone H2AX phosphorylation on serine 139. J Biol Chem. 1998;273:5858-68.

106. Celeste A, Petersen S, Romanienko PJ, Fernandez-Capetillo O, Chen HT, Sedelnikova OA, et al. Genomic instability in mice lacking histone H2AX. Science. 2002;296:922-7.

107. Kinner A, Wu W, Staudt C, Iliakis G. g-H2AX in recognition and signaling of DNA double-strand breaks in the context of chromatin. Nucleic Acids Res. 2008;36(17):5678-94.

108. Burma S, Chen BP, Murphy M, Kurimasa A, Chen DJ. ATM phosphorylates histone H2AX in response to DNA double-strand breaks. J Biol Chem. 2001;276:42462-7.

109. Stucki M, Clapperton JA, Mohammad D, Yaffe MB, Smerdon SJ, Jackson SP. MDC1 directly binds phosphorylated histone H2AX to regulate cellular responses to DNA double-strand breaks. Cell. 2005;123:1213-26.

110. Stucki M, Jackson SP. gH2AX and MDC1: Anchoring the DNA-damage-response machinery to broken chromosomes. DNA Repair. 2006;5(5):534-43.

111. Lou Z, Minter-Dykhouse K, Franco S, Gostissa M, Rivera MA, Celeste A, et al. MDC1 maintains genomic stability by participating in the amplification of ATM-dependent DNA damage signals. Mol Cell. 2006;21(2):187-200.

112. Mailand N, Bekker-Jensen S, Faustrup H, Melander F, Bartek J, Lukas C, et al. RNF8 ubiquitylates histones at DNA double-strand breaks and promotes assembly of repair proteins. Cell. 2007;131:887-900.

113. Makharashvili N, Tubbs AT, Yang SH, Wang H, Barton O, Zhou Y, et al. Catalytic and noncatalytic roles of the CtIP endonuclease in double-strand break end resection. Molecular cell. 2014;54(6):1022-33.

114. Steger M, Murina O, Hühn D, Ferretti Lorenza P, Walser R, Hänggi K, et al. Prolyl Isomerase PIN1 Regulates DNA Double-Strand Break Repair by Counteracting DNA End Resection. Mol Cell. 2013;50(3):333-43.

115. Davies OR, Forment JV, Sun M, Belotserkovskaya R, Coates J, Galanty Y, et al. CtIP tetramer assembly is required for DNA-end resection and repair. Nat Struct Mol Biol. 2015;22(2):150-7.

116. Kaidi A, Weinert BT, Choudhary C, Jackson SP. Human SIRT6 Promotes DNA End Resection Through CtIP Deacetylation. Science. 2010;329(5997):1348-53.

117. Yu X, Chen J. DNA Damage-Induced Cell Cycle Checkpoint Control Requires CtIP, a Phosphorylation-Dependent Binding Partner of BRCA1 C-Terminal Domains. Mol Cell Biol. 2004;24(21):9478-86.

118. Yu X, Fu S, Lai M, Baer R, Chen J. BRCA1 ubiquitinates its phosphorylation-dependent binding partner CtIP. Genes Dev. 2006;20(13):1721-6.

119. Cruz-García A, López-Saavedra A, Huertas P. BRCA1 Accelerates CtIP-Mediated DNA-End Resection. Cell Rep. 2014;9(2):451-9.

120. Goldberg M, Stucki M, Falck J, D'Amours D, Rahman D, Pappin D, et al. MDC1 is required for the intra-S-phase DNA damage checkpoint. Nature. 2003;421:952-6.

121. Stewart GS, Wang B, Rignell CR, Taylor AMR, Elledge SJ. MDC1 is a mediator of the mammalian DNA damage checkpoint. Nature. 2003;421:961-6.

122. Mochan TA, Venere M, DiTullio Jr. RA, Halazonetis TD. 53BP1 and NFBD1/MDC1-Nbs1 Function in Parallel Interacting Pathways Activating Ataxia-Telangiectasia Mutated (ATM) in Response to DNA Damage. Cancer Res. 2003;63:8586-91.

123. Bunting SF, Callén E, Wong N, Chen H-T, Polato F, Gunn A, et al. 53BP1 Inhibits Homologous Recombination in Brca1-Deficient Cells by Blocking Resection of DNA Breaks. Cell. 2010;141:243-54.

124. Bothmer A, Robbiani DF, Feldhahn N, Gazumyan A, Nussenzweig A, Nussenzweig MC. 53BP1 regulates DNA resection and the choice between classical and alternative end joining during class switch recombination. J Exp Med. 2010;207(4):855-65.

125. Zimmermann M, Lottersberger F, Buonomo SB, Sfeir A, de Lange T. 53BP1 Regulates DSB Repair Using Rif1 to Control 5′ End Resection. Science. 2013;339(6120):700-4.

126. Di Virgilio M, Callen E, Yamane A, Zhang W, Jankovic M, Gitlin AD, et al. Rif1 Prevents Resection of DNA Breaks and Promotes Immunoglobulin Class Switching. Science. 2013;339(6120):711-5.

127. Escribano-Diaz C, Orthwein A, Fradet-Turcotte A, Xing M, Young JTF, Tkac J, et al. A Cell Cycle-Dependent Regulatory Circuit Composed of 53BP1-RIF1 and BRCA1-CtIP Controls DNA Repair Pathway Choice. Mol Cell. 2013;49(5):872-83.

128. Chapman JR, Barral P, Vannier J-B, Borel V, Steger M, Tomas-Loba A, et al. RIF1 Is Essential for 53BP1-Dependent Nonhomologous End Joining and Suppression of DNA Double-Strand Break Resection. Mol Cell. 2013;49(5):858-71.

129. Wang B, Matsuoka S, Ballif BA, Zhang D, Smogorzewska A, Gygi SP, et al. Abraxas and RAP80 Form a BRCA1 Protein Complex Required for the DNA Damage Response. Science. 2007;316:1194-8.

130. Sobhian B, Shao G, Lilli DR, Culhane AC, Moreau LA, Xia B, et al. RAP80 targets BRCA1 to specific ubiquitin structures at DNA damage sites. Science. 2007;316:1198-202.

131. Kim H, Chen J, Yu X. Ubiquitin-Binding Protein RAP80 Mediates BRCA1-Dependent DNA Damage Response. Science. 2007;316:1202-5.

132. Kakarougkas A, Ismail A, Katsuki Y, Freire R, Shibata A, Jeggo PA. Co-operation of BRCA1 and POH1 relieves the barriers posed by 53BP1 and RAP80 to resection. Nucleic Acids Res. 2013;41(22):10298-311.

133. Liu S, Bekker-Jensen S, Mailand N, Lukas C, Bartek J, Lukas J. Claspin Operates Downstream of TopBP1 To Direct ATR Signaling towards Chk1 Activation. Mol Cell Biol. 2006;26(16):6056-64.

134. Parrilla-Castellar ER, Arlander SJH, Karnitz L. Dial 9-1-1 for DNA damage: the Rad9-Hus1-Rad1 (9-1-1) clamp complex. DNA Repair. 2004;3:1009-14.

135. Neal JA, Dang V, Douglas P, Wold MS, Lees-Miller SP, Meek K. Inhibition of Homologous Recombination by DNA-Dependent Protein Kinase Requires Kinase Activity, Is Titratable, and Is Modulated by Autophosphorylation. Mol Cell Biol. 2011;31(8):1719-33.

136. Allen C, Halbrook J, Nickoloff JA. Interactive Competition between Homologous Recombination and Non-Homologous End Joining. Mol Cancer Res. 2003;1(12):913-20.

137. Convery E, Shin EK, Ding Q, Wang W, Douglas P, Davis LS, et al. Inhibition of homologous recombination by variants of the catalytic subunit of the DNA-dependent protein kinase (DNA-PKcs). Proc Natl Acad Sci USA. 2005;102(5):1345-50.

138. Cui X, Yu Y, Gupta S, Cho Y-M, Lees-Miller SP, Meek K. Autophosphorylation of DNA-Dependent Protein Kinase Regulates DNA End Processing and May Also Alter Double-Strand Break Repair Pathway Choice. Mol Cell Biol. 2005;25(24):10842-52.

139. Walker AI, Hunt T, Jackson RJ, Anderson CW. Double-stranded DNA induces the phosphorylation of several proteins including the 90 000 mol. wt. heat-shock protein in animal cell extracts. EMBO J. 1985;4(1):139-45.

140. Gottlieb TM, Jackson SP. The DNA-dependent protein kinase: Requirement for DNA ends and association with Ku antigen. Cell. 1993;72:131-42.

141. Lees-Miller SP, Chen Y-R, Anderson CW. Human cells contain a DNA-activated protein kinase that phosphorylates simian virus 40 T antigen, mouse p53, and the human Ku autoantigen. Mol Cell Biol. 1990;10:6472-81.

142. Sibanda BL, Chirgadze DY, Blundell TL. Crystal structure of DNA-PKcs reveals a large open-ring cradle comprised of HEAT repeats. Nature. 2010;463(7277):118-21.

143. Smith GCM, Jackson SP. The DNA-dependent protein kinase. Genes Dev. 1999;13:916-34.

144. Hammarsten O, Chu G. DNA-dependent protein kinase: DNA binding and activation in the absence of Ku. Proc Natl Acad Sci USA. 1998;95:525-30.

145. Lempiäinen H, Halazonetis TD. Emerging common themes in regulation of PIKKs and PI3Ks. EMBO J. 2009;28(20):3067-73.

146. Hartley KO, Gell D, Smith GCM, Zhang H, Divecha N, Connelly MA, et al. DNA-dependent protein kinase catalytic subunit: A relative of phosphatidylinositol 3-kinase and the ataxia telangiectasia gene product. Cell. 1995;82:849-56.

147. Hunter T. When is a lipid kinase not a lipid kinase? When it is a protein kinase. Cell. 1995;83:1-4.

148. Dynan WS, Yoo S. Interaction of ku protein and DNA-dependent protein kinase catalytic subunit with nucleic acids. Nucleic Acids Res. 1998;26:1551-9.

149. Blunt T, Gell D, Fox M, Taccioli GE, Lehmann AR, Jackson SP, et al. Identification of a nonsense mutation in the carboxyl-terminal region of DNA-dependent protein kinase catalytic subunit in the *scid* mouse. Proc Natl Acad Sci USA. 1996;93:10285-90.

150. Blunt T, Finnie NJ, Taccioli GE, Smith GCM, Demengeot J, Gottlieb TM, et al. Defective DNA-dependent protein kinase activity is linked to V(D)J recombination and DNA repair defects associated with the murine *scid* mutation. Cell. 1995;80:813-23.

151. Finnie NJ, Gottlieb TM, Blunt T, Jeggo PA, Jackson SP. DNA-dependent protein kinase defects are linked to deficiencies in DNA repair and V(D)J recombination. Philos Trans R Soc Lond B Biol Sci. 1996;351:173-9.

152. Kirchgessner CU, Patil CK, Evans JW, Cuomo CA, Fried LM, Carter T, et al. DNA-dependent kinase (p350) as a candidate gene for the murine SCID defect. Science. 1995;267:1178-83.

153. Peterson SR, Kurimasa A, Oshimura M, Dynan WS, Bradbury EM, Chen DJ. Loss of the catalytic subunit of the DNA-dependent protein kinase in DNA double-strand break-repair mutant mammalian cells. Proc Natl Acad Sci USA. 1995;92:3171-4.

154. Zhu C, Bogue MA, Lim D-S, Hasty P, Roth DB. Ku86-deficient mice exhibit severe combined immunodeficiency and defective processing of V(D)J recombination intermediates. Cell. 1996;86:379-89.

155. Nussenzweig A, Chen C, da Costa Soares V, Sanchez M, Kokol K, Nussenzweig MC, et al. Requirement for Ku80 in growth and immunoglobulin V(D)J recombination. Nature. 1996;382:551-5.

156. Chan DW, Lees-Miller SP. The DNA-dependent protein kinase is inactivated by autophosphorylation of the catalytic subunit. J Biol Chem. 1996;271:8936-41.

157. Ding Q, Reddy YVR, Wang W, Woods T, Douglas P, Ramsden DA, et al. Autophosphorylation of the Catalytic Subunit of the DNA-Dependent Protein Kinase Is Required for Efficient End Procesing during DNA Double-Strand Break Repair. Mol Cell Biol. 2003;23:5836-48.

158. DeFazio LG, Stansel RM, Griffith JD, Chu G. Synapsis of DNA ends by DNA-dependent protein kinase. EMBO J. 2002;21:3192-200.

159. Meek K, Douglas P, Cui X, Ding Q, Lees-Miller SP. trans Autophosphorylation at DNA-Dependent Protein Kinase's Two Major Autophosphorylation Site Clusters Facilitates End Processing but Not End Joining. Mol Cell Biol. 2007;27(10):3881-90.

160. Ma Y, Lu H, Tippin B, Goodman MF, Shimazaki N, Koiwai O, et al. A Biochemically Defined System for Mammalian Nonhomologous DNA End Joining. Mol Cell. 2004;16:701-13.

161. Jovanovic M, Dynan WS. Terminal DNA structure and ATP influence binding parameters of the DNA-dependent protein kinase at an early step prior to DNA synapsis. Nucleic Acids Res. 2006;34(4):1112-20.

162. Meek K, Lees-Miller SP, Modesti M. N-terminal constraint activates the catalytic subunit of the DNA-dependent protein kinase in the absence of DNA or Ku. Nucleic Acids Res. 2012;40(7):2964-73.

163. Jin S, Kharbanda S, Mayer B, Kufe D, Weaver DT. Binding of Ku and c-Abl at the kinase homology region of DNA-dependent protein kinase catalytic subunit. J Biol Chem. 1997;272(40):24763-6.

164. Kharbanda S, Pandey P, Jin S, Inoue S, Bharti A, Yuan Z-M, et al. Functional interaction between DNA-PK and c-Abl in response to DNA damage. Nature. 1997;386:732-5.

165. Chen BPC, Uematsu N, Kobayashi J, Lerenthal Y, Krempler A, Yajima H, et al. Ataxia Telangiectasia Mutated (ATM) Is Essential for DNA-PKcs Phosphorylations at the Thr-2609 Cluster upon DNA Double Strand Break. J Biol Chem. 2007;282(9):6582-7.

166. Yajima H, Lee K-J, Zhang S, Kobayashi J, Chen BPC. DNA Double-Strand Break Formation upon UV-Induced Replication Stress Activates ATM and DNA-PKcs Kinases. J Mol Biol. 2009;385(3):800-10.

167. Ruscetti T, Lehnert BE, Halbrook J, Trong HL, Hoekstra MF, Chen DJ, et al. Stimulation of the DNA-dependent protein kinase by poly(ADP-ribose) polymerase. J Biol Chem. 1998;273:14461-7.

168. Myung K, He DM, Lee SE, Hendrickson EA. KARP-1: a novel leucine zipper protein expressed from the Ku86 autoantigen locus is implicated in the control of DNA-dependent protein kinase activity. EMBO J. 1997;16:3172-84.

169. Myung K, Braastad C, He DM, Hendrickson EA. KARP-1 is induced by DNA damage in a p53- and ataxia telangiectasia mutated-dependent fashion. Proc Natl Acad Sci USA. 1998;95:7664-9.

170. Wang H, Guan J, Wang H, Perrault AR, Wang Y, Iliakis G. Replication Protein A2 Phosphorylation after DNA Damage by the Coordinated Action of Ataxia Telangiectasia-Mutated and DNA-dependent Protein Kinase. Cancer Res. 2001;61:8554-63.

171. Ashley AK, Shrivastav M, Nie J, Amerin C, Troksa K, Glanzer JG, et al. DNA-PK phosphorylation of RPA32 Ser4/Ser8 regulates replication stress checkpoint activation, fork restart, homologous recombination and mitotic catastrophe. DNA Repair. 2014;21(0):131-9.

172. Serrano MA, Li Z, Dangeti M, Musich PR, Patrick S, Roginskaya M, et al. DNA-PK, ATM and ATR collaboratively regulate p53-RPA interaction to facilitate homologous recombination DNA repair. Oncogene. 2013;32(19):2452-62.

173. Allalunis-Turner J, Barron GM, Day RS, III. Intact G2-phase checkpoint in cells of a human cell line lacking DNA-dependent protein kinase activity. Radiat Res. 1997;147:284-7.

174. Guan J, DiBiase S, Iliakis G. The catalytic subunit DNA-dependent protein kinase (DNA-PKcs) facilitates recovery from radiation-induced inhibition of DNA replication. Nucleic Acids Res. 2000;28:1183-92.

175. Liu S, Opiyo SO, Manthey K, Glanzer JG, Ashley AK, Amerin C, et al. Distinct roles for DNA-PK, ATM and ATR in RPA phosphorylation and checkpoint activation in response to replication stress. Nucleic Acids Res. 2012;40(21):10780-94.

176. Tomimatsu N, Mukherjee B, Burma S. Distinct roles of ATR and DNA-PKcs in triggering DNA damage responses in ATM-deficient cells. EMBO Rep. 2009;10(6):629-35.

177. Jeggo PA, Taccioli GE, Jackson SP. Menage á trois: double strand break repair, V(D)J recombination and DNA-PK. Bioessays. 1995;17:949-57.

178. Kurimasa A, Kumano S, Boubnov NV, Story MD, Tung C-S, Peterson SR, et al. Requirement for the kinase activity of human DNA-dependent protein kinase catalytic subunit in DNA strand break rejoining. Mol Cell Biol. 1999;19:3877-84.

179. Jackson SP, MacDonald JJ, Lees-Miller S, Tjian R. GC box binding induces phosphorylation of Sp1 by a DNA-dependent protein kinase. Cell. 1990;63(1):155-65.

180. Dvir A, Peterson SR, Knuth MW, Lu H, Dynan WS. Ku autoantigen is the regulatory component of a template-associated protein kinase that phosphorylates RNA polymerase II. Proc Natl Acad Sci USA. 1992;89:11920-4.

181. Ju B-G, Lunyak VV, Perissi V, Garcia-Bassets I, Rose DW, Glass CK, et al. A Topoisomerase IIß-Mediated dsDNA Break Required for Regulated Transcription. Science. 2006;312:1798-802.

182. Goodwin Jonathan F, Kothari V, Drake Justin M, Zhao S, Dylgjeri E, Dean Jeffry L, et al. DNA-PKcs-Mediated Transcriptional Regulation Drives Prostate Cancer Progression and Metastasis. Cancer Cell. 2015;28(1):97-113.

183. Douglas P, Ye R, Trinkle-Mulcahy L, Neal JA, De Wever V, Morrice NA, et al. Polo-like kinase 1 (PLK1) and protein phosphatase 6 (PP6) regulate DNA-dependent protein kinase catalytic subunit (DNA-PKcs) phosphorylation in mitosis. Biosci Rep. 2014;34:Article: e00113.

184. Huang B, Shang Z-F, Li B, Wang Y, Liu X-D, Zhang S-M, et al. DNA-PKcs Associates With PLK1 and Is Involved in Proper Chromosome Segregation and Cytokinesis. J Cell Biochem. 2014;115(6):1077-88.

185. Tu W-Z, Li B, Huang B, Wang Y, Liu X-D, Guan H, et al. γH2AX foci formation in the absence of DNA damage: Mitotic H2AX phosphorylation is mediated by the DNA-PKcs/CHK2 pathway. FEBS Lett. 2013;587(21):3437-43.

186. Lees-Miller SP, Long MC, Kilvert MA, Lam V, Rice SA, Spencer CA. Attenuation of DNA-dependent protein kinase activity and its catalytic subunit by the herpes simplex virus type 1 transactivator ICP0. J Virol. 1996;70:7471-7.

187. Parkinson J, Lees-Miller SP, Everett RD. Herpes simplex virus type 1 immediate-early protein Vmw110 induces the proteasome-dependent degradation of the catalytic subunit of DNA-dependent protein kinase. J Virol. 1999;73:650-7.

188. Cooper A, Garcia M, Petrovas C, Yamamoto T, Koup RA, Nabel GJ. HIV-1 causes CD4 cell death through DNA-dependent protein kinase during viral integration. Nature. 2013;498(7454):376-9.

189. Gilley D, Tanaka H, Hande MP, Kurimasa A, Li GC, Oshimura M, et al. DNA-PKcs is critical for telomere capping. Proc Natl Acad Sci USA. 2001;98:15084-8.

190. Le PN, Maranon DG, Altina NH, Battaglia CLR, Bailey SM. TERRA, hnRNP A1 and DNA-PKcs interactions at human telomeres. Front Oncol. 2013;3:Article 91.

191. Williams ES, Klingler R, Ponnaiya B, Hardt T, Schrock E, Lees-Miller SP, et al. Telomere Dysfunction and DNA-PKcs Deficiency: Characterization and Consequence. Cancer Res. 2009;69(5):2100-7.

192. Carter T, Vancurová I, Sun I, Lou W, DeLeon S. A DNA-activated protein kinase from HeLa cell nuclei. Mol Cell Biol. 1990;10:6460-71.

193. Lees-Miller SP, Godbout R, Chan DW, Weinfeld M, Day RS, III, Barron GM, et al. Absence of p350 subunit of DNA-activated protein kinase from a radiosensitive human cell line. Science. 1995;267:1183-5.

194. Allalunis-Turner MJ, Barron GM, Day RS, Dobler KD, Mirzayans R. Isolation of two cell lines from a human malignant glioma specimen differing in sensitivity to radiation and chemotherapeutic drugs. Radiat Res. 1993;134:349-54.

195. Kenny MK, Schlegel U, Furneaux H, Hurwitz J. The role of human single-stranded DNA binding protein and its individual subunits in simian virus 40 DNA replication. J Biol Chem. 1990;265:7693-700.

196. Borrelli MJ, Mackey MA, Dewey WC. A method for freezing synchronous mitotic and G1 cells. Experimental cell research. 1987;170(2):363-8.

197. Fire A, Xu S, Montgomery MK, Kostas SA, Driver SE, Mello CC. Potent and specific genetic interference by double-stranded RNA in Caenorhabditis elegans. Nature. 1998;391:806-11.

198. Peng G, Dai H, Zhang W, Hsieh H-J, Pan M-R, Park Y-Y, et al. Human Nuclease/Helicase DNA2 Alleviates Replication Stress by Promoting DNA End Resection. Cancer Res. 2012;72(11):2802-13.

199. Gravel S, Chapman JR, Magill C, Jackson SP. DNA helicases Sgs1 and BLM promote DNA double-strand break resection. Genes Dev. 2008;22(20):2767-72.

200. Britton S, Coates J, Jackson SP. A new method for high-resolution imaging of Ku foci to decipher mechanisms of DNA double-strand break repair. J Cell Biol. 2013;202(3):579-95.

201. Yuan J, Chen J. MRE11-RAD50-NBS1 Complex Dictates DNA Repair Independent of H2AX. J Biol Chem. 2010;285(2):1097-104.

202. Shiotani B, Nguyen Hai D, Håkansson P, Maréchal A, Tse A, Tahara H, et al. Two Distinct Modes of ATR Activation Orchestrated by Rad17 and Nbs1. Cell Rep. 2013;3(5):1651-62.

203. Xu B, Kim S-T, Lim D-S, Kastan MB. Two Molecularly Distinct G_2/M Checkpoints Are Induced by Ionizing Irradiation. Mol Cell Biol. 2002;22:1049-59.

204. Bradford MM. A rapid and sensitive method for the quantitation of microgram quantities of protein utilizing the principle of protein-dye binding. Analytical biochemistry. 1976;72:248-54.

205. Fan X. Interplay between ATM and ATR for the regulation of cellular responses to DNA damage [Doctoral dissertation]: University of Duisburg-Essen; 2009.

206. Allalunis-Turner MJ, Zia PKY, Barron GM, Mirzayans R, Day RS, III. Radiation-Induced DNA Damage and Repair in Cells of a Radiosensitive Human Malignant Glioma Cell Line. Radiat Res. 1995;144:288-93.

207. Anderson CW, Dunn JJ, Freimuth PI, Galloway AM, Allalunis-Turner MJ. Frameshift mutation in PRKDC, the gene for DNA-PKcs, in the DNA repair-defective, human, glioma-derived cell line M059J. Radiat Res. 2001;156:2-9.

208. Izzard RA, Jackson SP, Smith GC. Competitive and noncompetitive inhibition of the DNA-dependent protein kinase. Cancer research. 1999;59(11):2581-6.

209. Leahy JJJ, Golding BT, Griffin RJ, Hardcastle IR, Richardson C, Rigoreau L, et al. Identification of a highly potent and selective DNA-dependent protein kinase (DNA-PK) inhibitor (NU7441) by screening of chromenone libraries. Bioorg Med Chem Lett. 2004;14(24):6083-7.

210. Hardcastle IR, Cockcroft X, Curtin NJ, El-Murr MD, Leahy JJJ, Stockley M, et al. Discovery of Potent Chromen-4-one Inhibitors of the DNA-Dependent Protein Kinase (DNA-PK) Using a Small-Molecule Library Approach. J Med Chem. 2005;48:7829-46.

211. Hollick JJ, Golding BT, Hardcastle IR, Martin N, Richardson C, Rigoreau LJ, et al. 2,6-disubstituted pyran-4-one and thiopyran-4-one inhibitors of DNA-Dependent protein kinase (DNA-PK). Bioorganic & medicinal chemistry letters. 2003;13(18):3083-6.

212. Jackman M, Firth M, Pines J. Human cyclins B1 and B2 are localized to strikingly different structures: B1 to microtubules, B2 primarily to the Golgi apparatus. The EMBO journal. 1995;14(8):1646-54.

213. Fattah F, Lee EH, Weisensel N, Wang Y, Lichter N, Hendrickson EA. Ku Regulates the Non-Homologous End Joining Pathway Choice of DNA Double-Strand Break Repair in Human Somatic Cells. PLoS Genet. 2010;6(2):e1000855.

214. Mimitou EP, Symington LS. Ku prevents Exo1 and Sgs1-dependent resection of DNA ends in the absence of a functional MRX complex or Sae2. EMBO J. 2010;29(19):3358-69.

215. Ng WL, Yan D, Zhang X, Mo Y-Y, Wang Y. Over-expression of miR-100 is responsible for the low-expression of ATM in the human glioma cell line: M059J. DNA Repair. 2010;9(11):1170-5.

216. Fan X, Mladenov E, Soni A, Dueva R, Paul-Konietzko K, Iliakis G. ATR controls G2-checkpoint through Chk1 and regulates resection by cooperating with ATM and DNA-PKcs in cells sustaining DNA double strand breaks in S- or G2-phase. Submitted. 2015.

217. Limbo O, Chahwan C, Yamada Y, de Bruin RAM, Wittenberg C, Russell P. Ctp1 Is a Cell-Cycle-Regulated Protein that Functions with Mre11 Complex to Control Double-Strand Break Repair by Homologous Recombination. Mol Cell. 2007;28:134-46.

218. Schaetzlein S, Chahwan R, Avdievich E, Roa S, Wei K, Eoff RL, et al. Mammalian Exo1 encodes both structural and catalytic functions that play distinct

roles in essential biological processes. Proc Natl Acad Sci USA. 2013;110(27):E2470-90.

219. Peng Y, Woods RG, Beamish H, Ye R, Lees-Miller SP, Lavin MF, et al. Deficiency in the Catalytic Subunit of DNA-Dependent Protein Kinase Causes Down-Regulation of ATM. Cancer Res. 2005;65(5):1670-7.

220. Lin Y-F, Shih H-Y, Shang Z, Matsunaga S, Chen BP. DNA-PKcs is required to maintain stability of Chk1 and Claspin for optimal replication stress response. Nucleic Acids Res. 2014;42(7):4463-73.

221. Vidal-Eychenié S, Décaillet C, Basbous J, Constantinou A. DNA structure-specific priming of ATR activation by DNA-PKcs. J Cell Biol. 2013;202(3):421-9.

222. Allen C, Kurimasa A, Brenneman MA, Chen DJ, Nickoloff JA. DNA-dependent protein kinase suppresses double-strand break-induced and spontaneous homologous recombination. Proc Natl Acad Sci USA. 2002;99:3758-63.

223. Dip R, Naegeli H. Binding of the DNA-dependent protein kinase catalytic subunit to Holliday junctions. The Biochemical journal. 2004;381(Pt 1):165-74.

224. Goedecke W, Eijpe M, Offenberg HH, van Aalderen M, Heyting C. Mre11 and Ku70 interact in somatic cells, but are differentially expressed in early meiosis. Nat Genet. 1999;23:194-8.

225. Sun J, Lee K-J, Davis AJ, Chen DJ. Human Ku70/80 Protein Blocks Exonuclease 1-mediated DNA Resection in the Presence of Human Mre11 or Mre11/Rad50 Protein Complex. J Biol Chem. 2012;287(7):4936-45.

226. Pierce AJ, Hu P, Han M, Ellis N, Jasin M. Ku DNA end-binding protein modulates homologous repair of double-strand breaks in mammalian cells. Genes Dev. 2001;15:3237-42.

227. Zhou Y, Paull TT. DNA-dependent Protein Kinase Regulates DNA End Resection in Concert with Mre11-Rad50-Nbs1 (MRN) and Ataxia Telangiectasia-mutated (ATM). J Biol Chem. 2013;288(52):37112-25.

228. Shiotani B, Zou L. Single-Stranded DNA Orchestrates an ATM-to-ATR Switch at DNA Breaks. Mol Cell. 2009;33(5):547-58.

229. Liu S, Shiotani B, Lahiri M, Maréchal A, Tse A, Leung Charles Chung Y, et al. ATR Autophosphorylation as a Molecular Switch for Checkpoint Activation. Mol Cell. 2011;43(2):192-202.

230. Goodarzi AA, Jeggo P, Lobrich M. The influence of heterochromatin on DNA double strand break repair: Getting the strong, silent type to relax. DNA Repair. 2010;9(12):1273-82.

231. Kousholt AN, Fugger K, Hoffmann S, Larsen BD, Menzel T, Sartori AA, et al. CtIP-dependent DNA resection is required for DNA damage checkpoint maintenance but not initiation. J Cell Biol. 2012;197(7):869-76.

232. Smith J, Mun Tho L, Xu N, A. Gillespie D, George FVWaGK. The ATM-Chk2 and ATR-Chk1 Pathways in DNA Damage Signaling and Cancer. Advances in Cancer Research. Volume 108: Academic Press; 2010. p. 73-112.

233. Wang X, Khadpe J, Hu B, Iliakis G, Wang Y. An Over-activated ATR/CHK1 Pathway is Responsible for the Prolonged G2 Accumulation in Irradiated AT Cells. J Biol Chem. 2003;278(33):30869-74.

234. Roth DB, Wilson JH. Relative rates of homologous and nonhomologous recombination in transfected DNA. Proc Natl Acad Sci USA. 1985;82:3355-9.

235. Shrivastav M, De Haro LP, Nickoloff JA. Regulation of DNA double-strand break repair pathway choice. Cell Res. 2008;18(1):134-47.

ACKNOWLEDGEMENTS

First and foremost, I would like to thank my supervisor Professor Dr. George Iliakis, the most remarkable person I know, for giving me the unique opportunity to perform this work in his laboratory and to be part of his team. I admire him for being always serene, patient and contagiously enthusiastic about science.

Special thanks to Dr. Emil Mladenov, who was the primary source for getting all my questions answered and stands out as an inspiration for me in many ways. I appreciate all his contributions of time, ideas and in the end as a first proofreader of my thesis. Best wishes to you and your wonderful family!

My PhD work was made possible by the financial support from DFG training program GRK1739 and I was lucky to be a part of this graduate school. I am particularly grateful to Professor Dr. Verena Jendrossek who is very devoted to the graduate program and my co-mentor Professor Dr. Hemmo Meyer for providing insightful discussions about my research at the retreats.

My sincere gratitude to all the members of Iliakis' lab, which has been a source of very good friendships, and all the people who I have come to depend on for help along the way. I also thank Drs. Katja Paul-Konietzko and Aashish Soni, who I worked with closely, and Vladimir Nikolov for filling the gaps in my knowledge and his suggestions in general. I value your friendship and support as well.

Thanks to all the members of GRK1739/1 for the great memories during the retreats and social events.

Finally, I would like to thank my family - my formula of success – for all their love and care, for their faith in me and support on all of my pursuits.

CURRICULUM VITAE

Der Lebenslauf ist in der veröffentlichten Version aus Gründen des Datenschutzes nicht enthalten.

Der Lebenslauf ist in der veröffentlichten Version aus Gründen des Datenschutzes nicht enthalten.

Der Lebenslauf ist in der veröffentlichten Version aus Gründen des Datenschutzes nicht enthalten.

DECLARATION

Erklärung:

Hiermit erkläre ich, gem. § 6 Abs. (2) g) der Promotionsordnung der Fakultät für Biologie zur Erlangung der Dr. *rer. nat.*, dass ich das Arbeitsgebiet, dem das Thema „*A role for DNA-PKcs in G_2 checkpoint response and DNA end-resection after exposure of cells to ionizing radiation*“ zuzuordnen ist, in Forschung und Lehre vertrete und den Antrag von Frau Rositsa Dueva befürworte und die Betreuung auch im Falle eines Weggangs, wenn nicht wichtige Gründe dem entgegenstehen, weiterführen werde.

Essen, den _____ _____

Unterschrift eines Mitglieds der Universität Duisburg-Essen

Erklärung:

Hiermit erkläre ich, gem. § 7 Abs. (2) d) + f) der Promotionsordnung der Fakultät für Biologie zur Erlangung des Dr. *rer. nat.*, dass ich die vorliegende Dissertation selbständig verfasst und mich keiner anderen als der angegebenen Hilfsmittel bedient, bei der Abfassung der Dissertation nur die angegeben Hilfsmittel benutzt und alle wörtlich oder inhaltlich übernommenen Stellen als solche gekennzeichnet habe.

Essen, den _____ _____

Unterschrift der Doktorandin

Erklärung:

Hiermit erkläre ich, gem. § 7 Abs. (2) e) + g) der Promotionsordnung der Fakultät für Biologie zur Erlangung des Dr. *rer. nat.*, dass ich keine anderen Promotionen bzw. Promotionsversuche in der Vergangenheit durchgeführt habe und dass diese Arbeit von keiner anderen Fakultät/Fachbereich abgelehnt worden ist.

Essen, den _____ _____

Unterschrift der Doktorandin